# TIMBER FRAME TENSION JOINERY

**Richard J. Schmidt**

**Robert B. MacKay**

**A Report on Research Sponsored by the**

**TIMBER FRAME BUSINESS COUNCIL**
**WASHINGTON, D. C.**

**Department of Civil and**
**Architectural Engineering**
**University of Wyoming**
**Laramie, WY 82071**

**October 1997**

**UNIVERSITY OF WYOMING**

50272-101

| REPORT DOCUMENTATION PAGE | 1. REPORT NO. | 2. | 3. Recipient's Accession No. |
|---|---|---|---|

**4. Title and Subtitle**
Timber Frame Tension Joinery

**5. Report Date**
October 1997

**6.**

**7. Author(s)**
Richard J. Schmidt & Robert B. MacKay

**8. Performing Organization Report No.**

**9. Performing Organization Name and Address**
Department of Civil and Architectural Engineering
University of Wyoming
Laramie, Wyoming 82071

**10. Project/Task/Work Unit No.**

**11. Contract(C) or Grant(G) No.**
(C)
(G)

**12. Sponsoring Organization Name and Address**
Timber Frame Business Council
1511 K Street NW, Suite 600
Washington, D. C. 20005

**13. Type of Report & Period Covered**
final

**14.**

**15. Supplementary Notes**

**16. Abstract (Limit: 200 words)**

Timber-frame connections use hardwood pegs to hold the main member (tenon) within the mortise. Design of these connections is currently beyond the scope of building codes and the National Design Specification for Wood Construction (NDS). The objective of this research is to determine the feasibility of the yield model approach for the design of these connections. The research includes a study of the mechanical properties of the pegs used in mortise and tenon tension connections. Properties of interest include the peg's flexural yield strength, the dowel bearing strength of a peg as it loads the frame material, and the peg's shear strength. The results of this research show that the existing yield model equations from the NDS are applicable to hardwood pegs used as dowel fasteners in mortise and tenon connections. However, additional yield modes specific to these connections are needed.

**17. Document Analysis**
**a. Descriptors**

traditional timber framing, heavy timber construction, structural analysis, wood peg fasteners, dowel connections, yield model

**b. Identifiers/Open-Ended Terms**

**c. COSATI Field/Group**

| 18. Availability Statement | 19. Security Class (This Report) | 21. No. of Pages |
|---|---|---|
| Release Unlimited | unclassified | 87 |
| | 20. Security Class (This Page) | 22. Price |
| | unclassified | |

## Acknowledgments

Acknowledgments go to the Timber Frame Business Council for their financial support of this project. For providing materials, thanks are extended to Scott Northcott; Christian & Son, Inc.; Resource Woodworks; Riverbend Timberframing, Inc.; Duluth Timbers; Timberpeg; The Cascade Joinery; and Timberhouse Post and Beam.

Table of Contents Page

List of Tables Page

List of Figures Page

## List of Appendices Page

## Nomenclature and Glossary

Special terms used in this report are defined below. Definitions are based on those given in (Macmillan, 1996), (Hewett, 1980), and (Hoadley, 1980), plus those offered by this researcher.

| | |
|---|---|
| 5% exclusion value | the value at which 95% of the values in the series of tests will exceed |
| allowable stress design | a method of design that uses allowable stresses to determine allowable loads on members, etc. Note that the allowable stresses have built in factors of safety. |
| balloon framing | a method of wood construction that uses dimensional lumber spaced at regular intervals to create walls, floors, etc. |
| confidence level | an indicator of the reliability of the results in a small sample and how closely they would match the entire population |
| correlation | having a mutual relationship |
| data acquisition system | an electronic system that retrieves data about the item or material being tested and records the information for later analysis |
| double shear | a condition in which two shear planes exist on a single object |
| dowel bearing strength | the strength of a material being loaded by a circular prismatic object that is oriented perpendicular to its long axis |
| edge distance | the distance measured perpendicular to the grain, from the center of the dowel to the edge of the member being loaded |

| | |
|---|---|
| elasto-plastic behavior | an ideal yield behavior that exhibits a perfectly linear elastic region on the stress-strain curve up to the yield stress and stays at that stress level as further strain occurs |
| end distance | the distance measured parallel to the grain, from the center of the dowel to the end of the member being loaded |
| European Yield Model | a model developed by European scientists that describes how a timber connection might fail in terms of various modes of failure |
| $F_e$ | variable representing the dowel bearing strength of a material |
| $F_{em}$ | the dowel bearing strength of the main member |
| $F_{es}$ | the dowel bearing strength of the side member |
| flexural yield strength | the yield strength in bending of a certain object or material |
| fork and tongue connection | a connection that contains a single, centered tongue that fits in a slot at the end of another member, commonly used at a roof peak, where rafters join end-to-end |
| $F_{v\perp}$ | the shear strength of the wood for loading perpendicular to the grain |
| $F_v$ | the shear strength of the wood for loading parallel to the grain |
| $F_{yb}$ | the yield strength in bending of a dowel |
| gravity loads | loads caused by gravity such as self weight and live loads |

| | |
|---|---|
| half-timber | a traditional name for a common European framing system which used timbers that were split in half |
| housing | a cavity large enough to hold the entire timber's end |
| linear potentiometer | an electronic device that measures displacements by returning a voltage signal that changes relative to the displacement |
| longitudinal direction | along the centerline of the tree (parallel to the grain) |
| $l_v$ | the distance from the center of the peg to the end of the tenon, end distance |
| Mode II | a single shear failure mode in which the peg rotates through both members |
| Mode III | a single or double shear failure mode in which the peg rotates through the main or side member(s) and a plastic hinge forms in the other member(s) |
| Mode I | a single or double shear failure mode in which dowel bearing failures occur in either the main or side member(s) |
| Mode IV | a single or double shear failure mode in which plastic hinges occur in the main and side member(s) |
| Mode V | a peg shear failure mode |
| Mode VI | a failure mode in which the relish fails in shear |
| Mode VII | a failure mode caused by mortise splitting |
| mortise | a hole cut into a member in which the tenon is fit |
| NDS | The National Design Specification for Wood Construction (see Bibliography) |

| | |
|---|---|
| normal distribution | a statistically ideal distribution of data about a mean value |
| orthotropic material | material that has significant strength differences along each axis of strength. These axes are 90° to each other. |
| pith | the small core of soft, spongy tissue located at the center of tree stems, branches and twigs |
| plastic hinge | a flexural hinge that develops in a dowel caused by material yielding plastically in tension and compression |
| platform framing | a method of timber construction similar to balloon framing that uses common elements and standard dimensions to create walls and floors that rest upon the platform below |
| pressure transducer | an electronic device that measures pressure in a system (such as a hydraulic system) by returning a voltage signal which changes relative to the changing pressure in a system |
| radial direction | the direction out from the center of the tree |
| $R_e$ | the ratio of dowel bearing strengths ($F_{em}/F_{es}$) |
| Recycled Timber | timber that came from an older building to be used again in a newer one |
| relish | the material directly behind the peg at the end of the tenon |
| $R_t$ | the ratio of member thicknesses ($t_m/t_s$) |
| shear span | the distance between the loading block and the reaction block |
| shear strength | the average shear stress on a cross-section at failure under shear loading |

| | |
|---|---|
| shoulder | a ledge cut into the joined member that carries the entire width of a joining member |
| single shear | a condition in which one shear plane exists on a single object |
| specific gravity | the ratio of the density of a material to the density of water |
| standard deviation | a numerical value representing how closely a series of data is grouped about the mean |
| stress-skin panel | an insulated panel composed of rigid foam insulation and covered by structural paneling on one or both sides |
| stroke rate | the speed that the piston on a test apparatus moves |
| $t$ | variable representing the thickness of a member |
| tangential direction | a direction tangent to the growth rings of a tree |
| tenon | the stub on the end of a member that fits into a mortise |
| tie beam | a beam oriented transversely in a building to tie walls together; tie beams have end joints subjected to withdrawal loads |
| timber frame | traditional, stand-alone, heavy timber structure with all-wood joinery |
| $t_m$ | thickness of the tenon or main member |
| $t_s$ | thickness of the mortise side |
| ultimate load | the maximum load that can be obtained |
| wattle and daub | a method of infilling a wall that used woven sticks and mud |
| yield strength | the capacity of a material or member associated with yield behavior |

# 1. Introduction

## 1.1 General Overview

The goal of this project was to quantify the strength of the timber mortise and tenon connection when loaded in tension. This connection is made entirely of wood and has been used for centuries; however, its behavior has never been described mathematically. A typical application of the mortise and tenon connection is to join a beam to a post (Figure 1-1) in a heavy timber structure. A mortise is notched out of the post and a tenon on the end of the beam is then fit into the mortise. The entire system is held together with hardwood pegs. An example of a situation in which this connection is loaded in tension in a timber frame is at the end of a tie beam (Figure 1-2) (Hewett, 1980).

This method of connecting wood members became obsolete in the early 1800's as inexpensive nails began to replace the all-timber connections (Elliot and Wallas, 1977). This traditional style of timber framing has only recently regained popularity in housing and other heavy timber construction. The modern timber frame is energy efficient (through use of stress-skin panel insulation), comfortable to live or work in, elegant in style, and efficient in its use of timbers.

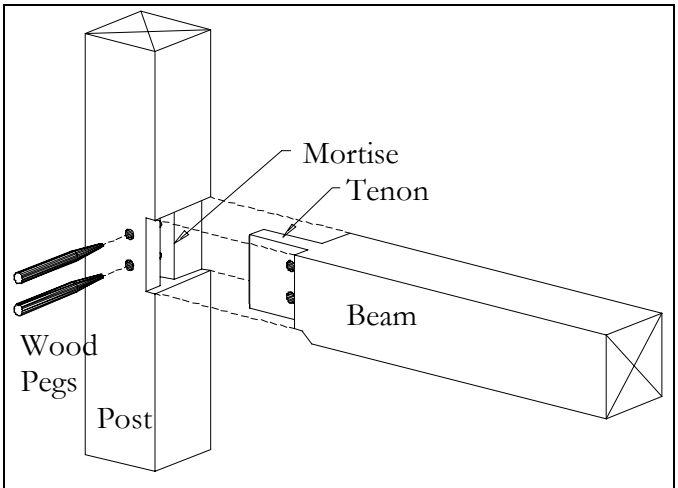


Figure 1-1 Typical Mortise and Tenon Connection

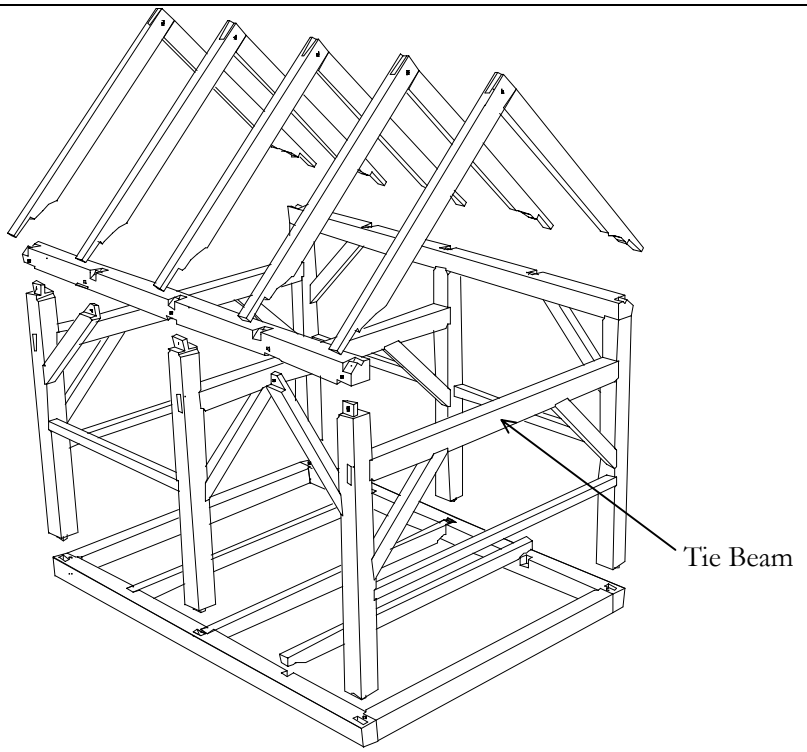


Figure 1-2 American Timber Frame (Redrawn from Sobon and Schroeder, 1984)

Structures made with the mortise and tenon joint have survived for hundreds of years. The mortise and tenon connection has been used in countless applications from furniture, to house construction, to ship building, and has proven itself time and again.

An analytical model was needed to verify the strength of the mortise and tenon connection. This was not with the intent to change traditional construction practices but to quantify the strength of the joint.

## 1.2 Objective and Scope

The objective of this project was to develop an analytical model to predict the strength of the mortise and tenon connection when loaded in tension. The overall connection strength is dependent on many different factors. These factors include the bending and shear strengths of the peg, the dowel bearing strength of the peg in the frame

materials, and the shear strength of the frame material. These factors must be combined into an appropriate analytical model. The model is an extension of the European Yield Model (EYM) (Larsen, 1973). The EYM was developed for connections using steel bolts and was extended by this research for use with wood peg connections. One important aspect of this project was the need to obtain material data for wood pegs. To this end, tests were conducted to obtain the material properties of species commonly used in mortise and tenon connections. Full-size connection tests were also conducted to validate the analytical model.

The final objective of the project was to develop design procedures and recommendations for construction using connections of this type.

# 2. Timber Framing Background

## 2.1 History of Timber Framing

The timber frame has been in existence for more than two thousand years. Timber framing came about slowly, as the tools became available and the laborers grew to be talented enough to do the work. The mortise and tenon joint was created sometime between 500 B.C. and 200 B.C. (Benson, 1997). This joint allowed a semi-rigid connection between the members of a frame. The first timber-frame buildings were constructed about the time of Christ (Benson, 1997). Early timber frames were made rigid by digging holes for the posts and compacting earth around the posts. This provided lateral support for the building, but the posts rotted quickly. The carpenters were forced to modify the structures to make them able to stand above the ground on stone foundations. To do this, the frames needed to be made stiffer. This was accomplished by means of diagonal bracing and stronger joinery.

As architectural systems emerged in Europe, the most common style was the framed wall system. In this system, the exterior walls were capable of supporting the weight of the roof above, and they contained the secondary elements of door and window openings, interior panels, and a weather resistant exterior covering. These systems varied by region, but in all cases they used the mortise and tenon connection and used beams made from logs that were split in half. From this method came the more traditional name, half-timber (Charles, 1984).

Timber frames became available to the common homeowner around 1450 (Charles, 1984). In the 1600's, the craft of timber framing reached its peak in Europe (Sobon and Schroeder, 1984). But as the supply of long, straight timbers dwindled, carpenters were

required to use shorter posts and beams, and crooked members wherever possible. Architectural styles began to show these modifications.

When colonists settled in America they naturally built homes similar to those in their homeland. These homes were meant to be functional. Long, straight timbers from virgin forests were plentiful so craftsmen began to build homes like those in Europe. The homes were small and usually had one room, but were sturdy and kept out the harsh New England weather. Communities worked together to build the structures. The designs for the timber frames were modified and constructed so that they could be assembled on the ground as large units and raised into place, to fit precisely into other members. American architecture did not have the limits of short timbers, for it was common to have 9" x 12" x 50' timbers in barns (Sobon and Schroeder, 1984). American timber framing gained a style all to its own.

The first buildings in the colonies used a wattle and daub method of infilling. This method came from Europe and called for branches and twigs to be woven between the main timbers and packed with mud to seal the wall. This proved ineffective in New England since the extreme weather caused shrinkage and swelling in the wattle and daub and eventually cracking. The colonists shifted to a wooden clapboard siding with a plaster interior.

In the 1600's, craft guilds comprised of carpenters were common. In these guilds, masters would teach apprentices the skills of the trade. The guilds were very competitive with each other, so they had to survive on good reputation and quality work. Timber frames were commonly built until around the 1830's when a machine was introduced that could produce nails quickly and inexpensively (Elliot and Wallas, 1977). Also, hand-hewn timbers were being replaced with standardized sawn lumber cut with steam-powered circular saws (Sobon and Schroeder, 1984). At this time, the demand for fast, inexpensive housing was growing in America due to the number of people moving and settling in the western

territories. Using the new construction materials, new forms of framing, called balloon and platform framing, were introduced and homes could be built quickly to meet the demand. Another benefit at the time was that the labor force did not need to be as skilled. Thus, timber framing was replaced with alternative construction methods and the craft guilds, needed to pass along the traditions, were no more.

## 2.2 Review of Relevant Research

Research in timber framing in general, and traditional joinery in particular, is limited not only in the United States but also internationally. Since the mid-1970's when the revival of the craft began, the research community has regarded timber framing as indistinct from conventional heavy-timber, post and beam construction. The first significant research work done in timber framing was that by Brungraber (1985). Dr. Brungraber's research was broad in scope and examined full structure, as well as individual joint, behavior via both experimental and numerical studies.

A more recent research project has just been completed at Michigan Technological University under the direction of Dr. William M. Bulleit (Sandberg *et al.*, 1996; Bulleit *et al.*, 1996). Bulleit's research was guided in part by the path taken by Dr. Brungraber. However, Bulleit defined a more narrow objective and conducted a comprehensive investigation of timber frame subassemblies under gravity loads. A major objective of Bulleit's work was the identification of joint behavior and its role in the overall structural response. He developed a special-purpose structural analysis computer program that includes semi-rigid joint behavior.

One of the major findings from Bulleit's research was that tightly fitting joints, in which little movement is allowed between the tenon and mortise, carry gravity loads with less peg damage than occurs in loose joints. Also, mortise and tenon connections with a

shoulder that can carry the entire width of the beam perform better under gravity loads than unshouldered mortise and tenon connections or fork and tongue-type connections. An overall impression from these tests is that these joints have remarkable load capacity and resistance to catastrophic failure (Sandberg *et al.*, 1996).

Preliminary work done at the University of Wyoming on the design of tension joinery was discussed in (Schmidt *et al.*, 1996). Emphasis was on the applicability of the NDS yield modes to all-wood connections and the presentation of material strength test data.

Other research efforts in the U. S. have focused on peg characteristics and joint design. An investigation of dowel bearing strength for pegged joints was performed at the University of Idaho by J. R. Church (Church and Tew, 1997; Church, 1995). Church performed bearing tests on Red Oak and Douglas Fir specimens using White Oak pegs. One of his findings was that the bearing strength of both materials was higher when the peg was loaded in the radial orientation (perpendicular to growth rings) than when loaded in the tangential orientation, regardless of the orientation of the base material. Another finding was that the bearing strength of the Red Oak was independent of the base material orientation. That is, dowel bearing strength parallel to the grain is not significantly higher than that perpendicular to the grain when the dowel consists of a white oak peg. Also there seemed to be no significant effect from the variation in hole size for a given peg size.

A program of joint specimen tests and analytical analysis for timber bridge construction was performed at the Massachusetts Institute of Technology (Brungraber and Morse-Fortier, 1996). Both of these studies have produced valuable data regarding the bending, shear and bearing characteristics of hardwood pegs.

Although timber framing is still a popular building method in Europe (especially England and Germany) and in the Orient, little useful international research has been located. Oriental construction styles differ markedly from that used in the United States (Abe and Kawaguchi, 1995; King *et al.*, 1996). Timber-frame structures in Japan and China generally involve complex joinery and ornate structural forms. In addition, Oriental practice commonly relies on stacked and interlocked members in order to assure structural integrity. In sharp contrast, United States practice involves longer members that are fewer in number with less intricate joinery. Hence, the results of the available research do not apply to U. S. practice.

Traditional techniques in Europe closely resemble U. S. practice. However, little is published that pertains specifically to timber framing. Two valuable research articles in German have been translated (Peavy and Schmidt, 1995; 1996). While limited in scope, the recommendations contained in the second of these two reports form the basis of all timber frame reconstruction and restoration now performed in Germany (Kessel, 1996). Due to the high costs of good-quality, solid-sawn timber in Europe, new timber frames are not built in the traditional manner. Reconstructions are limited to structures of significant historical importance for which cost is (almost) no object (Kessel, 1988).

M. H. Kessel performed 120 tests on full-size all-wood connections constructed of freshly-cut Oak and dry Spruce timber, of which 80 were traditional mortise and tenon joints. These connections were each held together with two Oak pegs. The cross sections of the members ranged in size from 5.5"x5.5" to 7.9"x7.9" (140mm x 140mm to 200mm x 200mm). The Oak pegs ranged in diameter from 0.9" to 1.6" (24mm to 40mm). Results from the all-Oak connections (Peavy and Schmidt, 1996) are presented as design recommendations in this report (see Table 6-1).

Studies in the U. S. that adapt and apply the European yield model to domestic practice for bolted connections are reported in (Thangjitham, 1981; McLain and Thangjitham, 1983; Soltis *et al.*, 1986; Soltis *et al.*, 1987; Soltis and Wilkinson, 1987; Wilkinson, 1993).

Technical literature on timber frame joinery design is limited. Reviews of current practice, which is based on interpretations of past research and available design standards, are found in (Brungraber, 1992a; Brungraber, 1992b). Alternatives to all-wood joinery involving metallic fasteners are described in (Brungraber, 1992a) and (Duff *et al.*, 1996).

There are several craft-oriented books that present the history, architectural design, and construction techniques for timber frames. These include (Elliot and Wallas, 1977; Benson and Gruber, 1980; Sobon and Schroeder, 1984; Benson, 1997; Sobon 1994). In these books, details related to engineering design are usually limited to span tables for bending members (floor beams). Carpentry details of Oriental joinery are found in (Seike, 1977).

Even though the joinery used in timber-frame structures resembles that used by carpenters in the furniture industry, significant differences exist. The basic mortise and tenon joint used in furniture construction (Hill and Eckelman, 1973) includes a relatively short (stub) tenon and relies on adhesives to secure the joint. Doweled joints in furniture (Eckelman, 1970; 1979) use the wood dowel as a replacement for the tenon, rather than as an anchor to prevent tenon withdrawal from the mortise. These joints also rely on adhesives to secure the joint. Hence, the relatively large body of literature in furniture joinery is not applicable to the structural systems considered here.

# 3. European Yield Model and Proposed Additions

## 3.1 Introduction

Today, the craft of timber framing is returning. Craftsmen are re-learning the skills of the trade by studying existing buildings and applying the techniques to modern construction. Building officials, however, are often not familiar with this construction method and will not rely on previous standards for today's practices. The problem is not in the structural members, for the behavior of beams and columns is well understood, but in the timber-frame connections. A method to determine the strength of these connections is therefore required.

This chapter will focus on the existing yield model and its derivation and will determine how it could be applied to timber-frame connections. An alternate analysis of one of the yield modes is shown and was used to determine its applicability to pegged mortise and tenon connections. As a result of this analysis, additional yield modes are introduced, specific to pegged mortise and tenon connections.

## 3.2 Development of European Yield Model

A mathematical model for determining connection strength was developed in 1941 by K. W. Johansen, who applied the theory to connections with metal dowel fasteners (Aune and Patton-Mallory, 1986). This model was used to analyze single and double shear timber connections that used bolts as the primary fasteners. To analyze the connections, Johansen compared the dowel bearing strength of the bolt to its bending strength to obtain the overall strength of the connection (Johansen, 1949). H. J. Larsen extended Johansen's development to include various failure modes for single and double shear connections (Larsen, 1973). Figures 3-1 and 3-2 illustrate the various failure modes for single and double shear connections. Labeling of the modes follows National Design Specification for Wood

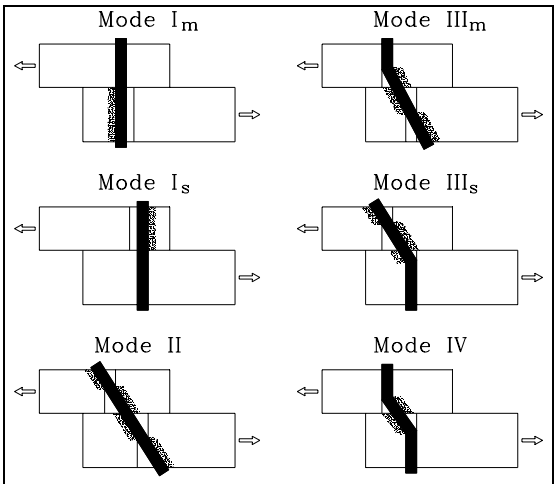


Figure 3-1 Single Shear Failure Modes

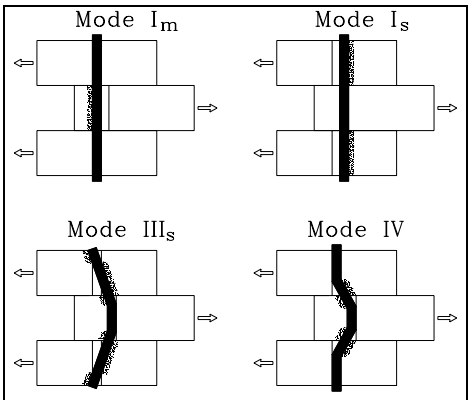


Figure 3-2 Double Shear Failure Modes

Construction (NDS) nomenclature (AFPA, 1991). The current code makes use of the work done by Johansen, Larsen and others.

Modes $I_m$ and $I_s$ are bearing failure modes of the base material. The shaded region near the dowel represents base material that has yielded in bearing. Mode II is a single shear failure mode in which the dowel rotates in both the main and side members, causing the base material to yield. Mode III and IV failures can occur in both single and double shear modes and is characterized by both dowel and base yielding. Mode III occurs when the dowel rotates in the main or side members and develops a plastic hinge in bending, while simultaneously crushing the base material. Mode IV occurs when hinges form in both main and side members in combination with base material crushing. Note that some of the single shear yield modes are not possible in double shear, since it is not possible for the dowel to rotate in the main member.

Larsen divided these failure modes into two possible scenarios of dowel rotation and dowel bending. If the dowel was very stiff, then it could rotate in the wood, crushing the fibers on either side. If the dowel was flexible and the surrounding wood had a high

strength, then the dowel could bend, causing a plastic hinge to form in the dowel. He assumed that both materials behaved elasto-plastically, meaning that when the stress in the material reached yielding, then no more stress could be applied. The scenarios are illustrated in Figure 3-3 and Figure 3-4.

For each scenario, the load can be found in terms of its eccentricity.

For the first scenario of the dowel rotating in the material (see Figure 3-3):

$$P = \left[\sqrt{(2e+t)^2 + t^2} - (2e+t)\right] DF_e \tag{3-1}$$

For the second scenario of the dowel yielding in the material (see Figure 3-4):

$$P = \left[\sqrt{e^2 + \frac{D^2 F_{yb}}{3F_e}} - e\right] DF_e \tag{3-2}$$

The figures come from the work of S. Thangjitham (Thangjitham, 1981). The key parameters for the above equations and figures are as follows: *P* represents the load applied

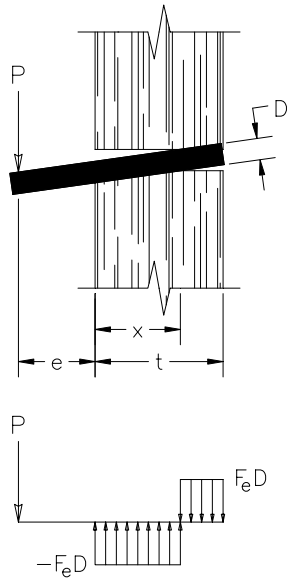


Figure 3-3 Assumed Dowel Rotation Load Diagram

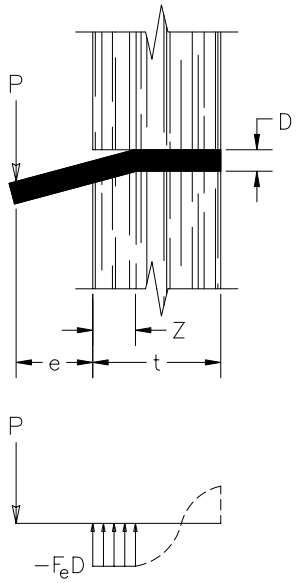


Figure 3-4 Assumed Dowel Yielding Load Diagram

to the dowel and $e$ is the eccentricity of the load; the material thickness and dowel diameter are $t$ and $D$, respectively; the positions of the dowel pivot point and plastic hinge point are $x$ and $Z$, respectively; the dowel bearing strength of the base material is $F_e$ and the bending yield strength of the dowel is $F_{yb}$. Equations 3-1 and 3-2 are derived in Appendices A and B, respectively.

These equations are applied to each yield mode to determine joint capacity. For instance, the single shear Mode IV has the same type of failure in both the main and side member. Therefore, Eq. 3-2 can be used for each member. From equilibrium, the yield load in each member must be equal, and is the following (Thangjitham, 1981):

$$P = D^2 \sqrt{\frac{2F_{em}F_{yb}}{3\left(1+\frac{F_{em}}{F_{es}}\right)}} \tag{3-3}$$

The above equation uses $F_{em}$ and $F_{es}$ for the dowel bearing strength in the main (thicker) and side (thinner) members, respectively.

The derivation of these equations is based on the assumption that a single, unique position for the eccentricity can be found and that the resultant of the load for the entire connection is at this location. Section 3.3 contains an alternative method for calculating the yield load for Mode IV.

The yield loads for the single shear modes are as follows:

$$P_{I_m} = D \cdot t_m \cdot F_{em} \tag{3-4}$$

$$P_{I_s} = D \cdot t_s \cdot F_{es} \tag{3-5}$$

$$P_{II} = k_1 \cdot D \cdot t_s \cdot F_{es} \tag{3-6}$$

$$P_{III_m} = \frac{k_2 \cdot D \cdot t_m \cdot F_{em}}{(1+2 \cdot R_e)} \tag{3-7}$$

$$P_{III_s} = \frac{k_3 \cdot D \cdot t_s \cdot F_{em}}{(2 + R_e)} \tag{3-8}$$

$$P_{IV} = D^2 \sqrt{\frac{2 \cdot F_{em} \cdot F_{yb}}{3 \cdot (1 + R_e)}} \tag{3-9}$$

where:

$$k_1 = \frac{\sqrt{R_e + 2 \cdot R_e^{\,2} \cdot (1 + R_t + R_t^{\,2}) + R_t^{\,2} \cdot R_e^{\,3}} - R_e \cdot (1 + R_t)}{(1 + R_e)} \tag{3-10}$$

$$k_2 = -1 + \sqrt{2 \cdot (1 + R_e) + \frac{2 \cdot F_{yb} \cdot (1 + 2 \cdot R_e) \cdot D^2}{3 \cdot F_{em} \cdot t_m^{\,2}}} \tag{3-11}$$

$$k_3 = -1 + \sqrt{\frac{2 \cdot (1 + R_e)}{R_e} + \frac{2 \cdot F_{yb} \cdot (2 + R_e) \cdot D^2}{3 \cdot F_{em} \cdot t_s^{\,2}}} \tag{3-12}$$

The other key parameters for these equations are $R_e$ which is the ratio of main and side bearing strengths ($F_{em}/F_{es}$), and $R_t$ which is the ratio of main to side thicknesses ($t_m/t_s$).

For the double shear yield modes, simply multiply the single shear yield mode that applies, by two.

### 3.3 Alternate Derivation of the Mode IV Yield Model Equation

As a check on the derivation of the yield model equations, another approach was taken in this research. Instead of looking at the equilibrium of the entire connection, the equilibrium of the dowel was the main concern. An assumed load distribution was to be applied to the dowel for the failure mode in question as a means to obtain a more intuitive derivation (see Figure 3-5). The single shear Mode IV is one that contains two plastic hinges in the dowel. This scenario could occur if the side and main members had high dowel bearing strengths while the peg was flexible.

In Figure 3-5, the loading outside of each plastic hinge was unknown so the dowel bearing strength was used arbitrarily. This assumption allowed calculations to be performed

and the results obtained match those of others.

In Figure 3-5, the deformed shape and the stress distribution on the peg are assumed. Joint capacities from the model generally agree well with experimental observations. Nevertheless, there are inconsistencies in the theory. For instance, the location of maximum bending moment in the peg does not coincide with the location of the hinge in the assumed deformed shape (Figure 3-5).

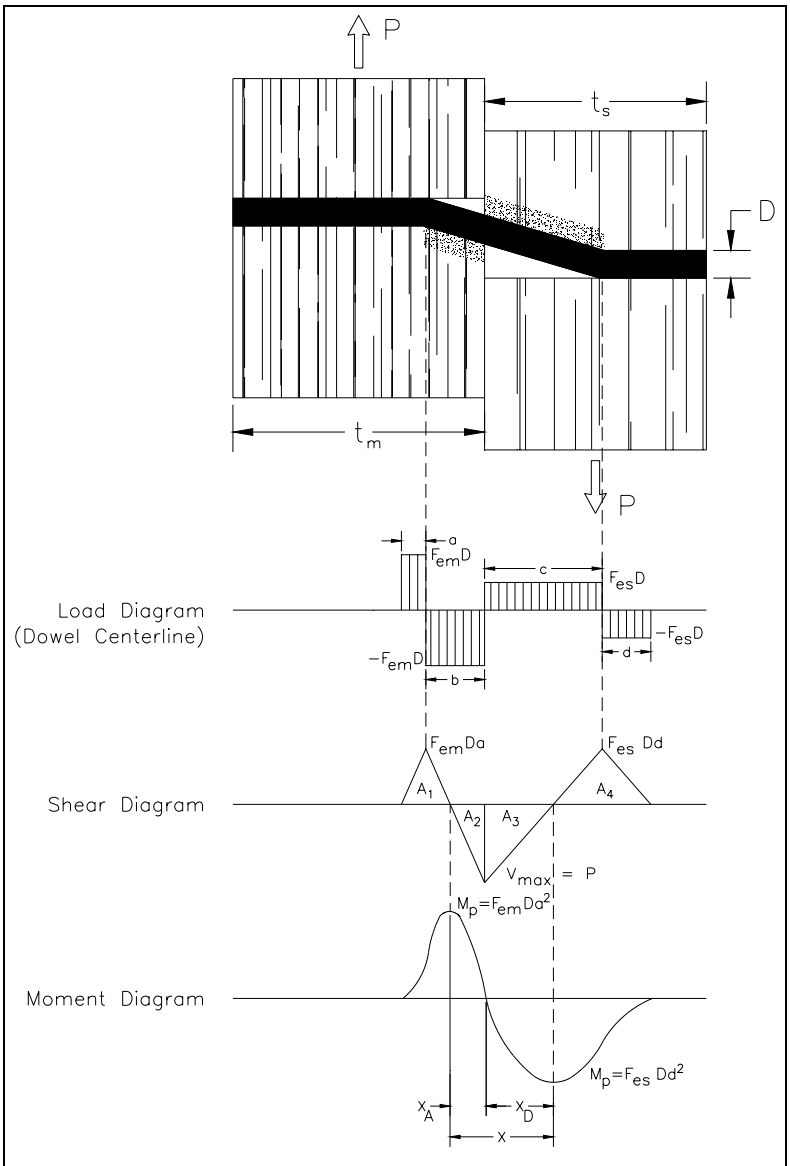


Figure 3-5 Assumed Load, Moment and Shear Diagrams

The areas under the shear diagram can be represented as follows:

$$A_1 = \frac{F_{em} D a (2a)}{2} = F_{em} D a^2 \tag{3-13}$$

$$A_2 = \frac{(\sqrt{2}a)(F_{em} D \sqrt{2}a)}{2} = F_{em} D a^2 \tag{3-14}$$

$$A_3 = F_{es} D d^2 \tag{3-15}$$

$$A_4 = F_{es} D d^2 \tag{3-16}$$

From mechanics of materials, the plastic moment capacity for a circular cross-section in bending is:

$$M_p = \frac{F_{yb} D^3}{6} \tag{3-17}$$

From the moment diagram, we have

$$M_p = F_{em} D a^2 \tag{3-18}$$

$$2 \cdot M_p = A_2 + A_3 \tag{3-19}$$

Substituting for $M_p$, $A_2$ and $A_3$, and solving for $a$, we obtain:

$$a = \sqrt{\frac{F_{yb} D^2}{3 F_{em} \left(1 + \frac{F_{em}}{F_{es}}\right)}} \tag{3-20}$$

$$P = F_{em} D \sqrt{2} a \tag{3-21}$$

For single shear, the Mode IV capacity is:

$$P = D^2 \sqrt{\frac{2 F_{em} F_{yb}}{3\left(1 + \frac{F_{em}}{F_{es}}\right)}} \tag{3-22}$$

In actual mortise and tenon connections, hinges similar to the Mode IV hinges have been observed but at a very close spacing. The purpose of the following analysis is to predict the spacing between the Mode IV hinges from a strength of materials approach and compare it to actual distances to learn if this mode occurs or if something else is happening.

Plastic hinges occur in the peg due to bending and are located at points of maximum moment (see Figure 3-5). This derivation is as follows:

From equilibrium:

$$x_A = \frac{P}{DF_{em}} \tag{3-23}$$

For failure to occur, two plastic hinges must occur in the peg. Areas under the shear diagram give

$$\frac{DF_{em}(a-b)x_A}{2} + \frac{DF_{es}(d-c)x_D}{2} = 2M_p \tag{3-24}$$

$$DF_{em}(a-b) = P \tag{3-25}$$

$$DF_{es}(d-c) = P \tag{3-26}$$

Simplifying Equation 3-24, we obtain

$$Px_A + Px_D = 4M_p \tag{3-27}$$

$$x_D = \frac{4M_p}{P} - x_A \tag{3-28}$$

Total distance between hinges is

$$x = x_A + x_D \tag{3-29}$$

$$x = \frac{4M_p}{P} = \frac{4F_{yb}D^3}{6P} \tag{3-30}$$

Substituting Eq. 3-22 into Eq. 3-30 we obtain

$$x = D\sqrt{\frac{2F_{yb}\left(1+\frac{F_{em}}{F_{es}}\right)}{3F_{em}}} \tag{3-31}$$

As a numerical example, typical values for 1" Red Oak Pegs in Douglas Fir give a total distance between plastic hinges of 3.0 inches (using $F_{yb}$ = 12,601 psi, $F_{em}$ = 2070 psi,

and $F_{es}$ = 1728 psi) (see Sections 5.2 and 5.4). As will be discussed later, typical test results show hinges that are much closer together than is predicted with this yield mode.

### 3.4 Application of the European Yield Model to Timber-Frame Connections

The yield model failure modes may be applied to timber frame connections since they are based on equilibrium and compatibility of materials and the only difference in the equations is the material used for the dowel. The wood pegs are assumed to yield in bending similarly to the steel dowels in the original derivation. Steel dowels yield plastically in bending with the entire cross-section deforming plastically after yielding is reached. It is important to note that the cross-section continues to gain resistance to load after the extreme fibers yield in tension or compression, up to the point where all of the material in the cross-section has yielded. After the entire section is yielded, the dowel can resist little additional load. Similar behavior occurs in wood as can be seen in Figure 3-6. Wood pegs are therefore assumed to yield plastically in bending.

In the typical mortise and tenon joint (Figure 1-1), a state of double shear exists. For this reason, the following discussion will focus on the double shear yield model failure modes (Figure 3-2).

The four modes of double shear failure can be assumed to apply. However, additional modes of failure have been observed in timber-frame connections. After comparing the theoretical hinge spacing of Mode IV to actual failed connections, where the hinge spacing is much closer than predicted, one must conclude that other factors exist to cause failure. The Mode IV equations are based on a simple bending failure in the dowel. Wood pegs, quite possibly, fail due to the combined effect of bending and shear on the cross-section. Since wood is so highly orthotropic, its strength is dependent on the loading orientation. Also, wood is typically weak in shear. This combined effect would tend to

cause the hinges to form closer together than as predicted by pure bending, since the shear strength would influence the overall strength of the system and the resulting shape would be similar to that seen in Figure 3-7.

Another failure possible in timber-frame connections is known as a relish failure and is related to the end distance ($l_v$) of the peg in the tenon. When the tenon is loaded in tension, the material behind the peg (or relish) can be broken away from the tenon (see Figure 3-8). This type of failure is different than the splitting failure seen in steel bolted connections. In a splitting failure, the wood directly behind the bolt splits and the bolt slides through the gap created (see Figure 3-9). Also, the splitting-type failure of the tenon is not typical in mortise and tenon connections since the tenon is usually restrained tightly in the mortise.

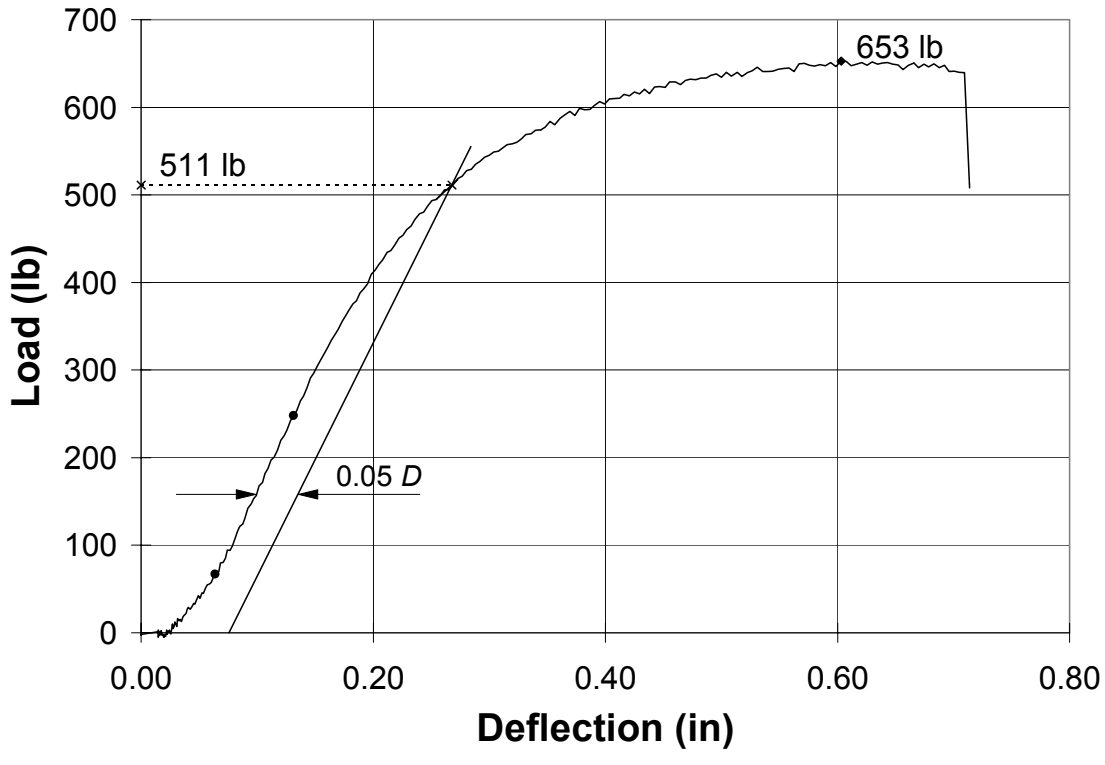


Figure 3-6 Typical Load Deflection Curve (Bending Test, ¾" Dia. Red Oak Peg)

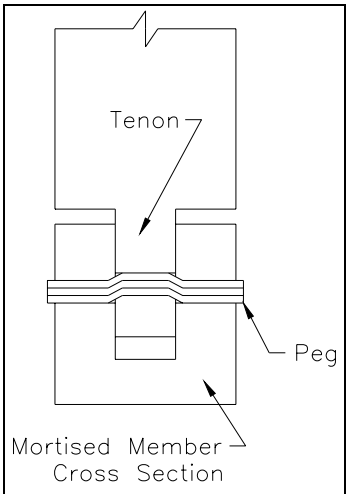


Figure 3-7 Combined Shear - Bending Failure

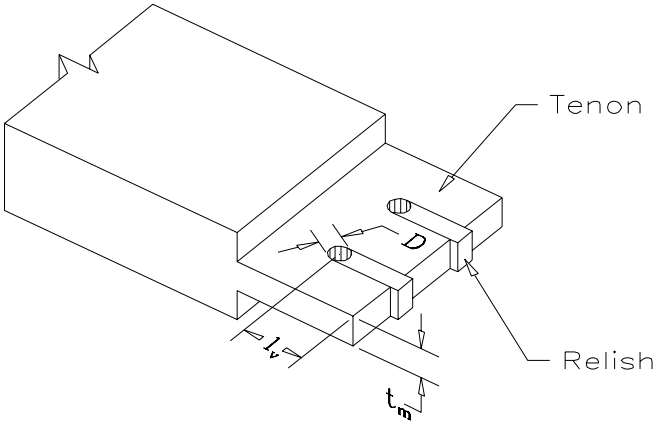


Figure 3-8 Relish Failure

The last failure mode observed in mortise and tenon connections pertains to the splitting of the material around the mortise. As the connection is loaded in tension, two things occur. First, the mortise material is loaded in direct tension, perpendicular to the grain, and secondly, the bending in the peg causes the sides of the mortise to spread out and finally split apart (see Figure 3-10). A method to quantify the strength of the material surrounding the mortise is left for future research. This will be a difficult matter since the material on all sides of the mortise provides constraint to the joint. This additional material helps to keep the sides of the mortise from spreading outward and provides additional

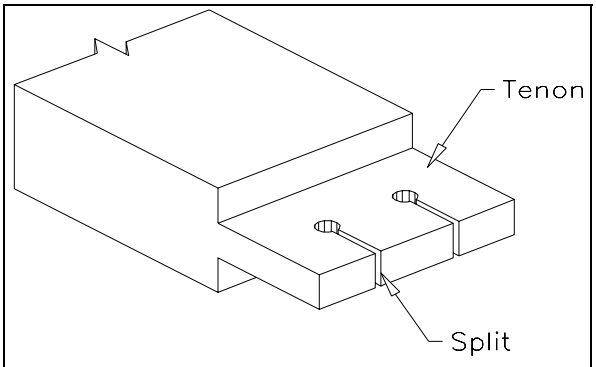


Figure 3-9 Tenon Splitting Failure

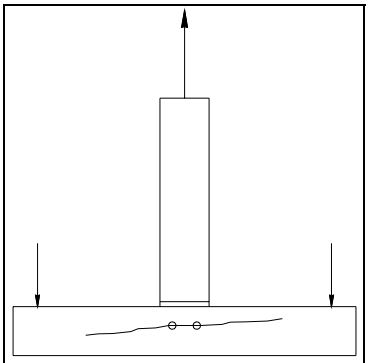

Figure 3-10 Mortise Splitting Failure

material needed in direct tension.

### 3.5 Additional Yield Model Equations

A comprehensive mortise and tenon yield model will need to include the existing four NDS yield modes for double shear and the three additional yield modes, specific to mortise and tenon connections. The existing NDS modes are based on peg bearing and bending, and the proposed yield modes will account for combined shear and bending, relish failure, and mortise splitting.

The first proposed yield mode will be known as Mode V, for purposes of discussion, and takes into account the effect of the combined bending and shear behavior of the connection (Fig. 3-7). The double shear strength for $n$ pegs is the following:

$$P_V = 2nF_{v\perp}A \tag{3-32}$$

Where $F_{v\perp}$ is the vertical shear strength of the wood peg and $A$ is the cross-sectional area of the peg. This equation takes into account the combined bending and shear effects by using an allowable shear strength that is determined by testing as shall be described in the next section.

The relish failure mode shall be known as Mode VI (Fig. 3-8) and is related to the distance from the center of the peg to the end of the tenon ($l_v$), the tenon thickness ($t_m$), peg diameter ($D$), and the horizontal shear strength of the tenon ($F_{vm}$).

$$P_{VI} = 2nF_{vm}t_m\left(l_v - \frac{D}{2}\right) \tag{3-33}$$

In the case of the mortise material splitting, known as Mode VII (Fig. 3-10), no specific test or numerical model has been devised to quantify the strength of the material around the mortise. Therefore, minimum edge distances, such as those required by the NDS, shall be developed to ensure that this failure mode does not control.

For softwood members the NDS requires that a distance of 7*D* be provided from the center of the bolt to the end of the tension member ($l_v$) and that a distance of 4*D* be provided from the edge of the mortise to the center of the bolt ($l_e$) (where *D* is the diameter of the steel bolt).

Since these requirements are based on connections tests with steel bolts, a wood peg used in the same application would have a much larger diameter than a steel bolt. It does not seem reasonable to assume that for a given load, a much larger end distance is required for a wood peg than a steel bolt, just because the diameter needs to be greater. Therefore, relationships must be drawn between the required wood peg diameter and an equivalent steel bolt diameter. End distances and perhaps edge distances would then be determined by using the equivalent steel bolt diameter.

To determine the size of a wood peg or pegs needed in a connection, one would

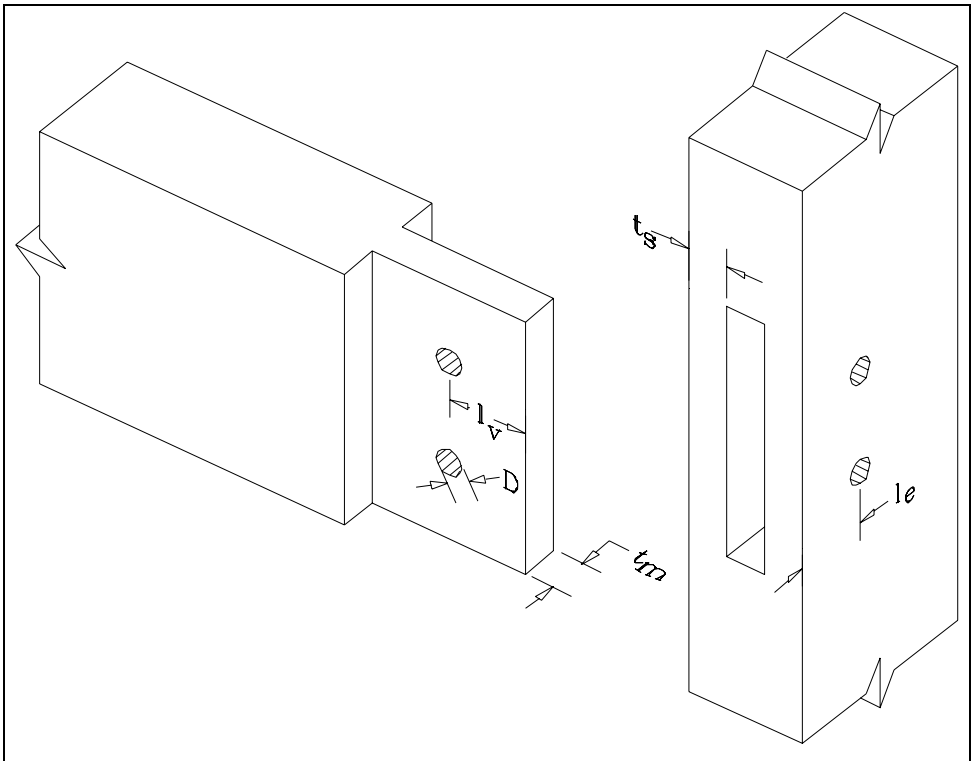


Figure 3-11 Standard Connection Geometry

need to know the required load and available materials and then use the yield mode equations to size the connection (see Figure 3-11). Assuming that a state of double shear exists, the yield modes are as follows: (Note: The factors of safety have been removed to obtain yield loads.)

$$P_{Im} = nDt_m F_{em} \tag{3-34}$$

$$P_{Is} = 2nDt_s F_{es} \tag{3-35}$$

$$P_{IIIs} = \frac{2nk_3 Dt_s F_{em}}{\left(2 + R_e\right)} \tag{3-36}$$

$$P_{IV} = 2nD^2 \sqrt{\frac{2F_{em}F_{yb}}{3\left(1 + R_e\right)}} \tag{3-37}$$

$$P_V = 2nF_{v\perp}\left(\pi \frac{D^2}{4}\right) \tag{3-38}$$

$$P_{VI} = 2nF_{vm}t_m\left(l_v - \frac{D}{2}\right) \tag{3-39}$$

where:

$$k_3 = -1 + \sqrt{\frac{2(1 + R_e)}{R_e} + \frac{2F_{yb}(2 + R_e)D^2}{3F_{em}t_s{}^2}} \tag{3-40}$$

Note that $R_e$ is the ratio of the wood peg dowel bearing stresses ($F_{em}/F_{es}$) in the main and side member, respectively, and $F_{yb}$ is the bending yield stress for the wood peg. $F_{v\perp}$ and $F_{vm}$ are the shear yield stresses in the wood peg and main member, respectively.

Once the loads are determined for each mode, the lowest load ($P$) is used as the yield load for the entire connection. This yield load is then used to solve for equivalent bolt diameters for each mode. Solving for $D$ in each mode equation:

$$D_{Im} = \frac{P}{t_m F_{em}} \tag{3-41}$$

$$D_{Is} = \frac{P}{2 t_s F_{es}} \tag{3-42}$$

$D_{IIIs} =$ positive root of following equation: (3-43)

$$\frac{2}{3} F_{yb}\left(2 + R_e\right) F_{em} D^4 + \left(\frac{2\left(1 + R_e\right)}{R_e} - 1\right) {t_s}^2 {F_{em}}^2 D^2 + \frac{P}{n}\left(2 + R_e\right) t_s F_{em} D - \frac{1}{4}\left(\frac{P}{n}\right)^2 \left(2 + R_e\right)^2 = 0$$

$$D_{IV} = \sqrt{\frac{P}{2n}\sqrt{\frac{3\left(1 + R_e\right)}{2 F_{em} F_{yb}}}} \tag{3-44}$$

$$D_V = \sqrt{\frac{2P}{n\pi F_{v\perp} t_m}} \tag{3-45}$$

Where $R_e$ is now the ratio of the dowel bearing stresses ($F_{em}/F_{es}$), for the bolted connection and $F_{yb}$ and $F_v$ are the bolt bending and yield stresses, respectively. Mode VI has been excluded from this analysis for bolt diameter because the shear yield stress in the main member will not change between a wood peg and a steel bolt, and the bolt diameter will only increase due to the end distance. For instance, if a connection is sized based on the shear in the peg, then the end distance is not a concern. When an equivalent steel bolt is determined using this mode, it will be much larger than the wood peg, due to the fact that less end distance is needed to balance out the load.

From these equations, the largest diameter ($D$) is used as the equivalent bolt diameter. The following example (Figure 3-12) shows how a wood connection, with a yield load of 5,184 lb using two 1" Red Oak pegs, can carry an equivalent load using a 0.53" diameter steel bolt.

Using the equivalent bolt diameter, the end distance can be determined from the NDS requirements. The end distance requirement of 7*D*, suggests that for a bolt that is 0.53" in diameter, an end distance of 3.71" is needed. For the equivalent 1" Red Oak peg, the same end distance of 3.71" should be adequate to develop the full load of the connection.

There is also the possibility that another yield mode, similar to Mode $III_s$ is needed. In failed mortise and tenon connections, a common failure mode is one that contains a

**Connection Geometry**

| | | | | | |
|---|---|---|---|---|---|
| $D$ = | 1.00 in | (25 mm) | $t_m$ = | 2.00 in | (51 mm) |
| $n$ = | 2 | | $t_s$ = | 1.75 in | (44 mm) |
| | | | $l_v$ = | 3.00 in | (76 mm) |

| **Wood Peg Properties** | | | **Steel Bolt Properties** | | |
|---|---|---|---|---|---|
| $F_{yb}$ = | 12,600 psi | (86.9 MPa) | $F_{yb}$ = | 45,000 psi | (310.3 MPa) |
| $F_{v\perp}$ = | 1,650 psi | (11.4 MPa) | $F_{v\perp}$ = | 27,000 psi | (186.2 MPa) |
| $F_{em}$ = | 1,547 psi | (10.7 MPa) | $F_{em}$ = | 4,050 psi | (27.9 MPa) |
| $F_{es}$ = | 930 psi | (6.4 MPa) | $F_{es}$ = | 1,950 psi | (13.4 MPa) |
| $F_{vm}$ = | 280 psi | (1.9 MPa) | $F_{vm}$ = | 280 psi | (1.9 MPa) |

Based on Red Oak Pegs and
Eastern White Pine Mortise and Tenon

| **Load Analysis** | | | **Equivalent Steel Bolt Analysis** | | |
|---|---|---|---|---|---|
| $P_{Im}$ = | 6,188 lb | (27.53 kN) | $D_{Im}$ = | 0.32 in | (8 mm) |
| $P_{Is}$ = | 6,510 lb | (28.96 kN) | $D_{Is}$ = | 0.38 in | (10 mm) |
| $P_{IIIs}$ = | 6,249 lb | (27.80 kN) | $D_{IIIs}$ = | 0.53 in | (14 mm) |
| $P_{IV}$ = | 8,835 lb | (39.30 kN) | $D_{IV}$ = | 0.45 in | (12 mm) |
| $P_{V}$ = | 5,184 lb | (23.06 kN) | $D_{V}$ = | 0.17 in | (4 mm) |
| $P_{VI}$ = | 6,720 lb | (29.89 kN) | | | |
| $P$ = | 5,184 lb | (23.06 kN) | $D$ = | 0.53 in | (14 mm) |

Figure 3-12 Equivalent Bolt Diameter Example

single hinge in the peg, at the center of the tenon. In Mode $III_s$ the ends of the peg rotate through the side material and two hinges form, but this mode does not allow those two hinges to form at the same location (thus actually being one hinge) (see Figure 3-13).

Mode $III_s$ is based on a single shear condition, where one end of the peg is held securely in the material of the main member. As the connection is loaded, the peg rotates through the side material and a hinge forms in the peg (see Figure 3-14).

A mathematical model that properly reflects the strength of the peg and the surrounding material is necessary for Mode $III_s$'.

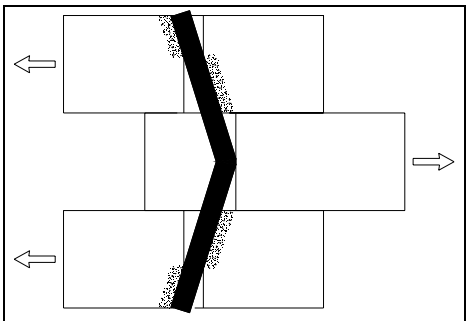

Figure 3-13 Proposed Mode $III_s$'

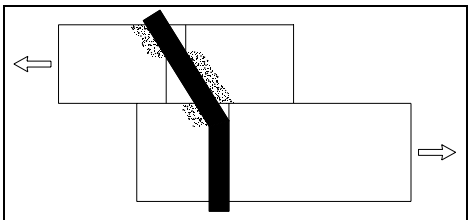

Figure 3-14 Mode $III_s$ (Single Shear)

# 4. Peg Testing Procedures and Analysis

## 4.1 General Testing Procedures for Hardwood Pegs

This section introduces the tests performed by this researcher and the procedures followed for all tests. Testing procedures that are unique to the specific type of test are discussed in the section for that individual test. The tests performed were dowel bending tests, dowel bearing tests, dowel shear tests, and full-sized tests.

The yield models require material properties specific to hardwood pegs. These properties include the bending strength of the pegs, the dowel bearing strength of the pegs in the main and side members, and the combined shear and bending strength of the pegs. Whenever possible, ASTM test procedures were followed.

The primary species selected for peg testing were Red Oak and White Oak, with some additional testing of Locust, Birch, Maple, and Ash. The pegs were in diameters of ¾", 1" and 1¼" and ranged in length from 8" to 12". For the dowel bearing tests, the base materials were Douglas Fir, Red Oak, and Eastern White Pine. The samples were cut from 8x8 timbers roughly 4 feet in length.

The pegs and base materials arrived approximately one year before this writing from various locations around the United States. They were placed in an environmental chamber, as per the ASTM standard D4933-91 for Moisture Conditioning of Wood and Wood-Base Materials, and kept at or near a temperature of 70° F and 65% relative humidity until they were needed for testing (ASTM, 1995a). The purpose for this was to condition the wood at a constant moisture content of 12%. Even though constancy would have been ideal, some fluctuations did occur due to seasonal effects and some mechanical breakdowns. The moisture content was determined for each test sample as required by ASTM D4442-92 (ASTM, 1995a).

The pegs for each test were selected randomly from the limited supply. Occasionally it was necessary to discard pegs from the supply due to serious defects such as severe splits or extreme wane. It was judged that these would not have been used in stress-critical applications during construction.

For the dowel bearing tests, the samples which had severe splits or knots were discarded since they would affect the yield strength of such small samples.

The samples used for the dowel bearing tests came from a limited number of large timbers. Therefore, the population variety is not what would be desired, but the confidence levels help to adjust for this in the 5% exclusion values.

For all tests, it was important to note the orientation of the grain, to determine if the strength was dependent on this orientation. For example, the pegs were loaded in the radial and tangential directions, where radial means coming out from the center of the tree or perpendicular to the growth rings, and tangential being parallel to the growth rings.

Test data included the diameter of the pegs for two orientations (e.g. radial and tangential) at the middle and both ends of the peg, the specific gravity of the material, the slope of the grain, and the number of rings per inch. For the dowel bearing tests, the specific gravity, the moisture content, and the number of rings per inch for the base material were also determined. Any defects in the materials such as knots or splits were noted.

For all precise measurements such as peg diameters or specific gravity sample measurements, calipers that were capable of measurements accurate to $1/128^{th}$ of an inch were used.

In all tests, the yield point was determined by a 5% offset method per ASTM D5652 (ASTM, 1995a). In this method, a plot is made of the load versus deflection for the test. Then, using the slope of the initial portion of the curve, a parallel line is offset by 5% of the

dowel diameter and the intercept of that offset line with the load-deflection curve is defined as the yield value for the test. A typical load-deflection curve for a peg in bending is shown in Figure 4-1. The two points chosen to define the initial slope are highlighted and the yield load is indicated as 511 lb.

Note that if the ultimate load for the test occurs before the intercept point, the ultimate load is used as the yield point.

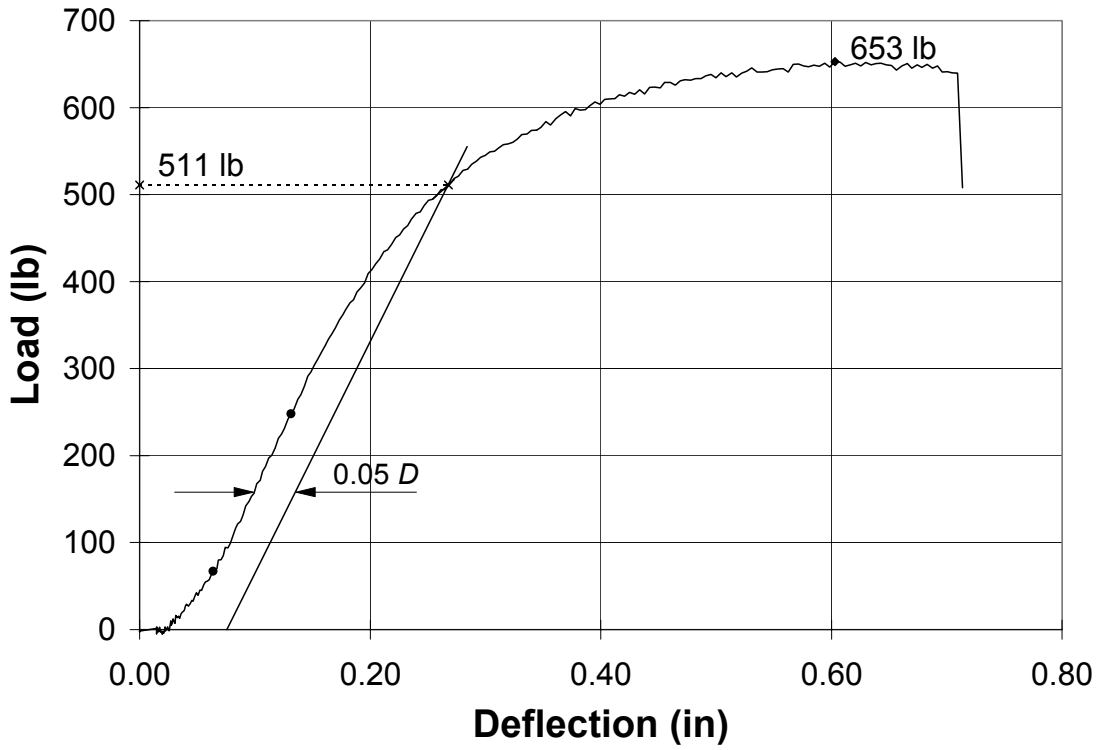


Figure 4-1 Typical Load Deflection Curve (Bending Test, ¾" Dia. Red Oak Peg)

## 4.2 Bending Test Procedure

The test procedure used to determine the bending strength of the peg was based on ASTM D198-94 (ASTM, 1995a). Due to the limited length of the pegs, the shear span to diameter ratio ($a/D$) ranged from 4.2 to 3.1, though ASTM D198-94 recommends a

minimum value of 5 to ensure a flexural failure (see Figure 4-2). Nevertheless, all pegs broke with typical flexural failures within the constant-moment portion of the span.

Red Oak and White Oak pegs in ¾", 1" and 1¼" diameters were tested. Also tested were Locust, Ash, Maple, and Birch pegs of various diameters.

The majority of the bending tests were done in previous research (Schmidt *et al.*, 1996). Although similar methods were used by both persons, it was decided later that additional information should be gathered about the pegs, including the number of growth rings per inch and the slope of the grain.

The testing was accomplished with an Instron model 1332 testing machine and a Strawberry Tree data acquisition system. The pegs were supported on saddles that provided a span of 9" and loaded through additional saddles spaced 2.75" apart (see Figure 4-2).

The pegs were loaded at a stroke rate of 0.05" per minute. This loading rate caused the pegs to reach their ultimate load in about ten minutes as suggested by ASTM D143-94 (ASTM, 1995a).

A typical bending test was conducted in the following manner: A peg was removed from the environmental chamber and labeled for identification. Diameter measurements

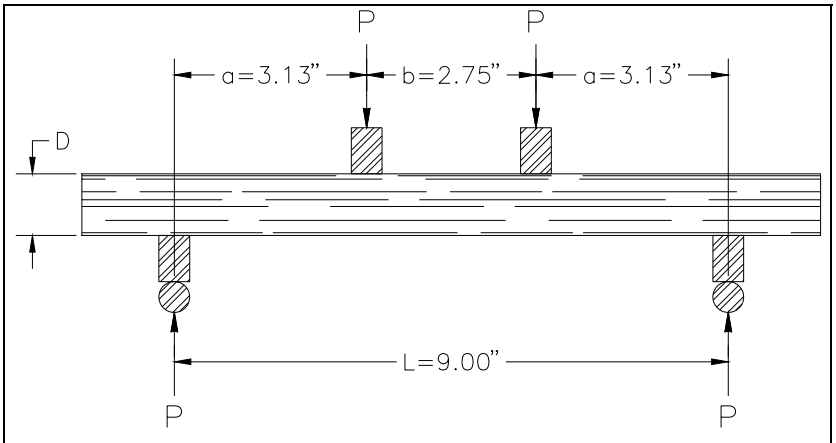


Figure 4-2 Bending Test Setup

were taken for two orientations (e.g. tangential and radial) at both ends and in the middle of the peg. The slope of the grain in the peg was measured with a protractor. Any defects in the peg were noted. The number of rings per inch was counted at one end of the peg. The peg was placed on the test machine in the support saddles and at the proper orientation (tangential or radial). Then a machined alignment guide was placed next to the peg and the upper load saddles were set in place. The alignment guide was removed and the loading head, with load spreader was then lowered into place so that it would barely touch the load saddles. The data acquisition program was started and the loading began.

After the load reached a maximum value, the data acquisition program and test machine were stopped and the characteristics of flexural failure were noted. The peg was then removed and a sample, three inches in length, was cut out of the peg, measured, weighed, and placed in an oven at 212° F for more than 24 hours. The oven-dry peg was removed and weighed again.

The data file obtained from the test was used to create a load versus deflection chart. The 5% offset method was used to determine the yield load, and the average diameter was used to calculate the bending yield stress $F_{yb}$.

### 4.3 Shear Test Procedure

For the shear tests, geometric data was measured on the pegs in the same way as was done for the bending tests. The testing apparatus and procedure were different.

A test fixture was devised to study the combined bending and shear behavior of the pegs. This fixture was used to hold the peg securely and test the peg in shear using varying spans (see Figure 4-3). The shear span is the distance between the faces of the outside reaction block and the middle load block. The purpose of this test fixture is to model the

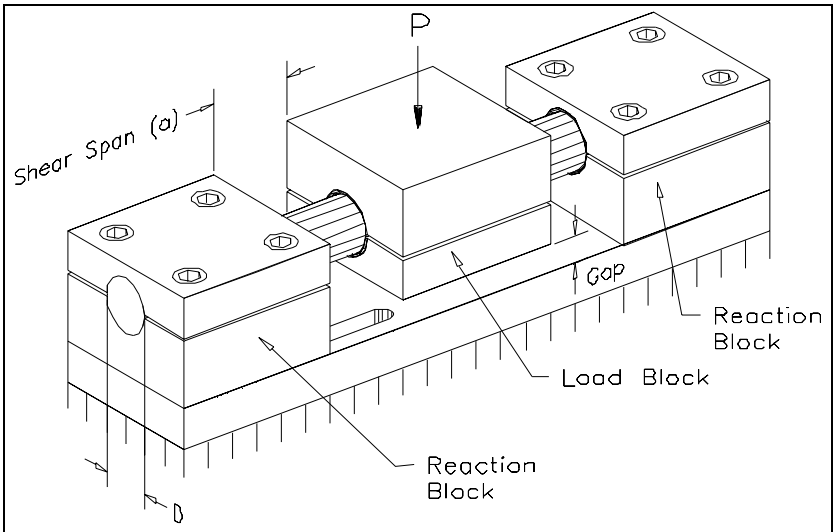


Figure 4-3 Shear Test Fixture

restraint within the mortise and tenon connection and to determine relationships between the shear span and the shear capacity of the peg.

When actual mortise and tenon connections are loaded to failure, the observed shear spans have been in the range of 1*D* or less (where *D* is the peg diameter). These shear spans were observed by removing the peg from the failed connection and measuring the length of the region with fibers disturbed by bending. Hence, it is necessary to understand how the shear spans affect the strength of the peg.

The pegs were tested using shear spans of 1/4*D*, 1/2*D* and 1*D*. The load rate for the shear tests was 0.024 inches per minute in order to conform to ASTM D143-94 (ASTM, 1995a). This load produced a test duration between six and ten minutes in all but a few cases. In these cases, the ultimate load was reached in just under six minutes and was probably due to abnormally weak pegs.

## 4.4 Dowel Bearing Test Procedure

The dowel bearing tests determine the compressive strength of the material surrounding the dowel. For a wood peg the dowel bearing yield strength of the material is

affected by the deformation in the peg as well as in the base material. It is important to test the dowel bearing strengths with pegs of different materials and at different orientations relative to the base material.

This test was based on ASTM D5652-95 (ASTM, 1995b) which stated that the maximum load should be achieved in approximately ten minutes, but in no less time than five minutes.

The base material testing blocks were cut from the 8x8 timbers using a chainsaw and an industrial bandsaw. The minimum dimensions for each block were 4*D* x 4*D* x 2*D*. Two of the blocks were then clamped together (end-to-end) and a hand-powered brace and auger bit were used to drill a hole to create a half-round hole or trough in the edge of each sample (see Figure 4-4). Note, in this figure the peg is loaded in the tangential orientation.

Similar data were taken for the dowel bearing tests as for previously described tests. Pegs were measured in the same way that they were measured for bending and shear tests. The base material was measured for its trough length and the number of rings per inch. When each test was completed, a 3" sample was removed from the peg and a 2"x2"x1"

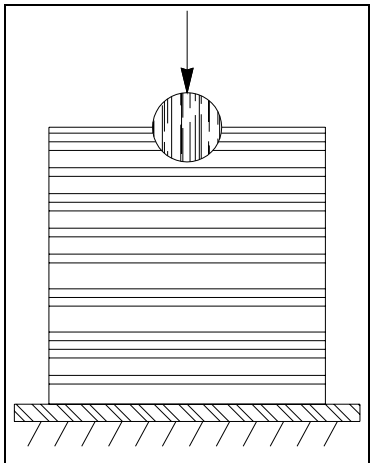

Figure 4-4 Standard Dowel Bearing Test

sample was removed from the base material. These were measured using calipers, weighed, and placed in an oven. After more than 24 hours, the samples were removed and weighed again to obtain the moisture content and the specific gravity.

The test fixture held an oak peg securely to a steel base plate so that the base material could be placed on the peg, under the loading head (see Figure 4-5). The load rate for the dowel bearing tests was 0.02" per minute.

Preliminary tests were performed in previous research (Schmidt *et al.*, 1996) using White Oak pegs and Douglas Fir base material. The peg diameters were ¾", 1" and 1¼", with 18 1" pegs tested and six each of the ¾" and 1¼" pegs. The pegs were tested in the radial and tangential orientations. The blocks were tested in a variety of orientations. These orientations are labeled RL, LR, LT, and TR (see Figure 4-6). The two characters refer to the direction the load is applied and the orientation of the peg. For instance, the LT block orientation has the load applied in the longitudinal direction of the block with the axis of the peg parallel to the tangential axis of the block (see Figure 4-5 and Figure 4-6).

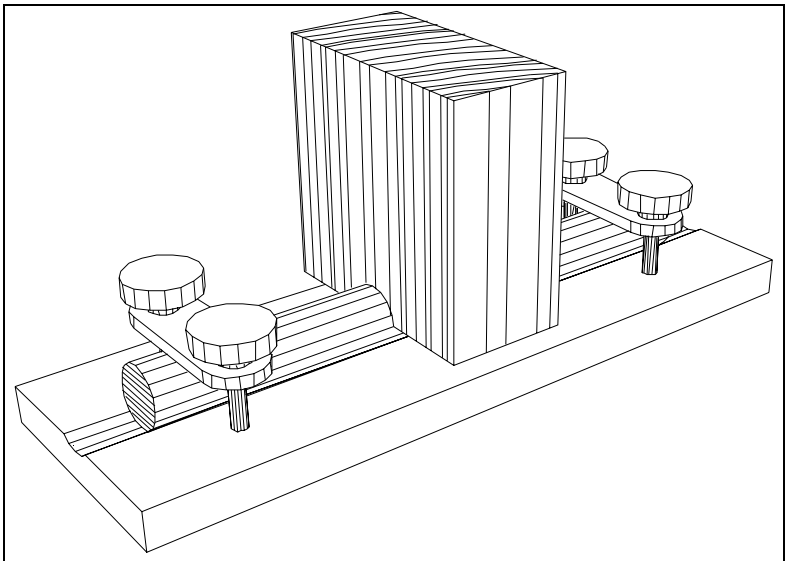

Figure 4-5 Dowel Bearing Test Fixture

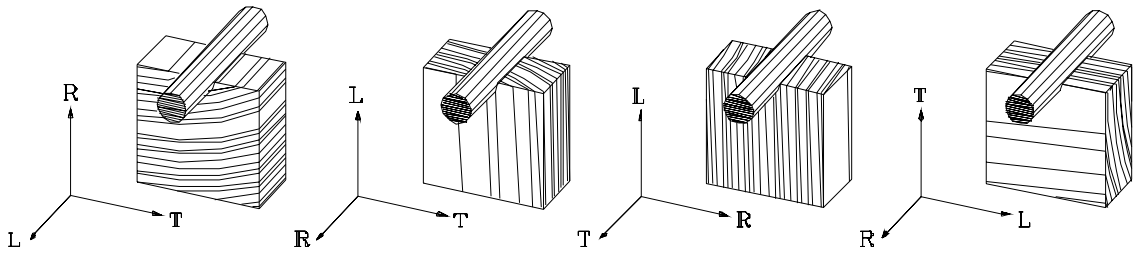


Figure 4-6 Orientation of Preliminary Test Blocks (RL, LR, LT, and TR)

Additional tests were conducted as part of this research using Red Oak pegs in base materials of Eastern White Pine, and Recycled Douglas Fir. To simplify the testing procedures, only 1" pegs were tested and only two orientations of base material were used. The selection of these orientations was based on the orientation of the wood in large mortise and tenon connections. The two orientations for the base materials are RT and LT (see Figure 4-7 and Figure 4-8). Note that for both diagrams the peg is shown loaded in the radial direction.

When the connection is loaded in tension, the fibers around the mortise are loaded perpendicular to the grain and the tenon fibers are loaded parallel to the grain. The RT orientation represents bearing of the peg in the mortise material where the load is applied perpendicular to the grain in the mortise. The LT orientation represents peg bearing in the

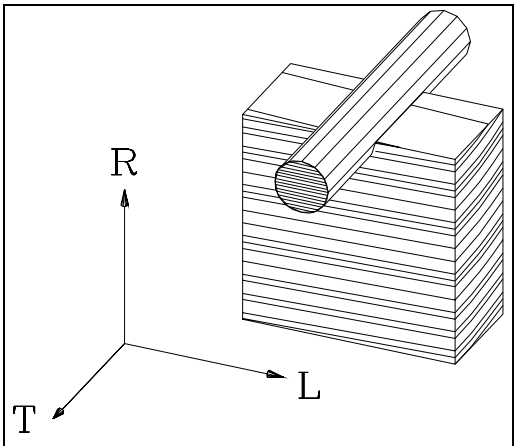


Figure 4-7 RT Block Orientation

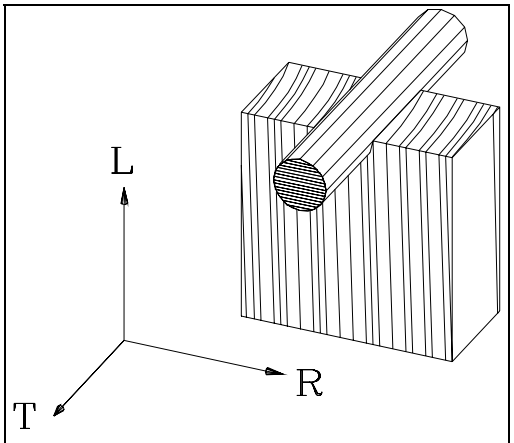


Figure 4-8 LT Block Orientation

tenon material where the load is applied parallel to the grain in the tenon. Tension loading of the mortise and tenon joint is assumed. These orientations were chosen based on the typical grain patterns in the mortise and tenon (see Figure 4-9).

The results of the tests give dowel bearing strengths for a variety of base materials in the perpendicular and parallel directions. These dowel bearing strengths can then be used directly in the yield model equations.

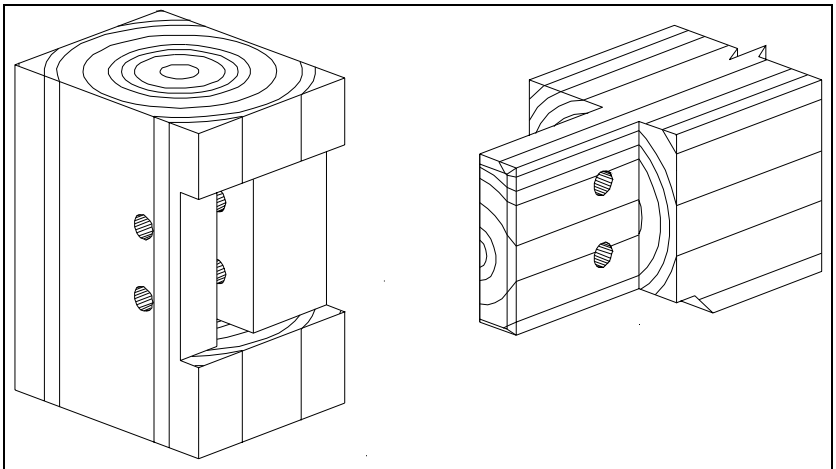

Figure 4-9 Mortise and Tenon Grain Patterns

## 4.5 Full-size Joint Test Procedures

Full-size joints were tested using a steel test frame (see Figure 4-10), an Enerpac RCH 123 hydraulic ram, hand-operated hydraulic pump, and Labview data acquisition software. A pressure transducer was used to acquire hydraulic pressure data and two linear potentiometers were used to average the deflection between the mortise and tenon members at the joint.

The main purpose of the full-size tests was to determine a shear yield criteria. To do this, the connection needed to fail in the peg. The resulting yield stress in the pegs was compared to the yield stresses obtained from the shear tests to obtain an approximate shear span in the full-size connections. A secondary purpose of the full-size tests was to establish minimum end and edge distances in the tenon and mortise material, respectively.

The construction of the joints was simplified by using 2x6 Douglas Fir dimension lumber (see Figure 4-11 and Figure 4-11). One 2x6 was used for the tenon, and two 2x6's were used to represent the mortised member, with all pieces coming from the same 12'-2x6 member. Six full-size joints were tested and a variety of peg configurations were used. Members that contained the pith were avoided.

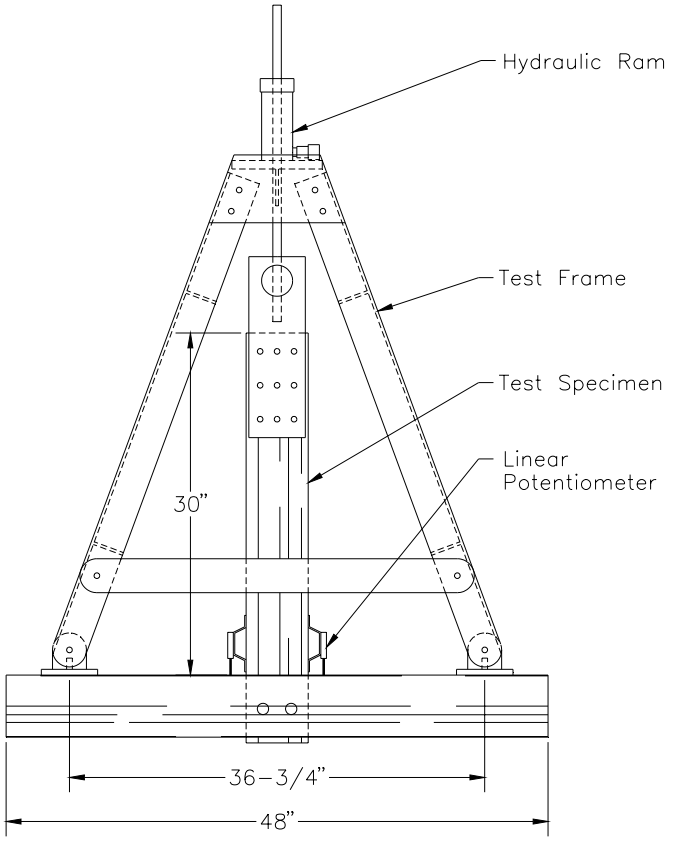


Figure 4-10 Full-size Joint Test Apparatus

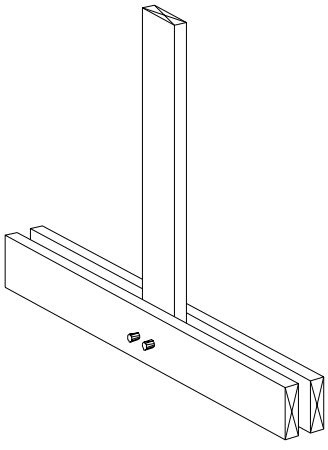

Figure 4-11 Full-size Test Specimen

To keep the stroke rate constant during testing, a chart was displayed on the computer which compared the actual rate of deflection to an ideal rate. It was then up to the operator to keep the rate of deflection the same as the ideal rate. The stroke rate of the piston was approximately 0.02" per minute. This caused the connection to yield in under ten minutes.

After each test was complete, the joint was taken apart by carefully pulling the members apart or by splitting the wood of the tenon and mortise. The peg and holes were then inspected to determine the cause of failure.

To induce shear failures to occur in the pegs, ¾" Red Oak pegs were used and the end and edge distances were adjusted until other failures no longer occurred.

# 5. Test Results

## 5.1 Introduction

The following sections contain the results of the experimental tests. The factors that affect the material properties are also explained. For almost every load type tested, the specific gravity or density of the material affected the yield strength. As the specific gravity increased, the material's yield strength increased.

The mean yield strength for each series of tests is presented along with other statistical data, such as the standard deviation and the 5% exclusion value. The 5% exclusion value is the strength that 95% of the tests can exceed. Therefore, only 5% of the tests will have strength values lower than this number. This assumes a normal distribution and a 75% confidence level (see Figure 5-1). The 5% exclusion values were calculated using ASTM D2915-94 (ASTM, 1995b) and were determined as $F_{.05} = \overline{F} - K\sigma$, where $\overline{F}$ is the mean value, $\sigma$ is the standard deviation, and $K$ is a factor that accounts for the confidence level, the number of tests, and the percent exclusion.

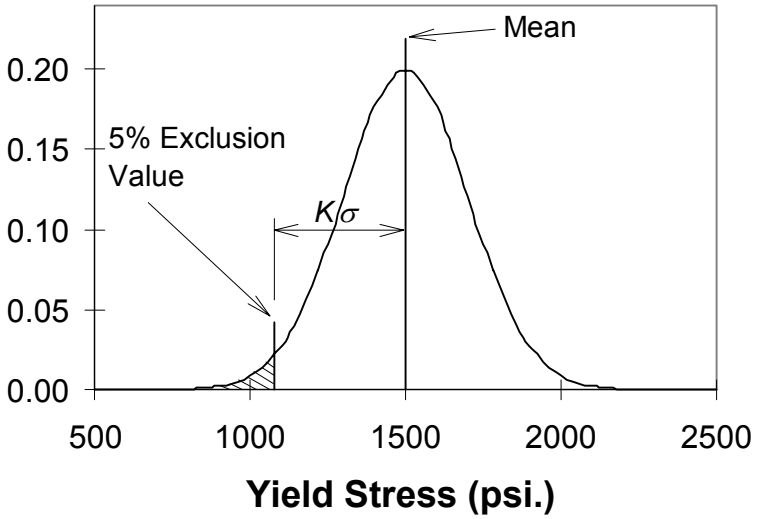


Figure 5-1 Normal Distribution

The mean and 5% exclusion values are important to the designer. The mean values can be used to understand at what load the average connection should actually fail, however, the 5% exclusion values are used as a safe limit of yield stress for limit states design. The 5% exclusion values are later modified with factors of safety to result in values useful for allowable stress design.

## 5.2 Bending Test Results

The major factor affecting the bending strength of hardwood pegs is the specific gravity of the material. As the peg increases in density, the bending strength tends to increase.

A correlation function was used to analyze the data to determine how the specific gravity and the moisture content in the pegs affected the yield strength (see Table 5-1). This correlation function shows when a relationship exists between two sets of data. For instance, a positive correlation coefficient shows that as one set of data increases, the other set of data tends to increase. A negative correlation coefficient would mean that as one set of data increases, the other set decreases. This correlation function is linear and it ranges from 1.0 to -1.0, with 1.0 being a perfect linear correlation of the data.

The results shown in Table 5-1 summarize all of the bending tests that had specific gravity and moisture content data. A total of 136 bending tests were accomplished by two researchers, of which 75 had specific gravity and moisture content information. This information is missing from the other tests because they were from an earlier series of tests, used for preliminary strength information. As in the case of the 1" Red and White Oak bending tests, only two tests in each set had specific gravity and moisture content data. That is why a perfect linear correlation coefficient exists for these tests. For the clear majority of the tests, a significant positive correlation coefficient exists between the yield stress and the

Table 5-1 Bending Test Correlation Coefficients

| Material | Dia. | Yield Stress vs. Specific Gravity | Yield Stress vs. Moisture Content |
|---|---|---|---|
| Red Oak | 3/4" | 0.912 | -0.755 |
| Red Oak | 1" | 1.000 | 1.000 |
| Red Oak | 1-1/4" | 0.549 | -0.113 |
| White Oak | 3/4" | -0.158 | 0.538 |
| White Oak | 1" | 1.000 | 1.000 |
| White Oak | 1-1/4" | 0.439 | -0.625 |
| Locust | 3/4" | 0.811 | 0.475 |
| Locust | 1" | 0.983 | -0.998 |
| Ash | 3/4" | 0.374 | 0.049 |
| Ash | 1" | 0.725 | 0.939 |
| Maple | 3/4" | -0.107 | -0.731 |
| Birch | 1" | 0.013 | -0.220 |

specific gravity. This shows that as the specific gravity increases, the yield strength tends to increase. Due to the variability of the correlation coefficients for the moisture content, no clear relationship can be determined for how the moisture content affects the yield strength of the pegs.

Twenty bending tests were conducted by this researcher on ¾" diameter pegs from four different materials. The materials were Red Oak, White Oak, Maple and Ash. For these pegs, the number of rings per inch and the slope of the grain were noted. As can be seen from the correlation data in Table 5-2 a correlation does exist between the moisture content and the bending yield strength. As the moisture content decreases, the yield strength increases. No clear correlation can be determined between the slope of the grain and the yield strength from the correlation data, however, sloping grain will cause early yielding when

Table 5-2 Additional Correlation Coefficients

| Material | Yield Stress vs. Rings per Inch | Yield Stress vs. Slope of Grain |
|---|---|---|
| Red Oak | -0.370 | -0.750 |
| White Oak | -0.939 | 0.038 |
| Maple | -0.697 | -0.296 |
| Ash | -0.466 | -0.165 |

the peg is loaded in the radial direction. In this orientation, the peg is allowed to split along the growth rings.

A negative correlation did exist between the peg diameter and the average yield strength of the Red Oak and White Oak pegs as can be seen in Table 5-3. This shows that as the peg diameter increased, the bending strength tended to decrease.

The bending yield strength results in Table 5-4 are separated into groups based on the material, the peg diameter and the peg orientation. These results show that for Red Oak and White Oak, the bending strength is typically higher in the radial direction. The data also shows that in order of decreasing strength, the materials are as follows: Maple, Locust, Birch, Ash, Red Oak, and White Oak.

In Table 5-5, the bending yield strengths are summarized for each material and peg diameter, and the 5% exclusion values are shown for the material and diameter.

The data shows, in many cases, a wide discrepancy between the average yield stress and the 5% exclusion value. This is usually because the standard deviation is high and/or the number of tests conducted is low. Data for individual pegs can be found in the appendix.

A possible way to ensure quality pegs would be to create a standard to limit the specific gravity of the wood used in pegs (see Figure 5-2). This figure shows how the specific gravity for the ¾" Red Oak pegs affects the bending yield strength. Such a standard was developed by M.H. Kessel (Peavy and Schmidt, 1996). Kessel recommends a minimum

Table 5-3 Correlation Between Peg Dia. and Bending Strength

| | Correlation |
|---|---|
| Red Oak | -0.748 |
| White Oak | -0.117 |

Table 5-4 Bending Yield Strength Results

| Material | Peg Dia. | Orient-ation | No. of Tests | Avg. Yield Stress (psi.) | Standard Deviation (psi.) | COV |
|---|---|---|---|---|---|---|
| Red Oak | 3/4" | R | 10 | 18,921 | 2,941 | 0.16 |
| | | T | 8 | 15,193 | 4,872 | 0.32 |
| Red Oak | 1" | R | 5 | 12,127 | 1,347 | 0.11 |
| | | T | 5 | 13,074 | 2,362 | 0.18 |
| Red Oak | 1-1/4" | R | 5 | 15,062 | 2,184 | 0.14 |
| | | T | 4 | 11,750 | 1,538 | 0.13 |
| Red Oak Combined | | | 37 | 15,110 | 3,928 | 0.26 |
| White Oak | 3/4" | R | 8 | 14,130 | 4,379 | 0.31 |
| | | T | 9 | 13,639 | 3,932 | 0.29 |
| White Oak | 1" | R | 5 | 12,929 | 3,614 | 0.28 |
| | | T | 5 | 12,295 | 1,360 | 0.11 |
| White Oak | 1-1/4" | R | 5 | 14,585 | 2,319 | 0.16 |
| | | T | 6 | 12,981 | 1,696 | 0.13 |
| Wht. Oak Combined | | | 38 | 13,493 | 3,176 | 0.24 |
| Locust | 3/4" | R | 1 | 16,997 | N/A | N/A |
| | | T | 2 | 21,247 | 733 | 0.03 |
| Locust | 1" | R | 2 | 21,079 | 774 | 0.04 |
| | | T | 2 | 27,098 | 503 | 0.02 |
| Locust Combined | | | 7 | 22,263 | 3,668 | 0.16 |
| Ash | 3/4" | R | 5 | 16,668 | 2,978 | 0.18 |
| | | T | 4 | 18,455 | 1,605 | 0.09 |
| Ash | 1" | R | 2 | 20,804 | 5,173 | 0.25 |
| | | T | 2 | 17,241 | 159 | 0.01 |
| Ash Combined | | | 13 | 17,942 | 2,836 | 0.16 |
| Maple | 3/4" | R | 4 | 25,157 | 6,845 | 0.27 |
| | | T | 5 | 27,097 | 9,586 | 0.35 |
| Maple Combined | | | 9 | 26,235 | 8,035 | 0.31 |
| Birch | 1" | R | 2 | 18,170 | 960 | 0.05 |
| | | T | 2 | 18,221 | 392 | 0.02 |
| Birch Combined | | | 4 | 18,196 | 600 | 0.03 |
| WO Octag | 3/4" | R | 5 | 12,698 | 1,923 | 0.15 |
| | | T | 5 | 13,966 | 2,986 | 0.21 |
| WO Octag | 1" | R | 5 | 19,608 | 1,664 | 0.08 |
| | | T | 5 | 19,607 | 605 | 0.03 |
| WO Octag Combined | | | 20 | 16,470 | 3,727 | 0.23 |

specific gravity of G=0.57 for pegs in critical connections. (A specific gravity of 0.57 corresponds to a unit weight of about 36 pcf).

Table 5-5 Combined Bending Results

| Material | Peg Dia. | Avg. Yield Stress (psi.) | Standard Deviation (psi.) | 5% Exclusion Value (psi.) |
|---|---|---|---|---|
| Red Oak | 3/4" | 17,264 | 4,241 | 8,986 |
| Red Oak | 1" | 12,601 | 1,881 | 8,644 |
| Red Oak | 1-1/4" | 13,590 | 2,514 | 8,205 |
| Red Oak Combined | | 15,110 | 3,928 | 7,871 |
| White Oak | 3/4" | 13,870 | 4,023 | 5,969 |
| White Oak | 1" | 12,612 | 2,596 | 7,151 |
| White Oak | 1-1/4" | 13,710 | 2,071 | 9,414 |
| Wht. Oak Combined | | 13,493 | 3,176 | 7,649 |
| Locust | 3/4" | 19,830 | 2,507 | 11,927 |
| Locust | 1" | 24,088 | 3,515 | 14,663 |
| Locust Combined | | 22,263 | 3,668 | 14,006 |
| Ash | 3/4" | 17,463 | 2,507 | 12,092 |
| Ash | 1" | 19,022 | 3,628 | 9,296 |
| Ash Combined | | 17,942 | 2,836 | 12,716 |
| Maple | 3/4" | 26,235 | 8,035 | 9,025 |
| Birch | 1" | 18,196 | 600 | 16,588 |
| WO Octag | 3/4" | 13,332 | 2,460 | 8,156 |
| WO Octag | 1" | 19,608 | 1,181 | 17,124 |
| WO Octag Combined | | 16,470 | 3,727 | 9,269 |

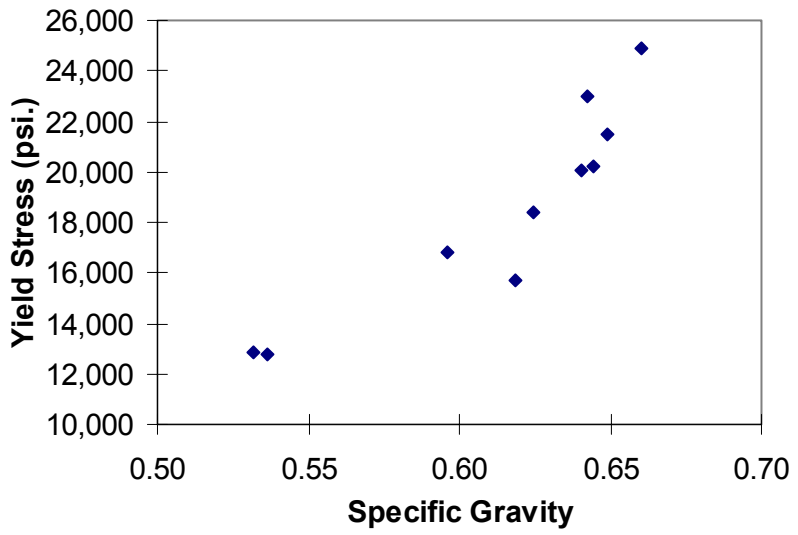


Figure 5-2 Relationship Between Specific Gravity and Bending Yield Stress

## 5.3 Shear Test Results

181 shear tests were conducted for this project, using Red Oak and White Oak pegs of ¾", 1", and 1¼" diameters at shear spans of 1/4D, 1/2D, and 1D. For each of the pegs, data was gathered for specific gravity, moisture content, the number of rings per inch, and the slope of the grain.

The major factor affecting the shear yield stress at a given shear span is the specific gravity of the peg. This can be seen in the correlation data from all of the series of tests (see Table 5-6). Also, there is a minor relationship between the moisture content in the pegs and the shear yield strengths as can be seen by the typically negative correlation coefficients. This means that as the moisture content decreases, the yield strength tends to increase.

Primarily for Red Oak, and to a lesser extent for White Oak, the number of rings per inch also seemed to be correlated to the shear yield strength of the pegs. This could be caused by a change in specific gravity as the number of growth rings per inch changed. To verify this assumption, plots were made to compare the specific gravity and the number of rings per inch, using data from all tests (bending, bearing, and shear). The plots included data from the Red Oak pegs tested (129) and all the White Oak pegs tested (89) that had data for specific gravity and growth rings per inch (see Figure 5-3 and Figure 5-4). As the growth rings got closer together, the specific gravity tended to decrease.

Table 5-6 Correlation Data for Shear Tests

| 3/4" Red Oak Pegs | Correlation | | |
|---|---|---|---|
| | 1/4D | 1/2D | 1D |
| Yield Stress vs. Specific Gravity | 0.903 | 0.864 | 0.866 |
| Yield Stress vs. Moisture Content | 0.153 | 0.014 | 0.545 |
| Yield Stress vs. Rings per Inch | -0.623 | -0.255 | -0.448 |
| Yield Stress vs. Grain Slope | -0.273 | 0.206 | -0.388 |
| | | | |
| 1" Red Oak Pegs | Correlation | | |
| | 1/4D | 1/2D | 1D |
| Yield Stress vs. Specific Gravity | 0.706 | 0.685 | 0.964 |
| Yield Stress vs. Moisture Content | 0.102 | 0.449 | -0.449 |
| Yield Stress vs. Rings per Inch | -0.760 | -0.106 | -0.505 |
| Yield Stress vs. Grain Slope | -0.373 | 0.146 | 0.111 |
| | | | |
| 1 1/4" Red Oak Pegs | Correlation | | |
| | 1/4D | 1/2D | 1D |
| Yield Stress vs. Specific Gravity | 0.878 | 0.482 | 0.589 |
| Yield Stress vs. Moisture Content | 0.044 | -0.399 | -0.109 |
| Yield Stress vs. Rings per Inch | -0.585 | -0.384 | -0.633 |
| Yield Stress vs. Grain Slope | -0.235 | 0.179 | -0.163 |
| | | | |
| 3/4" White Oak Pegs | Correlation | | |
| | 1/4D | 1/2D | 1D |
| Yield Stress vs. Specific Gravity | 0.516 | 0.672 | 0.722 |
| Yield Stress vs. Moisture Content | 0.346 | -0.324 | -0.455 |
| Yield Stress vs. Rings per Inch | -0.278 | -0.349 | 0.124 |
| Yield Stress vs. Grain Slope | 0.065 | 0.526 | -0.399 |
| | | | |
| 1" White Oak Pegs | Correlation | | |
| | 1/4D | 1/2D | 1D |
| Yield Stress vs. Specific Gravity | 0.797 | 0.208 | 0.856 |
| Yield Stress vs. Moisture Content | 0.630 | -0.303 | 0.458 |
| Yield Stress vs. Rings per Inch | -0.115 | -0.132 | -0.487 |
| Yield Stress vs. Grain Slope | 0.070 | 0.296 | -0.181 |
| | | | |
| 1 1/4" White Oak Pegs | Correlation | | |
| | 1/4D | 1/2D | 1D |
| Yield Stress vs. Specific Gravity | 0.784 | 0.919 | 0.626 |
| Yield Stress vs. Moisture Content | -0.306 | -0.370 | -0.012 |
| Yield Stress vs. Rings per Inch | 0.010 | -0.352 | -0.071 |
| Yield Stress vs. Grain Slope | -0.118 | 0.242 | -0.083 |

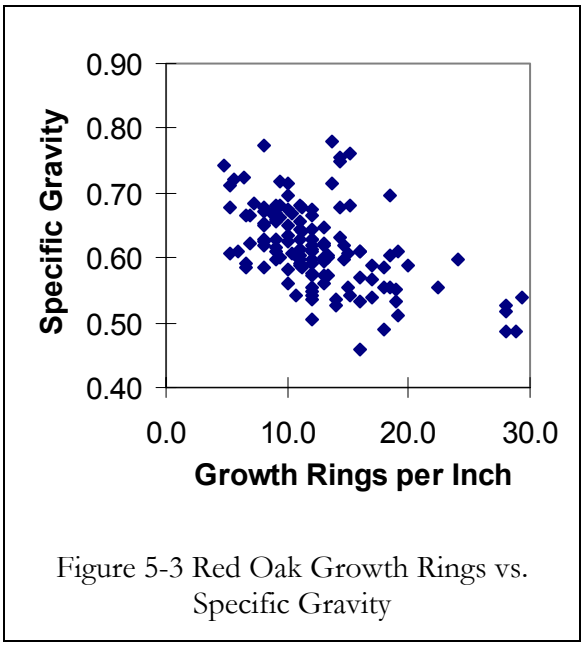


Figure 5-3 Red Oak Growth Rings vs. Specific Gravity

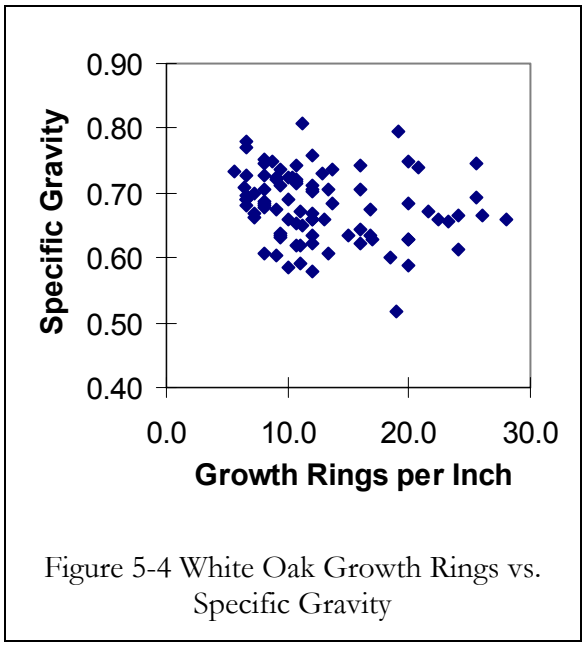


Figure 5-4 White Oak Growth Rings vs. Specific Gravity

A negative correlation did exist between the peg diameter and the yield strength as can be seen in Table 5-7. This shows that as the peg diameter increased, the average yield strengths tended to decrease.

The average shear capacity of the peg decreased as the shear spans increased. This can be seen in the average values of Table 5-8 for each of the peg diameters and materials tested. For the White Oak pegs, the yield strengths tended to be higher when the peg was loaded in the radial direction, however, the loading orientation made little difference for the Red Oak pegs. On average, the shear yield strengths for White Oak were 13% higher than for Red Oak.

From the data in Table 5-8, it can not be concluded that a strong relationship exists between the peg orientation and the yield strength.

Table 5-7 Correlation Between Peg Dia. and Yield Stress

| | Correlation | | |
|---|---|---|---|
| | 1/4D | 1/2D | 1D |
| RO - Diameter vs. Yield Stress | -0.423 | -0.518 | -0.870 |
| WO - Diameter vs. Yield Stress | -0.602 | -0.608 | -0.526 |

Table 5-8 Shear Results Summary

| Material | Dia. | Orient-ation | 1/4 D Shear Spans | | | 1/2 D Shear Spans | | | 1 D Shear Spans | | |
|---|---|---|---|---|---|---|---|---|---|---|---|
| | | | No. of Tests | Avg. Yield Stress (psi.) | Std. Dev. (psi.) | No. of Tests | Avg. Yield Stress (psi.) | Std. Dev. (psi.) | No. of Tests | Avg. Yield Stress (psi.) | Std. Dev. (psi.) |
| Red Oak | 3/4" | R | 5 | 1,950 | 284 | 5 | 1,706 | 209 | 5 | 1,614 | 261 |
| | | T | 5 | 1,964 | 228 | 5 | 1,776 | 191 | 5 | 1,502 | 140 |
| Red Oak | 1" | R | 5 | 1,956 | 186 | 5 | 1,783 | 126 | 5 | 1,465 | 222 |
| | | T | 5 | 2,168 | 330 | 5 | 2,078 | 159 | 5 | 1,644 | 109 |
| Red Oak | 1-1/4" | R | 5 | 1,928 | 159 | 5 | 1,688 | 340 | 5 | 1,205 | 159 |
| | | T | 5 | 1,832 | 310 | 5 | 1,387 | 82 | 5 | 1,156 | 157 |
| Red Oak Combined | | | 30 | 1,966 | 255 | 30 | 1,736 | 276 | 30 | 1,431 | 253 |
| Wht. Oak | 3/4" | R | 5 | 2,299 | 275 | 5 | 2,045 | 167 | 5 | 1,708 | 299 |
| | | T | 5 | 2,233 | 176 | 5 | 1,906 | 191 | 5 | 1,525 | 197 |
| Wht. Oak | 1" | R | 5 | 2,433 | 348 | 5 | 2,033 | 83 | 5 | 1,743 | 275 |
| | | T | 6 | 2,337 | 225 | 5 | 2,028 | 221 | 5 | 1,593 | 187 |
| Wht. Oak | 1-1/4" | R | 5 | 2,146 | 99 | 5 | 2,015 | 158 | 5 | 1,688 | 45 |
| | | T | 5 | 2,033 | 168 | 5 | 1,762 | 189 | 5 | 1,431 | 132 |
| Wht. Oak Combined | | | 31 | 2,250 | 247 | 30 | 1,965 | 189 | 30 | 1,615 | 220 |

The summaries for each diameter and the 5% exclusion values are shown in Table 5-9.

The average and 5% exclusion values for each shear span are important because plots can be made that show how the values change with the shear span (*a*) (see Figure 5-5). After using full-sized tests to cause peg shear failures, the resulting shear stresses can be inserted into the trend function for the proper material and diameter and a corresponding shear span-to-depth ratio (*a*/*D*) can be obtained. From this non-dimensional value the actual shear span can be calculated. The shear span-to-depth ratio obtained can then be used

Table 5-9 Shear Test Results Summary

| Material | Diameter | 1/4 D Shear Spans | | | 1/2 D Shear Spans | | | 1 D Shear Spans | | |
|---|---|---|---|---|---|---|---|---|---|---|
| | | Avg. Yield Stress (psi.) | Std. Dev. (psi.) | 5% Exclusion Value (psi.) | Avg. Yield Stress (psi.) | Std. Dev. (psi.) | 5% Exclusion Value (psi.) | Avg. Yield Stress (psi.) | Std. Dev. (psi.) | 5% Exclusion Value (psi.) |
| Red Oak | 3/4" | 1,957 | 243 | 1,446 | 1,741 | 192 | 1,336 | 1,558 | 206 | 1,124 |
| Red Oak | 1" | 2,062 | 276 | 1,482 | 1,930 | 206 | 1,497 | 1,555 | 190 | 1,155 |
| Red Oak | 1-1/4" | 1,880 | 238 | 1,379 | 1,537 | 282 | 944 | 1,180 | 151 | 862 |
| Red Oak Combined | | 1,966 | 255 | 1,489 | 1,736 | 276 | 1,221 | 1,431 | 253 | 958 |
| Wht. Oak | 3/4" | 2,266 | 221 | 1,802 | 1,976 | 185 | 1,587 | 1,617 | 258 | 1,075 |
| Wht. Oak | 1" | 2,380 | 276 | 1,808 | 2,031 | 157 | 1,700 | 1,668 | 236 | 1,173 |
| Wht. Oak | 1-1/4" | 2,090 | 143 | 1,789 | 1,888 | 211 | 1,443 | 1,559 | 164 | 1,214 |
| Wht. Oak Combined | | 2,250 | 247 | 1,789 | 1,965 | 189 | 1,612 | 1,615 | 220 | 1,204 |

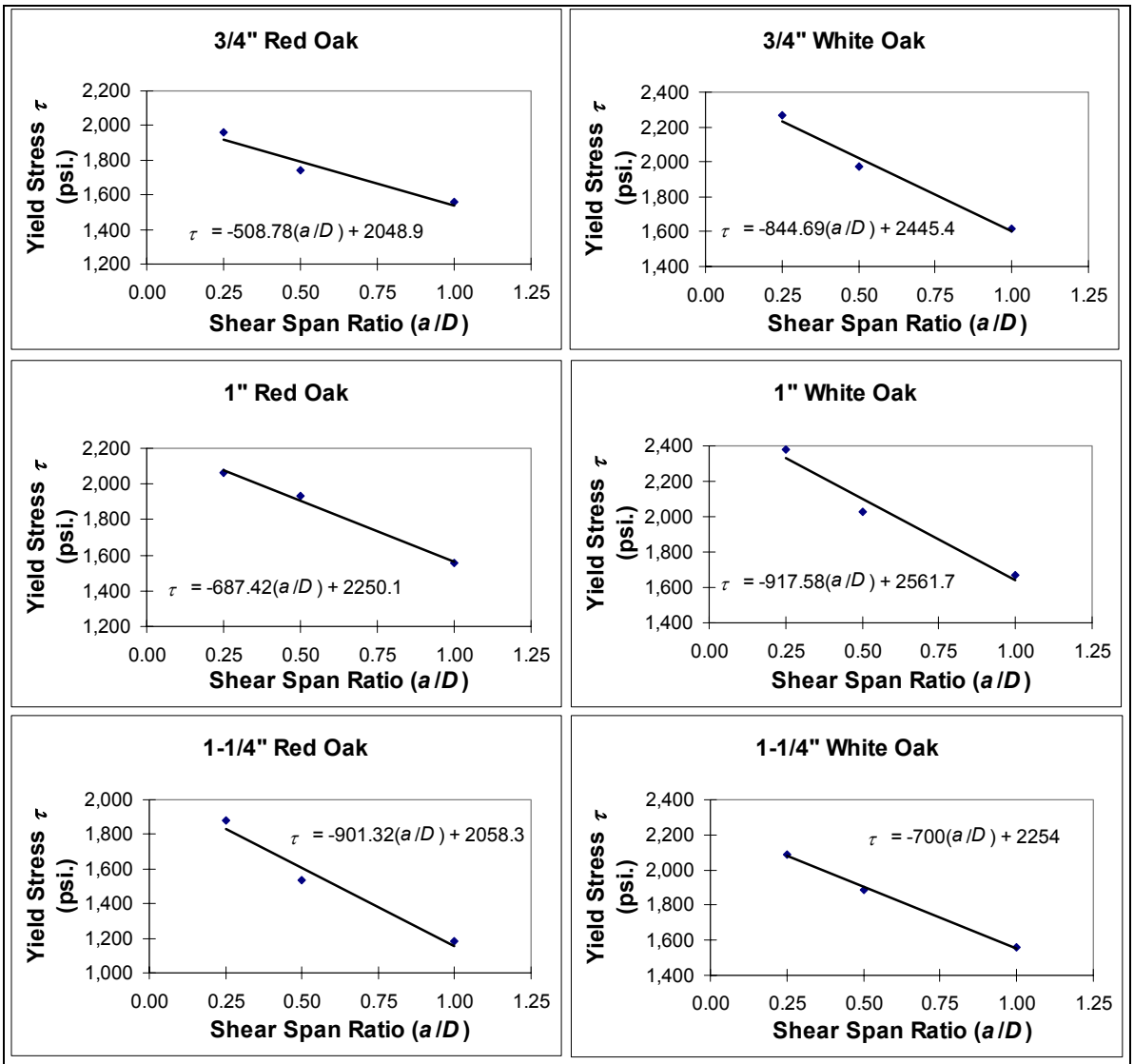


Figure 5-5 Average Shear Yield Stresses

in the trend function for the proper material combination and diameter of the 5% exclusion values, and a corresponding 5% exclusion value will be obtained.

The combined average moisture content and specific gravity information for the shear tests is listed in Table 5-10.

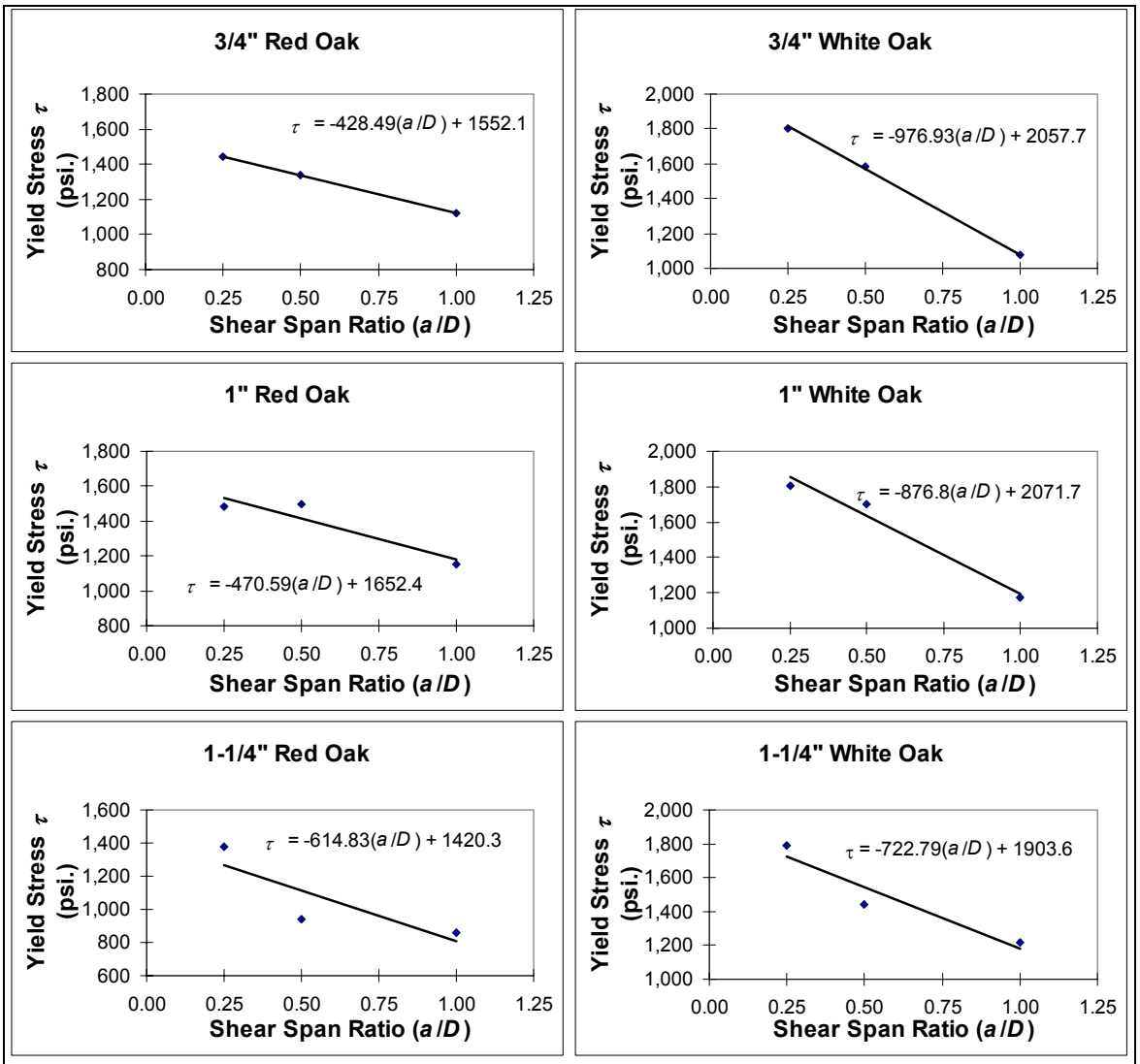


Figure 5-6 5% Exclusion Values From Shear Tests

Table 5-10 Average Values of Moisture Content and Specific Gravity

| | Average Moisture Content | Average Specific Gravity |
|---|---|---|
| Red Oak 3/4" | 10.3% | 0.60 |
| Red Oak 1" | 8.7% | 0.61 |
| Red Oak 1-1/4" | 14.9% | 0.65 |
| White Oak 3/4" | 11.8% | 0.68 |
| White Oak 1" | 10.2% | 0.67 |
| White Oak 1-1/4" | 13.5% | 0.69 |

## 5.4 Dowel Bearing Test Results

The dowel bearing strengths are shown in Table 5-12 for Eastern White Pine and Recycled Douglas Fir, using 1" Red Oak pegs. Logically, the LT orientation (parallel to grain) has higher bearing strengths than the RT orientation (perpendicular to grain) for both Eastern White Pine and Recycled Douglas Fir. It was interesting to note that, when either the Eastern White Pine or the Recycled Douglas Fir were loaded in the RT orientation crushing was visible in the base material; whereas, when the base material was loaded in the LT orientation, crushing was visible in the peg.

The results of preliminary tests done by another researcher can be seen in Table 5-11.

Table 5-11 Preliminary Dowel Bearing Strength Results (WO Pegs in Doug. Fir)

| Peg Orientation | RL Block Orientation | | | LR Block Orientation | | |
|---|---|---|---|---|---|---|
| | Number of Tests | Average Value | 5% Exclusion Value | Number of Tests | Average Value | 5% Exclusion Value |
| Radial | 9 | 734 psi. | 508 psi. | 5 | 2,494 psi. | 1,832 psi. |
| Tangential | 3 | 924 psi. | 717 psi. | 1 | 2,000 psi. | N/A |

| Peg Orientation | LT Block Orientation | | | TR Block Orientation | | |
|---|---|---|---|---|---|---|
| | Number of Tests | Average Value | 5% Exclusion Value | Number of Tests | Average Value | 5% Exclusion Value |
| Radial | 4 | 2,784 psi. | 1,970 psi. | 3 | 1,578 psi. | 971 psi. |
| Tangential | 2 | 1763 psi. | N/A | 3 | 1,411 psi. | 1,199 psi. |

Table 5-12 Dowel Bearing Test Summary

| Base Material | Base Orient. | Peg Material | Peg Orient. | No. of Tests | Average Stiffness (lb/in) | Avg. Yield Stress (psi.) | Std. Dev. (psi.) | COV | 5% Exclusion Value (psi.) |
|---|---|---|---|---|---|---|---|---|---|
| RDF | LT | RO | R | 5 | 68,426 | 2,021 | 344 | 0.17 | |
| RDF | LT | RO | T | 5 | 59,538 | 2,118 | 206 | 0.10 | |
| RDF | LT | RO | | 10 | 63,982 | 2,070 | 272 | 0.13 | 1,497 |
| | | | | | | | | | |
| RDF | RT | RO | R | 5 | 35,102 | 1,728 | 174 | 0.10 | 1,300 |
| EWP | LT | RO | R | 5 | 63,200 | 2,285 | 115 | 0.05 | |
| EWP | LT | RO | T | 5 | 61,039 | 2,268 | 199 | 0.09 | |
| EWP | LT | RO | | 10 | 62,120 | 2,277 | 153 | 0.07 | 1,954 |
| EWP | RT | RO | R | 5 | 24,776 | 1,438 | 166 | 0.12 | |
| EWP | RT | RO | T | 5 | 25,916 | 1,501 | 57 | 0.04 | |
| EWP | RT | RO | | 10 | 24,977 | 1,469 | 122 | 0.08 | 1,213 |

No conclusion can be made from the data available regarding the relationship between the peg orientation and the bearing strength of the material. Also, no clear correlations can be seen between the yield stresses and the material properties (see Table 5-13).

Table 5-13 Dowel Bearing Test Correlation Data

| | RDF-LT | RDF-RT | EWP-LT | EWP-RT |
|---|---|---|---|---|
| Yield Stress vs. Peg Specific Gravity | 0.777 | -0.413 | 0.233 | -0.189 |
| Yield Stress vs. Peg Moisture Content | -0.197 | 0.078 | 0.078 | 0.126 |
| Yield Stress vs. Peg Rings per Inch | -0.666 | 0.099 | -0.522 | -0.078 |
| Yield Stress vs. Peg Grain Slope (deg) | -0.483 | 0.191 | -0.659 | -0.001 |
| Yield Stress vs. Base Specific Gravity | -0.179 | -0.716 | 0.199 | -0.048 |
| Yield Stress vs. Base Moisture Content | -0.171 | 0.221 | 0.607 | 0.028 |
| Yield Stress vs. Base Rings per Inch | -0.527 | -0.742 | -0.185 | -0.586 |

## 5.5 Full-size Test Results

The major purpose of the full-size tests was to determine a relationship between the shear strength of the pegs in the full-size connections and the average shear strengths

obtained from shear tests at various spans. Secondly, initial estimates of minimum end and edge distances were developed to assure peg shear failure.

Table 5-14 shows the initial geometry and results from each individual test. The failure mode is noted. All tests used 2x6 Douglas Fir and two Red Oak pegs. The first test used 1" pegs with end and edge distances of 3*D*. The yield load is not recorded for this test because of setup problems, but the load obtained was much less than desired because of the mortise splitting failure. For this reason the edge distance was increased to 4*D*. The next two tests also used 1" pegs, but the desired shear failure in the pegs was not observed. The second of these failed in a mode similar to Mode $III_s$, but only contained a single hinge. After reviewing the derivation of the Mode $III_s$ equation, it was determined that Mode $III_s$ would not permit this type of failure. Therefore another failure mode is needed pertaining to this scenario (thus the nomenclature Mode $III_s$').

The last three tests used ¾" pegs and end and edge distances of 3*D* and 4*D* respectively, to assure shear failures in the pegs. Only two of these tests were considered valid since the side 2x6's representing the mortised member on the last test spread apart approximately ¼" on each side, thus increasing the shear spans in the pegs and causing an early shear failure. This much spreading of the mortise was considered unlikely in a full-size

Table 5-14 Full-size Test Results

| Peg Diameter (in.) | End Dist. ($l_v$) | Edge Dist. ($l_e$) | Yield Load (lb.) | Failure Type | Shear Stress (psi.) | Equiv. Shear Span |
|---|---|---|---|---|---|---|
| 1.00 | 3*D* | 3*D* | N/A | Mortise Split | N/A | N/A |
| 1.00 | 3*D* | 4*D* | 4843 | Tenon Split | 1,542 | N/A |
| 1.00 | 3*D* | 4*D* | 5563 | Mode $III_s$' | 1,771 | N/A |
| 0.75 | 3*D* | 4*D* | 3285 | Peg Shear | 1,859 | 0.37 |
| 0.75 | 3*D* | 4*D* | 3490 | Peg Shear | 1,975 | 0.15 |
| 0.75 | 3*D* | 4*D* | 2756 | 2x6 Spread | 1,560 | N/A |

connection. Therefore, the shear stresses from the two valid tests were inserted into the trend line from the average shear stresses of the ¾" Red Oak pegs and the approximate shear span was calculated for each. The average of these two shear spans (0.26 *D*) can then be used in the trend line for the 5% exclusion values to calculate the 5% exclusion values.

Assuming that all Oak pegs fail in full-size connections in a similar manner, the resulting 5% exclusion values for Red Oak and White Oak pegs can be seen in Table 5-15. Needless to say, many additional full-size tests are needed to verify this assumption.

Table 5-15 5% Shear Exclusion Value Summary

| Material | Peg Dia. (in.) | Shear Span of Interest | Average Yield Stress (psi.) | 5% Exclusion Value (psi.) |
|---|---|---|---|---|
| Red Oak | 3/4" Dia. | 0.26 | 1,917 | 1,441 |
| Red Oak | 1" Dia. | 0.26 | 2,071 | 1,530 |
| Red Oak | 1-1/4" Dia. | 0.26 | 1,824 | 1,260 |
| Red Oak Combined | | 0.26 | 1,937 | 1,410 |
| White Oak | 3/4" Dia. | 0.26 | 2,226 | 1,804 |
| White Oak | 1" Dia. | 0.26 | 2,323 | 1,844 |
| White Oak | 1-1/4" Dia. | 0.26 | 2,072 | 1,703 |
| White Oak Combined | | 0.26 | 2,207 | 1,783 |

# 6. Overall Connection Strength and Design Recommendations

## 6.1 Application of Factors of Safety

The 5% exclusion values obtained from testing are useful to a designer wanting to do allowable stress design when factors of safety have been applied to them. These allowable stresses should be applied to a comprehensive analytical model that includes the NDS double shear yield modes and the other modes applicable to mortise and tenon connections (see Equations 3-34 through 3-39). These modes include the combined bending and shear mode, the relish failure mode, and the mortise splitting mode.

To obtain allowable stress design values for these equations, factors of safety must be applied to the 5% exclusion values for each material property. These factors of safety must account for the variability of loads, load duration, differences in construction practices, and the accuracy of the analysis model. Typical factors of safety from ASTM 5457-93 (ASTM, 1995a) for members subjected to bending, shear, and bearing are 2.54, 2.88, and 2.40, respectively. However, for connections, there is a standard factor of safety of 3.32.

From the results of his full-size connection tests, Kessel suggests that a factor of safety of 3.00 should be applied to the average ultimate load from a series of tests (in which the geometry and materials are kept the same for each series), and a factor of safety of 2.25 should be applied to the minimum ultimate load from the same series of tests. He also suggests that the allowable load for a connection should be the average load achieved for a series of tests at a joint displacement of 0.06" (1.5 mm) (Peavy and Schmidt, 1996). Further work needs to be done in this area to determine appropriate factors of safety.

## 6.2 Current Design Procedures

The designers in the timber-framing industry employ clearly understood principles in the design of beams and columns, but connections in these structures are designed based on traditional practices and the limited applicability of the NDS yield modes.

This method of design is appropriate and acceptable in parts of the country where building officials are familiar with this system of joinery; however, this practice is often regarded as unacceptable in other parts of the country.

## 6.3 Recommendations for Timber-Frame Joinery

The design community should adopt an analytical approach to timber-frame tension joinery design. In this way, a standard method can be used by all designers, thus validating the design practice and expanding it to all parts of the nation.

Such a standard design method is far from complete. Once the failure modes are completely understood, there should be much thought given to a desired or preferred failure mode. For instance, would it be better if the connection failed in the mortise material rather than in the tenon? Or would a peg shear failure be better than a bearing failure? Why would a designer choose one over another? Perhaps a bearing failure would dissipate more energy in an earthquake than a peg shear failure would. Perhaps a peg shear failure would allow a simple repair to the connection if it was ever overloaded. As another option entirely, perhaps the connections should be balanced so that all failure modes are equally possible, thus conserving material used in the connection. Whatever the case may be, these and many other questions need to be answered before thorough design recommendations can be made. However, some design recommendations can be established based on this work and on the work of others.

The following design recommendations stem from the work of this research project and the tests performed by M. H. Kessel (Peavy and Schmidt, 1996). Based on the full-size tests of this project, in which 2x6 Douglas Fir lumber was used to represent the tenon and mortise material of a connection, some conclusions about the end and edge distances can be obtained (see Figure 6-1). To prevent the tenon from splitting or the relish from pulling out, an end distance ($l_v$) from the center of the peg to the end of the tenon, should be greater than or equal to three times the peg diameter (see Figure 6-2). To prevent the sides of the mortise from splitting, an edge distance ($l_e$) from the center of the peg to the edge of the mortise material, should be greater than or equal to four times the peg diameter.

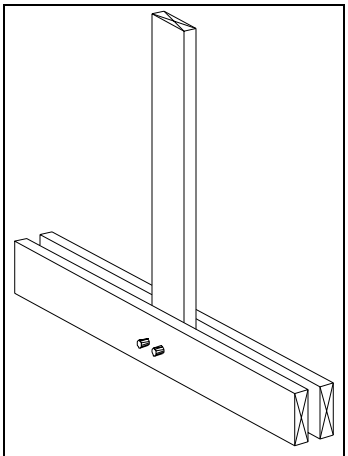

Figure 6-1 Full-size Test Diagram

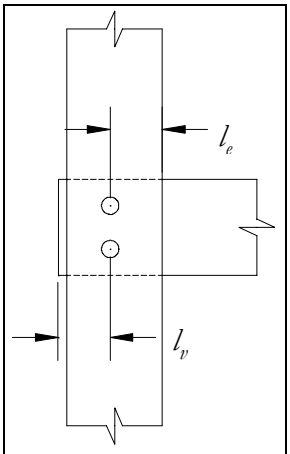


Figure 6-2 End, Edge Distances

These recommendations are appropriate when Oak pegs are used to connect individual softwood members in this fashion. They are likely conservative recommendations for full-size mortise and tenon connections (see Figure 6-3). The sides of the mortise are significantly strengthened by the additional material that surrounds the tenon. The effect this has on the strength of the mortise in tension is unknown. This additional mortise material would also prevent the sides of the mortise from splitting outward, whereas the 2x6's are free to rotate and spread outward. If the tenon is sufficiently surrounded by

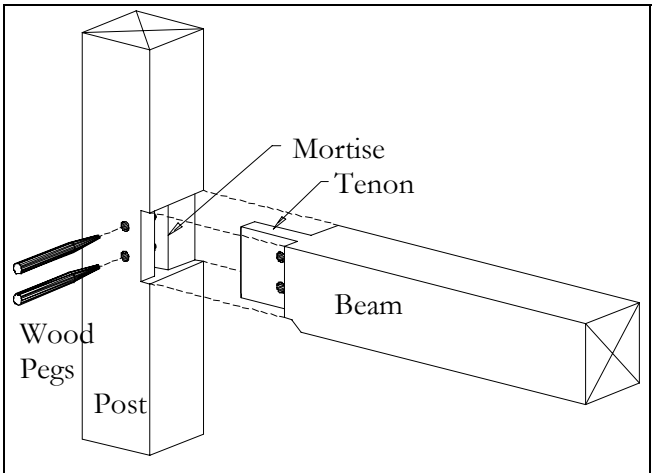


Figure 6-3 Full-size Mortise and Tenon Connection

material, the possibility of tenon splitting is most likely removed. The effect of this surrounding material is unknown.

Of the 120 full-size all-wood connections tested by M. H. Kessel, 60 mortise and tenon failures were summarized and some conclusions can be drawn. These connections were very similar to that in Figure 6-3 and used Oak members that ranged in size from 5.5"x5.5" to 7.9"x7.9" (140mm x 140mm to 200mm x 200mm). The pegs were also made of oak and ranged in diameter from 0.9" to 1.6" (24mm to 40mm). Table 6-1 shows how the types of failure modes are based on the connection geometry (Peavy and Schmidt, 1996). In many cases the connection failed in more than one mode. Some simple conclusions can be drawn from these test results. It is important to note that these conclusions are based on tests using oak timbers and oak pegs. Conclusions based on these tests may not directly correspond to other materials because of differing shear and other strengths.

To prevent mortise failures, a mortise edge distance ($l_e$) of 3.0$D$ or greater is required. To prevent tenon failures, the end distance ($l_v$) must be larger than 2.0$D$, since tenon failures still occurred with the peg failures in Series D. An end distance of 3.0$D$ is a more appropriate value. To balance out the design and create an equal possibility for tenon, mortise, and peg failures, the geometry in Series B should be used.

Figure 6-4 shows initial material parameters, connection geometry, and the results of

Table 6-1 Kessel Results Summary

| Series | End Dist. $l_v$ | Edge Dist. $l_e$ | Tot. No. of Tests | No. of Breaks In: | | |
|---|---|---|---|---|---|---|
| | | | | Tenon | Mortise | Peg |
| A | 2.0$D$ | 2.0$D$ | 15 | 3 | 10 | 9 |
| B | 1.5$D$ | 2.0$D$ | 15 | 7 | 7 | 9 |
| C | 1.5$D$ | 1.5$D$ | 15 | 8 | 11 | 9 |
| D | 2.0$D$ | 3.0$D$ | 15 | 11 | 1 | 15 |

each mode in the general yield model. These calculations are based on a mortise and tenon connection using Eastern White Pine 6x6's (full sawn) and two 1" Red Oak pegs. The calculations show that the peg shear condition will govern, but with the relish failure mode closely behind. They also show that the allowable load in tension on the connection should be 1334 pounds. The equations used in this general yield model are summarized in Figure 6-5.

| Given Information | | | Notes |
|---|---|---|---|
| Peg Diameter | $D$ = | 1.00 in. | |
| No. of Pegs | $n$ = | 2 | |
| Tenon Thickness | $t_m$ = | 2.00 in. | |
| Mortise Side Thickness | $t_s$ = | 2.00 in. | |
| Length from Peg Center To End of Tenon | $l_v$ = | 3.00 in. | |
| Peg Bending Stress | $F_{yb}$ = | 7,871 psi. | RO |
| Peg Shear Stress | $F_{v\perp}$ = | 1,410 psi. | RO |
| Tenon Dowel Bearing Stress | $F_{em}$ = | 1,954 psi. | EWP |
| Mortise Side Dowel Bearing Stress | $F_{es}$ = | 1,213 psi. | EWP |
| Tenon Shear Stress | $F_{vm}$ = | 70 psi. | EWP<br>NDS Allow. |

| Constants | |
|---|---|
| $R_e$ = | 1.611 |
| $k_3$ = | 1.380 |

Calculations

| | | | | |
|---|---|---|---|---|
| Mode $I_m$ | F.S. | 3.32 | $P$ = 2,354 lb. | Main Bearing |
| Mode $I_s$ | F.S. | 3.32 | $P$ = 2,923 lb. | Side Bearing |
| Mode $III_s$ | F.S. | 3.32 | $P$ = 1,800 lb. | |
| Mode IV | F.S. | 3.32 | $P$ = 2,388 lb. | |
| Mode V | F.S. | 3.32 | $P$ = 1,334 lb. | Peg Shear |
| Mode VI | F.S. | 1.00 | $P$ = 1,680 lb. | Relish Failure |
| | | | Max. Ultimate Load 1,334 lb. | |

Figure 6-4 Sample Connection Design Values

$$P_{Im} = nDt_m F_{em}$$

$$P_{Is} = 2nDt_s F_{es}$$

$$P_{IIIs} = \frac{2nk_3 Dt_s F_{em}}{\left(2 + R_e\right)}$$

$$P_{IV} = 2nD^2 \sqrt{\frac{2F_{em}F_{yb}}{3\left(1 + R_e\right)}}$$

$$P_V = 2nF_{v\perp}\left(\pi\frac{D^2}{4}\right)$$

$$P_{VI} = 2nF_{vm}t_m\left(l_v - \frac{D}{2}\right)$$

Where:

$n$ = Number of pegs

$D$ = Peg diameter

$t_m$ = Thickness of tenon (main) member

$t_s$ = Thickness of sides of mortised member

$F_{em}$ = Dowel bearing strength of main member

$F_{es}$ = Dowel bearing strength of mortise sides

$F_{yb}$ = Bending yield strength of peg

$F_{v\perp}$ = Peg shear yield strength

$F_{vm}$ = Shear yield strength of tenon (main) member

$$k_3 = -1 + \sqrt{\frac{2(1+R_e)}{R_e} + \frac{2F_{yb}(2+R_e)D^2}{3F_{em}t_s{}^2}}$$

$$R_e = \frac{F_{em}}{F_{es}}$$

Figure 6-5 Double Shear Yield Equations

# 7. Conclusions and Recommendations for Future Work

## 7.1 Concluding Statements

The existing yield model equations from the NDS are applicable to hardwood pegs used as dowel fasteners in mortise and tenon connections, however additional modes specific to these connections were necessary. One of these additional modes is regarding a peg shear condition. Hardwood pegs can fail in full-size connections under the combined stresses of shear and bending. Therefore this shear mode must take into account these combined effects. Another failure mode describes the shear failure of the material directly behind the peg in the tenon, also known as relish failure. Another type of failure specific to mortise and tenon connections is the mortise splitting failure.

The major findings of this research project are limited by the types of tests and materials used in this project. The material strengths were influenced by the specific gravity of the material. As the specific gravity increased, the yield strengths also increased. The orientation of the peg had a slight effect on the bending yield strengths, but it had little or no effect on the shear or dowel bearing yield strengths. No clear conclusions could be drawn regarding the effect of the moisture content on the material yield strengths.

The drastic failure modes of full-size joints, where the loads suddenly dropped off as deflection was occurring, were the mortise splitting and the peg bending modes. Although no tenon relish failures were witnessed, it is assumed that they would also fall into this category. The peg shear and dowel bearing failures were relatively ductile in that they allowed a significant amount of inelastic deformation before the loads dropped off.

## 7.2 Recommendations for Future Work

Much additional work is necessary. Additional wood species combinations need to be tested for their bending, shear, and dowel bearing strengths to account for other common

materials used in design. Specific tests to determine relish shear strengths must be devised to verify end distances and the possible effect of tenon thickness and peg diameter. The mortise splitting failure must be examined in great detail to determine the effects of the mortise side thicknesses, peg diameter, and the strength of the surrounding mortise material.

Many more full-size static tests of mortise and tenon connections of various materials and geometries are needed to validate the general yield model. These are also necessary to understand how specific yield modes occur and therefore to be able to predict their occurrences. Full-size tests should also be accomplished so that joint stiffnesses can be understood and predicted to a degree of accuracy.

Dynamic tests of full-size connections would result in an understanding of their energy absorption capabilities and their ability to withstand earthquake loads.

The NDS Mode $III_s$ does not seem to apply directly to a specific type of failure in mortise and tenon connections. The failure witnessed is similar to this mode, but contains only one plastic hinge, occurring in the middle of the tenon. By reviewing the derivation of Mode $III_s$, it seems that this type of failure is impossible due to the inability of the surrounding material to firmly hold the peg. Therefore, an additional failure mode, termed Mode $III_s$' herein, should be devised to account for this failure type.

Appropriate factors of safety should also be determined for use with these connections. They should account for the variability in loading, construction practices, and the accuracy of the general yield model.

Also, a full analysis should be made of the acceptable failure modes. It is unclear at this point if one failure mode is more desirable than another. Another possibility is for the connection to be balanced to allow all failure modes to be equally probable.

## Appendix A Derivation of Dowel Rotation Load

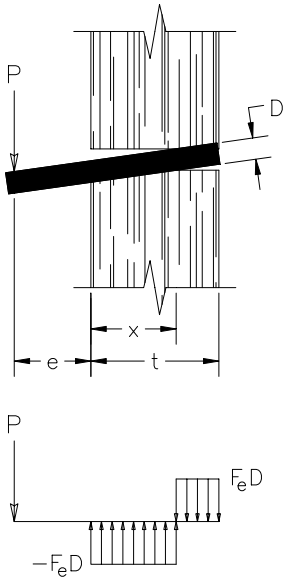


Figure A-1 Dowel Rotation Diagram

Sum forces in the *Y*-direction:

$$P = F_e D(2x - t) \tag{A-1}$$

Sum moments about load *P*:

$$F_e D(t - x)\left(e + x + \frac{t - x}{2}\right) - F_e D(x)\left(e + \frac{x}{2}\right) = 0 \tag{A-2}$$

$$x^2 + 2ex - te - \frac{t^2}{2} = 0 \tag{A-3}$$

Solve Eq. A-3 for *x*:

$$x = \frac{-2e \pm \sqrt{(2e + t)^2 + t^2}}{2} \tag{A-4}$$

Substitute into equation A-1 for *x*:

$$P = \left[\sqrt{(2e + t)^2 + t^2} - (2e + t)\right] D F_e \tag{A-5}$$

## Appendix B Derivation of Dowel Yielding Load

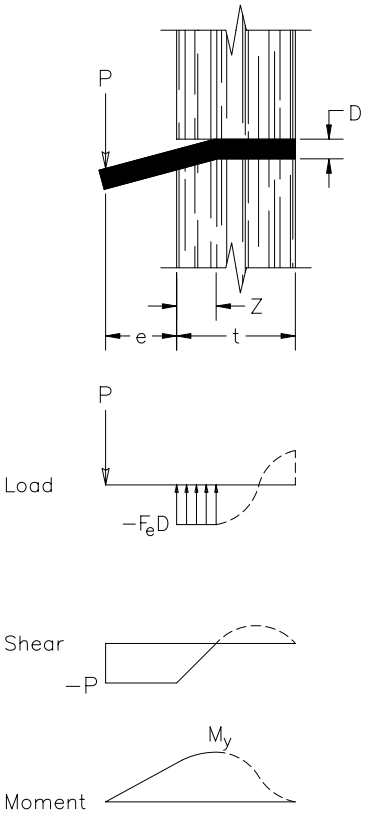


Figure B-1 Dowel Bending Diagrams

From shear and moment diagrams:

$$P = ZF_e D \tag{B-1}$$

Determine moment at plastic hinge location:

$$M_y = P(e+Z) - F_e D(Z)\left(\frac{Z}{2}\right) \tag{B-2}$$

Substitute for *P* Eq. B-1 into Eq. B-2:

$$M_y = Pe + PZ - P\left(\frac{Z}{2}\right) \tag{B-3}$$

$$Z = 2\left(\frac{M_y}{P} - e\right) \tag{B-4}$$

$$P = 2\left(\frac{M_y}{P} - e\right)F_e D \tag{B-5}$$

$$P^2 + 2eF_e DP - 2M_y F_e D = 0 \tag{B-6}$$

$$P = \left[\sqrt{e^2 + \frac{D^2 F_{yb}}{3F_e}} - e\right] DF_e \tag{B-7}$$

## Appendix C NDS Yield Mode II, Alternate Derivation

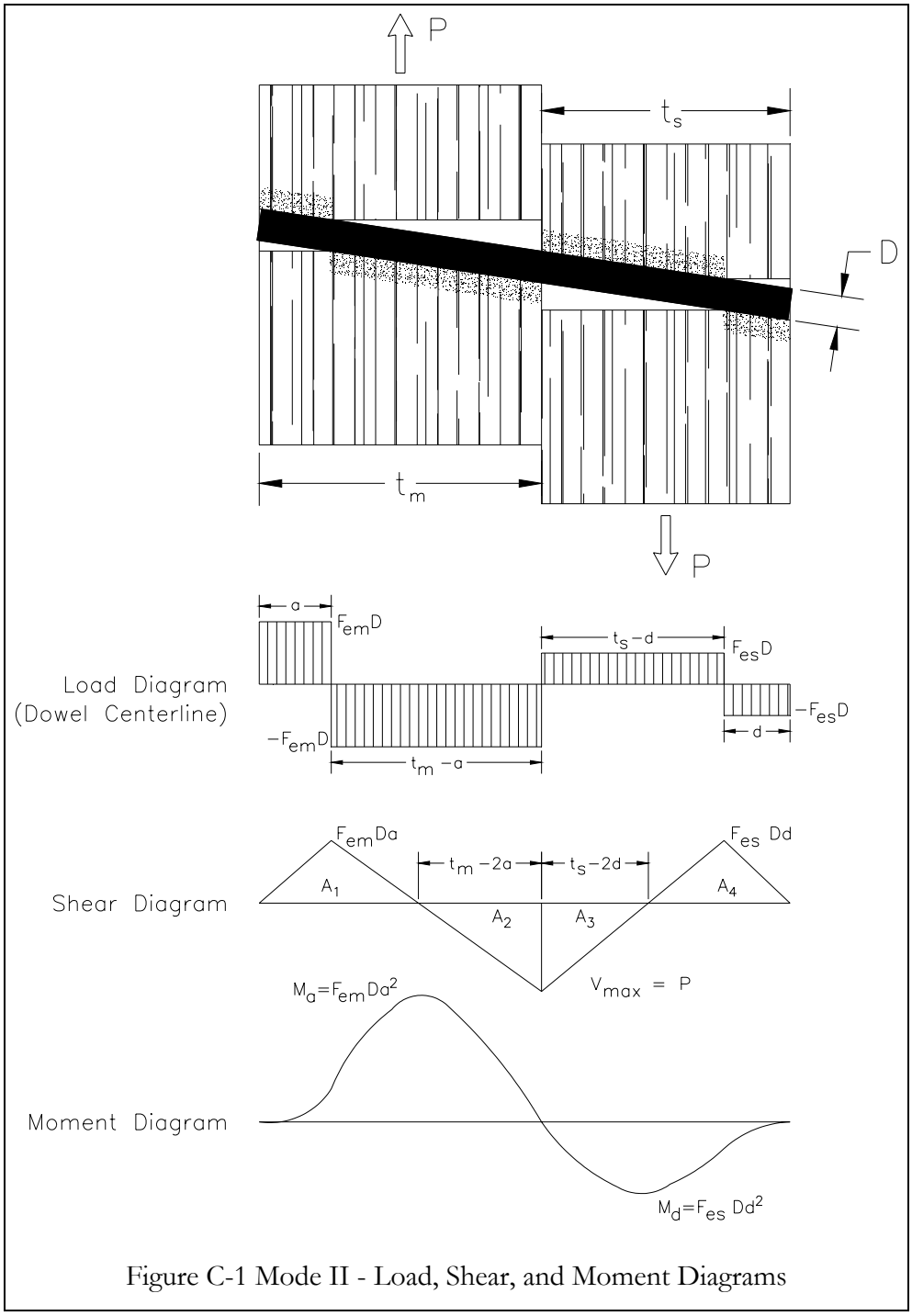


Figure C-1 Mode II - Load, Shear, and Moment Diagrams

From shear diagram equality:

$$F_{em}D\left(2a - t_m\right) = F_{es}D\left(2d - t_s\right) \tag{C-1}$$

Solving for *d*:

$$d = \frac{2F_{em}a - F_{em}t_m + F_{es}t_s}{2F_{es}} \tag{C-2}$$

From the moment diagram:

$$M_a + M_d = \frac{F_{em}D\left(t_m - 2a\right)^2}{2} + \frac{F_{em}D\left(t_s - 2d\right)^2}{2} = F_{em}Da^2 + F_{es}Dd^2 \tag{C-3}$$

Substitute for *d* and solve for *a*:

$$a = \frac{F_{em}t_s + \frac{F_{em}{}^2t_m}{F_{es}} + 2F_{em}t_m - \sqrt{2F_{em}{}^2t_s{}^2 + 2F_{em}{}^2t_mt_s + \frac{F_{em}{}^3t_m{}^2}{F_{es}} + 2F_{em}{}^2t_m{}^2 + F_{em}F_{es}t_s{}^2}}{2F_{em}\left(1 + \frac{F_{em}}{F_{es}}\right)}$$

(C-4)

$$P = 2F_{em}Da - F_{em}Dt_m \tag{C-5}$$

Substitute $R_e = F_{em}/F_{es}$ and $R_t = t_m/t_s$:

$$P = Dt_sF_{es}\left(\frac{R_e + R_eR_t - \sqrt{R_e + 2R_e{}^2\left(1 + R_t + R_t{}^2\right) + R_e{}^3R_t{}^2}}{\left(1 + R_e\right)}\right) \tag{C-6}$$

## Appendix D NDS Mode $III_s$, Alternate Derivation

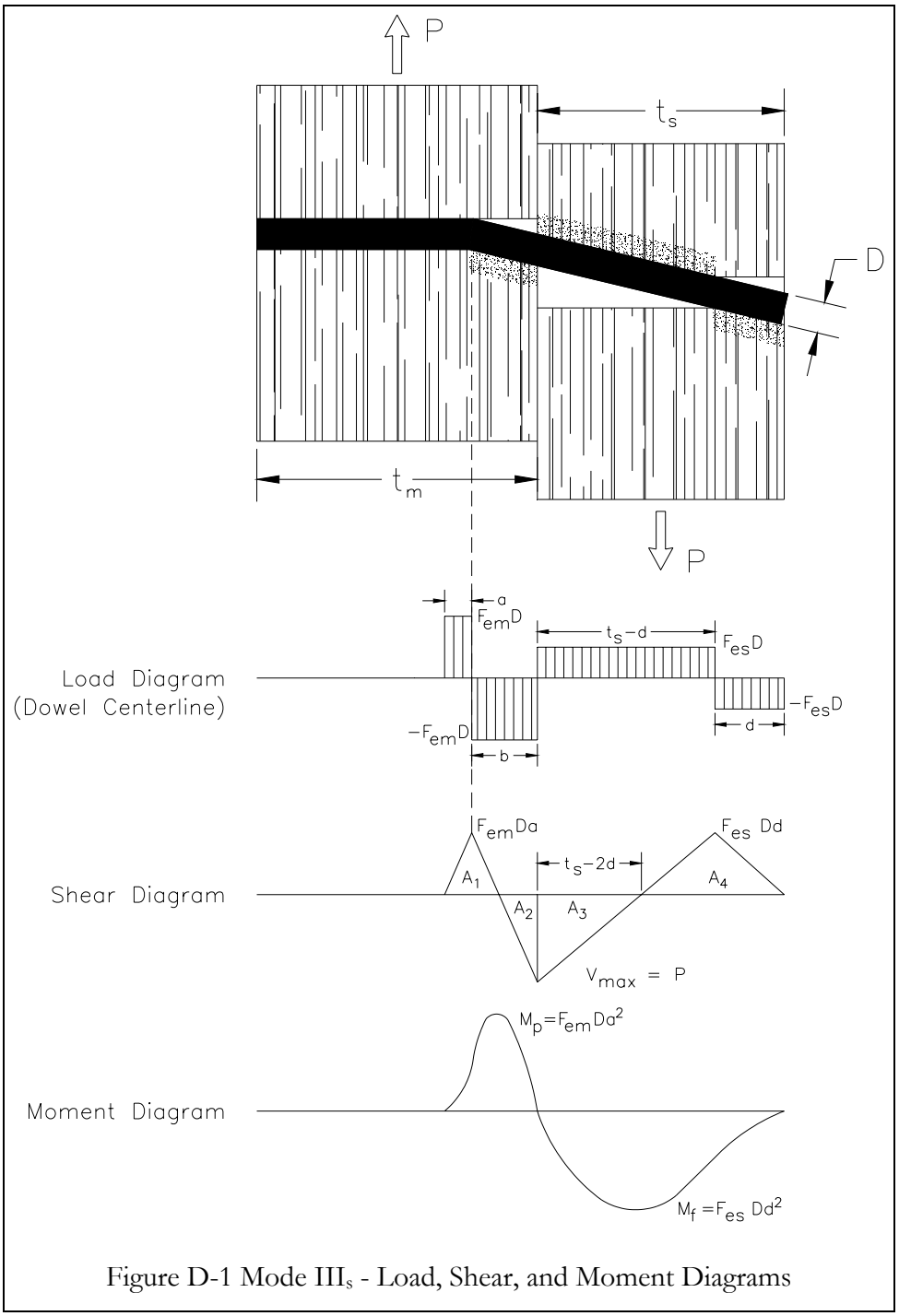


Figure D-1 Mode $III_s$ - Load, Shear, and Moment Diagrams

From shear diagram equality:

$$DF_{em}(a-b) = DF_{es}\left(2d - t_s\right) \tag{D-1}$$

Substitute for $b$ and solve for $d$:

$$d = \frac{F_{es}t_s - F_{em}a\sqrt{2}}{2F_{es}} \tag{D-2}$$

From the moment diagram:

$$M_f = F_{es}Dd^2 = \frac{DF_{es}{}^2t_s{}^2 - 2DF_{em}F_{es}t_sa\sqrt{2} + 2DF_{em}{}^2a^2}{4F_{es}} \tag{D-3}$$

$$M_p + M_f = \frac{F_{yb}D^3}{6} + F_{es}Dd^2 = -F_{em}Da^2 - \frac{F_{es}\left(2d - t_s\right)^2 D}{2} \tag{D-4}$$

Substitute for $d$:

$$-F_{em}a^2 - \frac{F_{em}{}^2a^2}{2F_{es}} - \frac{F_{em}t_sa}{\sqrt{2}} + \frac{F_{es}t_s{}^2}{4} + \frac{F_{yb}D^2}{6} = 0 \tag{D-5}$$

Solve for $a$:

$$a = \frac{\frac{F_{em}t_s}{\sqrt{2}} - \sqrt{\frac{F_{em}{}^2t_s{}^2}{2} + 4\left(F_{em} + \frac{F_{em}{}^2}{2F_{es}}\right)\left(\frac{F_{es}t_s{}^2}{4} + \frac{F_{yb}D^2}{6}\right)}}{2\left(-F_{em} - \frac{F_{em}{}^2}{2F_{es}}\right)} \tag{D-6}$$

Substituting:

$$P = F_{em}a\sqrt{2} \tag{D-7}$$

Substitute $R_e = F_{em}/F_{es}$ and $R_t = t_m/t_s$:

$$P = \frac{Dt_sF_{em}}{2 + R_e}\left(-1 + \sqrt{\frac{2\left(1 + R_e\right)}{R_e} + \frac{2F_{yb}\left(2 + R_e\right)D^2}{3F_{em}t_s{}^2}}\right) \tag{D-8}$$

## Appendix E Standard Test Setup for Instron Model 1332 Machine

Start the Strawberry Tree data acquisition system.
Turn on hydraulic pressure from Instron control panel.
Set load and stroke range

Example: 20% load range is 20% of 55 kips or 11 kips. While the output reads from 0 to -10 volts, the load will be changing from 0 to 11 kips (compression).

50% stroke range is 50% of 2 inches or 1 inch. While the output reads from 10 to 0 volts, the stroke will be changing from -1 to 0 inches.

Note: To adjust the stroke range, it is best to set the stroke position to 0, or the midpoint. This can be done by changing the readout to stroke and manually changing the position of the piston with the stroke dial. If the stroke position were not changed to zero, the current position of the stroke might be outside of the desired range.

Further note: To manually adjust the position of the stroke, the actuator must be turned on and set in the high position.

Insert object to be tested and secure it.
Lower top crossbar by turning the valve to unclamp the sides and opening the valve to lower the crossbar. Lower the head until it presses on the object to be tested. Then zero the load and stroke controllers (using the error lights and knobs) and make sure that the machine is set to stroke control (green light should be on at top of stroke controller).
Make sure the switch is in the interlock position at the bottom of the load controller.
Turn on the actuator and set it to the high position.
Move the piston to the bottom of the stroke (+100% of stroke range).
Open the Strawberry Tree file named loadefl.wbb (by using right mouse button) to allow reading of the load and stroke channels.
Double-click on log output file icon.
Type general description of test. (e.g. 1" White Oak Shear Test, 1/2" Spans, Radial, 20% Load Range, 20% Stroke Range)
Click on Save As button to save the output file under its own name (e.g. wo10200s.txt)
Make sure that the readings are continuous with an interval of 3 seconds.
Click OK to return to the main screen.
Set up function generator - Ramp mode, inverted (compression), sine waveform, gate.
Specify period of function. (e.g. 50% x 2" / 0.05"/min = 20 min. period)
In the Strawberry Tree main screen click with right mouse button and Enable, then Start All Logs.
Press Start on function generator.
Watch data output for load peak voltage and compute approximate peak load. Let run for about a minute after peak load. Compute approx. max. displacement.
Click with right mouse button and Enable, then Stop All Logs.
Press Hold on function generator, then Reset.
Turn off actuator.
Raise top crossbar by opening clamp valve and opening raise valve. Then close raise valve and clamp again.

## Appendix F Peg Testing Form

### Test Data

Date _____

Time _____

Peg Information

| | | | |
|---|---|---|---|
| Species | _____ | Peg No. | _____ |
| Diameter | _____ _____ | Filename | _____ |
| | _____ _____ | | |
| | _____ _____ | | |
| Slope of Grain | _____ | Orientation | _____ |
| No. Rings / Inch | _____ | Defects | _____ |
| Small Sample Exact Length | _____ | | |
| Initial Weight | _____ | Final Weight | _____ |

Base Material

| | | | |
|---|---|---|---|
| Species | _____ | | |
| Trough Length | _____ | Orientation | _____ |
| No. Rings / Inch | _____ | Defects | _____ |
| Small Sample Exact Size | _____ | | |
| Initial Weight | _____ | Final Weight | _____ |

Type of Test _____

_____

Load Rate _____

Load Range _____ Stroke Range _____

Approx. Ultimate Load _____ Approx. Stroke Distance _____

Failure Type _____

Oven Temp. _____ Total Time _____

# Appendix G Bending Test Data

## Summary of Bending Tests:

Last Revision: 8/11/97 Note: Formatting Changes

| SPECIES | ACTUAL DIA (IN.) | LOAD ORIENT. | BREAK TYPE | YIELD LOAD (lb) | $F_{yb}$ (psi) | M.C. % | SG | STIFFNESS (LB/IN) |
|---|---|---|---|---|---|---|---|---|
| RO | 0.742 | R | Cross-grain Tens. | 331 | 12,886 | 10.6% | 0.53 | 1343 |
| RO | 0.745 | R | Splintering Tens. | 436 | 16,796 | 10.8% | 0.60 | 1778 |
| RO | 0.775 | R | Splintering Tens. | 495 | 16,908 | | | |
| RO | 0.766 | R | Splintering Tens. | 513 | 18,147 | | | |
| RO | 0.774 | R | Cross-grain Tens. | 536 | 18,388 | | | |
| RO | 0.767 | R | Simple Tens. | 568 | 20,024 | 7.71 | 0.64 | |
| RO | 0.738 | R | Splintering Tens. | 511 | 20,210 | 10.6% | 0.64 | 2663 |
| RO | 0.774 | R | Cross-grain Tens. | 623 | 21,388 | | | |
| RO | 0.757 | R | X-grain Tens. & Shear | 586 | 21,502 | 8.68 | 0.65 | |
| RO | 0.763 | R | Splintering Tens. | 641 | 22,963 | 7.88 | 0.64 | |
| RO | 0.773 | T | Cross-grain Tens. | 234 | 8,052 | | | |
| RO | 0.751 | T | Cross-grain Tens. | 341 | 12,798 | 10.8% | 0.54 | 1668 |
| RO | 0.781 | T | Simple Tens. | 403 | 13,470 | | | |
| RO | 0.765 | T | Simple Tens. | 394 | 14,008 | | | |
| RO | 0.772 | T | Simple Tens. | 412 | 14,264 | | | |
| RO | 0.737 | T | Splintering Tens. | 394 | 15,666 | 11.0% | 0.62 | 1577 |
| RO | 0.750 | T | Splintering Tens. | 458 | 18,425 | 8.03 | 0.62 | |
| RO | 0.757 | T | Splintering Tens. | 678 | 24,862 | 7.99 | 0.66 | |
| | | | 18 | | 17,264 | Mean | | |
| | | | K Factor | 1.952 | 4,241 | Std. Dev. | | |
| | | | | | 8,986 | 5% Exclusion | | |
| RO | 1.004 | R | Brash Tens. | 632 | 9,937 | | | |
| RO | 1.005 | R | Cross-grain Tens. | 751 | 11,791 | | | |
| RO | 1.005 | R | Splintering Tens. | 806 | 12,629 | | | |
| RO | 1.007 | R | Splintering Tens. | 833 | 12,982 | | | |
| RO | 1.010 | R | Cross-grain tens. | 861 | 13,297 | 5.01 | 0.52 | |
| RO | 1.005 | T | Cross-grain Tens. | 641 | 10,041 | | | |
| RO | 1.009 | T | Cross-grain Tens. | 765 | 11,841 | | | |
| RO | 1.008 | T | Cross-grain Tens. | 824 | 12,795 | | | |
| RO | 1.007 | T | Cross-grain Tens. | 934 | 14,573 | | | |
| RO | 1.016 | T | Splinter tens./Simple tens. | 1062 | 16,120 | 5.87 | 0.61 | |
| | | | 10 | | 12,601 | Mean | | |
| | | | K Factor | 2.104 | 1,881 | Std. Dev. | | |
| | | | | | 8,644 | 5% Exclusion | | |
| RO | 1.2500 | R | Cross-grain Tens. | 1575 | 12,835 | 10.72 | 0.61 | |
| RO | 1.2463 | R | Cross-grain Tens. | 1667 | 13,701 | 11.41 | 0.62 | |
| RO | 1.2493 | R | Splinter Tens./Brash | 1809 | 14,761 | 12.19 | 0.64 | |
| RO | 1.2468 | R | Splintering Tens. | 1886 | 15,490 | 12.40 | 0.63 | |
| RO | 1.236 | R | Splintering tens. | 2198 | 18,525 | 9.49 | 0.58 | |
| RO | 1.2458 | T | Cross-grain Tens. | 1245 | 10,251 | 11.55 | 0.56 | |
| RO | 1.2502 | T | Cross-grain Tens. | 1392 | 11,338 | 10.17 | 0.55 | |
| RO | 1.2493 | T | Splintering Tens. | 1410 | 11,510 | 10.46 | 0.51 | |
| RO | 1.2427 | T | Cross-grain Tens. | 1676 | 13,899 | 10.43 | 0.59 | |
| | | | 9 | | 13,590 | Mean | | |
| | | | K Factor | 2.142 | 2,514 | Std. Dev. | | |
| | | | | | 8,205 | 5% Exclusion | | |

## Summary of Bending Tests:

Last Revision: 8/11/97 Note: Formatting Changes

| SPECIES | ACTUAL DIA (IN.) | LOAD ORIENT. | BREAK TYPE | | YIELD LOAD (lb) | $F_{yb}$ (psi) | M.C. % | SG | STIFFNESS (LB/IN) |
|---|---|---|---|---|---|---|---|---|---|
| WO | 0.756 | R | Splintering Tens. | | 252 | 9,276 | | | |
| WO | 0.741 | R | Cross-grain Tens. | | 238 | 9,301 | | | |
| WO | 0.756 | R | Splintering Tens. | | 293 | 10,808 | | | |
| WO | 0.759 | R | Splintering Tens. | | 353 | 12,833 | | | |
| WO | 0.740 | R | Simple tens./X-grain tens. | | 348 | 13,667 | 6.02 | 0.64 | |
| WO | 0.751 | R | Cross-grain Tens. | | 492 | 18,465 | 10.2% | 0.71 | 2126 |
| WO | 0.730 | R | Cross-grain Tens. | | 454 | 18,538 | 10.1% | 0.69 | 2283 |
| WO | 0.731 | R | Splintering tens. | | 495 | 20,148 | 6.83 | 0.74 | |
| WO | 0.751 | T | Cross-grain Tens. | | 256 | 9,647 | | | |
| WO | 0.735 | T | Minimal Splint. tens. | | 266 | 10,645 | 6.38 | 0.71 | |
| WO | 0.762 | T | Splintering Tens. | | 321 | 11,514 | | | |
| WO | 0.755 | T | Cross-grain Tens. | | 321 | 11,861 | | | |
| WO | 0.753 | T | Splintering Tens. | | 325 | 12,118 | | | |
| WO | 0.716 | T | Minimal Splint. tens. | | 288 | 12,507 | 7.92 | 0.75 | |
| WO | 0.749 | T | Cross-grain Tens. | | 368 | 13,956 | 9.9% | 0.74 | 1872 |
| WO | 0.738 | T | Compression | | 511 | 20,210 | 9.8% | 0.68 | 2972 |
| WO | 0.738 | T | Splintering Tens. | | 513 | 20,290 | 9.9% | 0.69 | 3439 |
| | | | | 17 | | 13,870 | Mean | | |
| | | | | K Factor | 1.964 | 4,023 | Std. Dev. | | |
| | | | | | | 5,969 | 5% Exclusion | | |
| WO | 0.996 | R | Simple Tens. | | 540 | 8,699 | | | |
| WO | 1.006 | R | Splintering Tens. | | 733 | 11,469 | | | |
| WO | 0.999 | R | Simple Tens. | | 733 | 11,683 | | | |
| WO | 1.003 | R | Cross-grain Tens. | | 925 | 14,581 | | | |
| WO | 0.992 | R | Simple Tens. | | 1117 | 18,215 | 11.66 | 0.74 | |
| WO | 1.003 | T | Splintering Tens. | | 678 | 10,689 | | | |
| WO | 0.999 | T | Splintering Tens. | | 705 | 11,256 | | | |
| WO | 0.994 | T | Cross-grain tens. | | 769 | 12,466 | 10.98 | 0.58 | |
| WO | 1.000 | T | Splintering Tens. | | 815 | 12,965 | | | |
| WO | 0.999 | T | Splintering Tens. | | 884 | 14,100 | | | |
| | | | | 10 | | 12,612 | Mean | | |
| | | | | K Factor | 2.104 | 2,596 | Std. Dev. | | |
| | | | | | | 7,151 | 5% Exclusion | | |
| WO | 1.250 | R | Cross-grain Tens. | | 1429 | 11,641 | 13.21 | 0.70 | |
| WO | 1.268 | R | Cross-grain Tens. | | 1722 | 13,440 | 13.50 | 0.63 | |
| WO | 1.258 | R | Cross-grain Tens. | | 1841 | 14,715 | 14.22 | 0.69 | |
| WO | 1.237 | R | Splintering tens. | | 1809 | 15,207 | 8.92 | 0.64 | |
| WO | 1.241 | R | Splintering tens. | | 2152 | 17,920 | 9.66 | 0.68 | |
| WO | 1.249 | T | Cross-grain Tens. | | 1355 | 11,084 | 13.54 | 0.57 | |
| WO | 1.245 | T | Cross-grain Tens. | | 1346 | 11,102 | 13.91 | 0.63 | |
| WO | 1.244 | T | Cross-grain Tens. | | 1502 | 12,421 | 13.52 | 0.68 | |
| WO | 1.240 | T | Splintering tens. | | 1648 | 13,760 | 10.27 | 0.66 | |
| WO | 1.241 | T | Cross-grain Tens. | | 1767 | 14,730 | 9.37 | 0.69 | |
| WO | 1.259 | T | Cross-grain Tens. | | 1854 | 14,789 | 13.57 | 0.69 | |
| | | | | 11 | | 13,710 | Mean | | |
| | | | | K Factor | 2.074 | 2,071 | Std. Dev. | | |
| | | | | | | 9,414 | 5% Exclusion | | |
| Locust | 0.758 | R | Cross-grain Tens. | | 451 | 16,997 | 9.00 | 0.68 | |
| Locust | 0.760 | T | Splintering Tens. | | 549 | 20,728 | 10.34 | 0.68 | |
| Locust | 0.759 | T | Splintering Tens. | | 577 | 21,765 | 9.26 | 0.70 | |
| | | | | 3 | | 19,830 | Mean | | |
| | | | | K Factor | 3.152 | 2,507 | Std. Dev. | | |
| | | | | | | 11,927 | 5% Exclusion | | |

## Summary of Bending Tests:

Last Revision: 8/11/97 Note: Formatting Changes

| SPECIES | ACTUAL DIA (IN.) | LOAD ORIENT. | BREAK TYPE | | YIELD LOAD (lb) | $F_{yb}$ (psi) | M.C. % | SG | STIFFNESS (LB/IN) |
|---|---|---|---|---|---|---|---|---|---|
| Locust | 1.010 | R | Cross-grain Tens. | | 1328 | 20,532 | | | |
| Locust | 1.009 | R | Splintering Tens. | | 1397 | 21,626 | 8.65 | 0.67 | |
| Locust | 1.021 | T | Splintering Tens. | | 1786 | 26,742 | 7.78 | 0.76 | |
| Locust | 1.013 | T | Cross-grain Tens. | | 1795 | 27,453 | 7.58 | 0.75 | |
| | | | | 4 | | 24,088 | Mean | | |
| | | | | K Factor | 2.681 | 3,515 | Std. Dev. | | |
| | | | | | | 14,663 | 5% Exclusion | | |
| Birch | 1.014 | R | Cross-grain Tens. | | 1145 | 17,491 | 10.35 | 0.58 | |
| Birch | 1.007 | R | Splintering Tens. | | 1209 | 18,849 | 9.81 | 0.58 | |
| Birch | 1.024 | T | Cross-grain Tens. | | 1209 | 17,944 | 10.92 | 0.64 | |
| Birch | 1.013 | T | Cross-grain Tens. | | 1209 | 18,498 | 11.19 | 0.65 | |
| | | | | 4 | | 18,196 | Mean | | |
| | | | | K Factor | 2.681 | 600 | Std. Dev. | | |
| | | | | | | 16,588 | 5% Exclusion | | |
| Maple | 0.742 | R | Cross-grain Tens. | | 503 | 19,582 | 8.0% | 0.60 | 3162 |
| Maple | 0.741 | R | Splintering Tens. | | 542 | 21,211 | 8.0% | 0.67 | 4183 |
| Maple | 0.749 | R | Simple Tens. | | 659 | 24,990 | 7.13 | 0.62 | |
| Maple | 0.743 | R | Simple Tens. | | 897 | 34,846 | 3.64 | 0.69 | |
| Maple | 0.743 | T | Cross-grain Tens. | | 472 | 18,278 | 8.6% | 0.68 | 2604 |
| Maple | 0.742 | T | Cross-grain Tens. | | 534 | 20,788 | 8.0% | 0.67 | 3524 |
| Maple | 0.738 | T | Cross-grain Tens. | | 542 | 21,437 | 7.8% | 0.70 | 3432 |
| Maple | 0.741 | T | Cross-grain Tens. | | 934 | 36,538 | 5.52 | 0.66 | |
| Maple | 0.745 | T | Cross-grain Tens. | | 998 | 38,446 | 7.37 | 0.63 | |
| | | | | 9 | | 26,235 | Mean | | |
| | | | | K Factor | 2.142 | 8,035 | Std. Dev. | | |
| | | | | | | 9,025 | 5% Exclusion | | |
| Ash | 0.745 | R | Cross-grain Tens. | | 316 | 12,173 | 8.9% | 0.58 | 1692 |
| Ash | 0.751 | R | Simple Tens. | | 412 | 15,464 | 7.64 | 0.72 | |
| Ash | 0.754 | R | Splintering tens. | | 462 | 17,160 | 8.5% | 0.62 | 1726 |
| Ash | 0.747 | R | Cross-grain Tens. | | 504 | 19,213 | 8.0% | 0.69 | 2313 |
| Ash | 0.757 | R | Splintering Tens. | | 527 | 19,331 | 11.85 | 0.64 | |
| Ash | 0.746 | T | Splintering Tens. | | 440 | 16,840 | 10.05 | 0.60 | |
| Ash | 0.749 | T | Simple Tens. | | 459 | 17,407 | 8.7% | 0.58 | 2440 |
| Ash | 0.755 | T | Splintering Tens. | | 522 | 19,303 | 7.41 | 0.68 | |
| Ash | 0.746 | T | Cross-grain Tens. | | 529 | 20,272 | 8.3% | 0.65 | 2445 |
| | | | | 9 | | 17,463 | Mean | | |
| | | | | K Factor | 2.142 | 2,507 | Std. Dev. | | |
| | | | | | | 12,092 | 5% Exclusion | | |
| Ash | 0.995 | R | Simple Tens. | | 1062 | 17,145 | 6.43 | 0.67 | |
| Ash | 0.994 | R | Simple Tens. | | 1511 | 24,462 | 13.63 | 0.75 | |
| Ash | 0.996 | T | Cross-grain Tens. | | 1062 | 17,128 | 6.17 | 0.58 | |
| Ash | 0.997 | T | Cross-grain Tens. | | 1081 | 17,354 | 3.37 | 0.70 | |
| | | | | 4 | | 19,022 | Mean | | |
| | | | | K Factor | 2.681 | 3,628 | Std. Dev. | | |
| LOAD ON: | | | | | | 9,296 | 5% Exclusion | | |

## Summary of Bending Tests:

Last Revision: 8/11/97 Note: Formatting Changes

| SPECIES | ACTUAL DIA (IN.) | LOAD ORIENT. | BREAK TYPE | | YIELD LOAD (lb) | $F_{yb}$ (psi) | M.C. % | SG | STIFFNESS (LB/IN) |
|---|---|---|---|---|---|---|---|---|---|
| WO | Face | R | Cross-grain Tens. | | 217 | 10,116 | | | |
| WO | Face | R | Cross-grain Tens. | | 250 | 11,654 | | | |
| WO | Face | R | Cross-grain Tens. | | 270 | 12,586 | | | |
| WO | Corner | R | Splintering Tens. | | 310 | 14,451 | | | |
| WO | Corner | R | Brash Tens. | | 315 | 14,684 | | | |
| WO | Face | T | Cross-grain Tens. | | 208 | 9,696 | | | |
| WO | Face | T | Cross-grain Tens. | | 275 | 12,819 | | | |
| WO | Corner | T | Cross-grain Tens. | | 305 | 14,218 | | | |
| WO | Face | T | Cross-grain Tens. | | 330 | 15,383 | | | |
| WO | Corner | T | Cross-grain Tens. | | 380 | 17,714 | | | |
| | | | | 10 | | 13,332 | Mean | | |
| | | | | K Factor | 2.104 | 2,460 | Std. Dev. | | |
| | | | | | | 8,156 | 5% Exclusion | | |
| WO | Corner | R | Cross-grain Tens. | | 880 | 18,337 | | | |
| WO | Face | R | Cross-grain Tens. | | 900 | 18,753 | | | |
| WO | Corner | R | Cross-grain Tens. | | 915 | 19,066 | | | |
| WO | Corner | R | Cross-grain Tens. | | 930 | 19,378 | | | |
| WO | Corner | R | Cross-grain Tens. | | 1080 | 22,504 | | | |
| WO | Face | T | Cross-grain Tens. | | 900 | 18,753 | | | |
| WO | Face | T | Cross-grain Tens. | | 925 | 19,274 | | | |
| WO | Face | T | Splintering Tens. | | 950 | 19,795 | | | |
| WO | Corner | T | Cross-grain Tens. | | 955 | 19,899 | | | |
| WO | Face | T | Cross-grain Tens. | | 975 | 20,316 | | | |
| | | | | 10 | | 19,608 | Mean | | |
| | | | | K Factor | 2.104 | 1,181 | Std. Dev. | | |
| | | | | | | 17,124 | 5% Exclusion | | |

**Tests with no strength results:**

| | | | | | |
|---|---|---|---|---|---|
| RO | 1.014 | T | Splintering tens. | 6.07 | 0.64 |
| RO | 1.012 | R | Cross-grain tens. | 5.36 | 0.68 |
| RO | 1.236 | T | Cross-grain tens. | 9.90 | 0.56 |
| RO | 1.236 | T | Cross-grain tens. | 9.61 | 0.53 |
| RO | 1.231 | R | Cross-grain tens. | 10.64 | 0.61 |
| | | | | | |
| WO | 0.990 | R | Cross-grain tens. | 10.54 | 0.66 |
| WO | 0.991 | T | Cross-grain tens. | 9.85 | 0.62 |
| WO | 1.248 | T | Splintering tens. | 9.98 | 0.65 |

# Appendix H Shear Test Data

## Summary of 3/4" Red Oak Shear Tests

Sorted by Yield Stress

| Avg. Dia. (in.) | Slope of Grain | No. Rings Per Inch | Span Lengths | Load Orientation | Yield Stress (psi) | Moisture Content | Dry Specific Gravity | Defects |
|---|---|---|---|---|---|---|---|---|
| 0.749 | 1/12 | 12.0 | 1/4 D | Radial | 1,685 | 10.0% | 0.55 | |
| 0.743 | 1/12 | 13.3 | 1/4 D | Radial | 1,806 | 10.0% | 0.57 | |
| 0.742 | 1/12 | 8.0 | 1/4 D | Radial | 1,879 | 10.0% | 0.63 | |
| 0.742 | 0/12 | 12.0 | 1/4 D | Radial | 1,954 | 10.4% | 0.63 | |
| 0.747 | 1/12 | 9.3 | 1/4 D | Radial | 2,426 | 9.9% | 0.72 | |
| 0.749 | 1/12 | 16.0 | 1/4 D | Tangential | 1,575 | 10.0% | 0.46 | |
| 0.737 | 1/12 | 12.0 | 1/4 D | Tangential | 1,989 | 11.2% | 0.62 | |
| 0.743 | 0/12 | 6.7 | 1/4 D | Tangential | 2,000 | 10.8% | 0.59 | |
| 0.747 | 1/12 | 10.7 | 1/4 D | Tangential | 2,112 | 10.2% | 0.61 | |
| 0.738 | 1/12 | 6.7 | 1/4 D | Tangential | 2,146 | 10.5% | 0.66 | |
| | | | | Mean | 1,957 | | | |
| | | | | Std. Dev. | 243 | K Factor 2.104 | | |
| | | | | 5% Exclusion | 1,446 [1] | | | |
| 0.745 | 0/12 | 28.0 | 1/2 D | Radial | 1,422 | 10.4% | 0.49 | |
| 0.750 | 1/12 | 12.0 | 1/2 D | Radial | 1,581 | 10.3% | 0.54 | |
| 0.742 | 1/12 | 5.3 | 1/2 D | Radial | 1,730 | 10.7% | 0.61 | Growth rings chipped out near edges |
| 0.745 | 1/12 | 12.0 | 1/2 D | Radial | 1,850 | 10.4% | 0.68 | |
| 0.745 | 0/12 | 24.0 | 1/2 D | Radial | 1,945 | 10.7% | 0.60 | |
| 0.747 | 0/12 | 10.7 | 1/2 D | Tangential | 1,594 | 10.6% | 0.54 | |
| 0.743 | 0/12 | 12.0 | 1/2 D | Tangential | 1,660 | 10.6% | 0.59 | |
| 0.743 | 0/12 | 6.7 | 1/2 D | Tangential | 1,752 | 10.3% | 0.59 | |
| 0.749 | 1/12 | 16.0 | 1/2 D | Tangential | 1,785 | 9.6% | 0.61 | |
| 0.747 | 0/12 | 9.3 | 1/2 D | Tangential | 2,090 | 10.4% | 0.66 | |
| | | | | Mean | 1,741 | | | |
| | | | | Std. Dev. | 192 | K Factor 2.104 | | |
| | | | | 5% Exclusion | 1,336 [1] | | | |
| 0.747 | 1/12 | 8.0 | 1 D | Radial | 1,270 | 10.3% | 0.59 | |
| 0.741 | 1/12 | 9.3 | 1 D | Radial | 1,440 | 10.2% | 0.60 | |
| 0.749 | 1/12 | 10.7 | 1 D | Radial | 1,650 | 10.1% | 0.61 | |
| 0.742 | 0/12 | 5.3 | 1 D | Radial | 1,803 | 10.2% | 0.68 | Wood light color, but same grain type |
| 0.747 | 1/12 | 5.3 | 1 D | Radial | 1,908 | 10.5% | 0.71 | |
| 0.745 | 1/12 | 14.0 | 1 D | Tangential | 1,318 | 9.6% | 0.53 | |
| 0.747 | 1/12 | 10.0 | 1 D | Tangential | 1,388 | 10.0% | 0.58 | |
| 0.749 | 0/12 | 13.3 | 1 D | Tangential | 1,563 | 10.1% | 0.60 | |
| 0.743 | 1/12 | 15.0 | 1 D | Tangential | 1,611 | 10.2% | 0.61 | |
| 0.745 | 1/12 | 9.3 | 1 D | Tangential | 1,629 | 10.4% | 0.68 | |
| | | | | Mean | 1,558 | | | |
| | | | | Std. Dev. | 206 | K Factor 2.104 | | |
| | | | | 5% Exclusion | 1,124 [1] | | | |

[1] From ASTM D 2915

## Summary of 1" Red Oak Shear Tests

Sorted by Yield Stress

| Avg. Dia. (in.) | Slope of Grain | No. Rings Per Inch | Span Lengths (in.) | Load Orientation | Yield Stress (psi) | Moisture Content | Dry Specific Gravity | Dbl. Shear Stiffness (lb/in) | Defects |
|---|---|---|---|---|---|---|---|---|---|
| 1.004 | 2/12 | 19.0 | 0.25 | Radial | 1,726 | 7.8% | 0.55 | 92,247 | Grain slope curves & steepens |
| 0.996 | 0/12 | 10.0 | 0.25 | Radial | 1,812 | 8.9% | 0.63 | 87,276 | |
| 1.001 | 1/12 | 11.0 | 0.25 | Radial | 2,004 | 9.0% | 0.60 | 102,899 | |
| 0.999 | 0/12 | 8.0 | 0.25 | Radial | 2,055 | 8.3% | 0.65 | 83,869 | |
| 0.997 | 0/12 | 10.0 | 0.25 | Radial | 2,184 | 8.8% | 0.65 | 129,443 | |
| 1.003 | 1/12 | 18.0 | 0.25 | Tangential | 1,618 | 9.1% | 0.49 | 87,785 | |
| 1.003 | 1/12 | 12.0 | 0.25 | Tangential | 2,102 | 9.3% | 0.61 | 90,256 | |
| 1.003 | 1/12 | 10.0 | 0.25 | Tangential | 2,363 | 8.9% | 0.68 | 130,657 | Chips missing out of sides |
| 1.003 | 1/12 | 9.0 | 0.25 | Tangential | 2,374 | 8.4% | 0.61 | 71,411 | |
| 1.003 | 1/12 | 9.0 | 0.25 | Tangential | 2,385 | 8.8% | 0.62 | 90,937 | |
| | | | | Mean | 2,062 | | | | |
| | | | | Std. Dev. | 276 | K Factor 2.104 | | | |
| | | | | 5% Exclusion | 1,482 [1] | | | | |
| 1.003 | 1/12 | 12.0 | 0.50 | Radial | 1,596 | 8.3% | 0.57 | 67,425 | |
| 0.995 | 0/12 | 9.0 | 0.50 | Radial | 1,761 | 8.7% | 0.60 | 80,383 | |
| 1.001 | 1/12 | 13.0 | 0.50 | Radial | 1,796 | 8.5% | 0.62 | 85,577 | |
| 1.008 | 1/12 | 13.3 | 0.50 | Radial | 1,813 | 8.7% | 0.60 | 91,438 | |
| 0.999 | 1/12 | 6.0 | 0.50 | Radial | 1,949 | 8.7% | 0.61 | 108,375 | |
| 1.010 | 1/12 | 29.3 | 0.50 | Tangential | 1,937 | 8.5% | 0.54 | 73,974 | |
| 1.001 | 1/12 | 13.0 | 0.50 | Tangential | 1,947 | 8.3% | 0.57 | 87,520 | |
| 0.999 | 1/12 | 13.0 | 0.50 | Tangential | 2,005 | 8.6% | 0.60 | 82,318 | |
| 1.003 | 1/12 | 9.0 | 0.50 | Tangential | 2,223 | 8.4% | 0.66 | 99,755 | |
| 1.004 | 1/12 | 10.0 | 0.50 | Tangential | 2,275 | 9.0% | 0.71 | 106,427 | |
| | | | | Mean | 1,930 | | | | |
| | | | | Std. Dev. | 206 | K Factor 2.104 | | | |
| | | | | 5% Exclusion | 1,497 [1] | | | | |
| 1.009 | 1/12 | 12.0 | 1.00 | Radial | 1,115 | 10.0% | 0.50 | 56,124 | |
| 1.001 | 0/12 | 17.0 | 1.00 | Radial | 1,424 | 8.1% | 0.57 | 58,719 | |
| 0.999 | 1/12 | 13.0 | 1.00 | Radial | 1,508 | 8.3% | 0.62 | 49,176 | Chips missing out of sides |
| 0.999 | 1/12 | 12.0 | 1.00 | Radial | 1,570 | 9.7% | 0.63 | 58,113 | |
| 1.004 | 0/12 | 7.0 | 1.00 | Radial | 1,709 | | | 67,436 | |
| 0.996 | 0/12 | 18.0 | 1.00 | Tangential | 1,482 | 8.7% | 0.58 | 53,847 | |
| 0.993 | 0/12 | 11.0 | 1.00 | Tangential | 1,582 | 8.1% | 0.63 | 51,639 | |
| 0.996 | 1/12 | 9.0 | 1.00 | Tangential | 1,710 | 8.3% | 0.66 | 45,301 | |
| 0.996 | 1/12 | 10.0 | 1.00 | Tangential | 1,723 | 9.0% | 0.70 | 49,274 | |
| 1.000 | 1/12 | 11.0 | 1.00 | Tangential | 1,725 | 8.7% | 0.66 | 42,859 | |
| | | | | Mean | 1,555 | | | | |
| | | | | Std. Dev. | 190 | K Factor 2.104 | | | |
| | | | | 5% Exclusion | 1,155 [1] | | | | |

[1] From ASTM D 2915

## Summary of 1-1/4" Red Oak Shear Tests

Sorted by Yield Stress

| Avg. Dia. (in.) | Slope of Grain | No. Rings Per Inch | Span Lengths | Load Orientation | Yield Stress (psi) | Moisture Content | Dry Specific Gravity | Defects |
|---|---|---|---|---|---|---|---|---|
| 1.275 | 1/12 | 19.2 | 1/4 D | Radial | 1,734 | 15.9% | 0.61 | Wane - 1/2" max. |
| 1.270 | 1/12 | 14.4 | 1/4 D | Radial | 1,830 | 16.3% | 0.63 | Wane - 1/2" flat face |
| 1.271 | 1/12 | 14.4 | 1/4 D | Radial | 1,894 | 16.0% | 0.75 | Wane - 1/2" max. and 1/2" flat |
| 1.273 | 1/12 | 13.6 | 1/4 D | Radial | 2,070 | 16.6% | 0.78 | Wane - 5/8" max. |
| 1.257 | 1/12 | 14.4 | 1/4 D | Radial | 2,110 | 15.2% | 0.75 | Wane - 1/2" flat face |
| 1.275 | 1/12 | 28.0 | 1/4 D | Tangential | 1,359 | 14.5% | 0.52 | |
| 1.266 | 0/12 | 6.4 | 1/4 D | Tangential | 1,682 | 15.0% | 0.72 | |
| 1.254 | 1/12 | 13.6 | 1/4 D | Tangential | 1,967 | 14.3% | 0.71 | Wane - 1/2" max. |
| 1.255 | 0/12 | 8.0 | 1/4 D | Tangential | 2,057 | 14.8% | 0.77 | Wane - 1/2" flat face |
| 1.253 | 1/12 | 15.2 | 1/4 D | Tangential | 2,095 | 13.8% | 0.76 | |
| | | | | Mean | 1,880 | | | |
| | | | | Std. Dev. | 238 | K Factor 2.104 | | |
| | | | | 5% Exclusion | 1,379 [1] | | | |
| 1.272 | 1/12 | 28.8 | 1/2 D | Radial | 1,195 | 15.9% | 0.49 | |
| 1.255 | 1/12 | 18.4 | 1/2 D | Radial | 1,547 | 14.8% | 0.60 | |
| 1.281 | 1/12 | 10.4 | 1/2 D | Radial | 1,725 | 16.2% | 0.61 | |
| 1.255 | 1/12 | 14.4 | 1/2 D | Radial | 1,889 | 14.4% | 0.68 | Wane - 1/2" flat face |
| 1.254 | 1/12 | 8.8 | 1/2 D | Radial | 2,085 | 14.2% | 0.67 | Wane - 1/2" max. and 1/2" flat |
| 1.280 | 2/12 | 10.4 | 1/2 D | Tangential | 1,288 | 16.9% | 0.67 | Wane - 1/2" flat face |
| 1.255 | 1/12 | 12.0 | 1/2 D | Tangential | 1,340 | 14.8% | 0.60 | |
| 1.251 | 0/12 | 11.2 | 1/2 D | Tangential | 1,363 | 14.3% | 0.59 | Wane - 1/2" flat face |
| 1.251 | 1/12 | 19.2 | 1/2 D | Tangential | 1,465 | 13.8% | 0.51 | |
| 1.258 | 2/12 | 5.6 | 1/2 D | Tangential | 1,478 | 15.7% | 0.72 | Wane - 1/2" flat face |
| | | | | Mean | 1,537 | | | |
| | | | | Std. Dev. | 282 | K Factor 2.104 | | |
| | | | | 5% Exclusion | 944 [1] | | | |
| 1.281 | 1/12 | 15.2 | 1 D | Radial | 1,029 | 13.6% | 0.54 | Wane - 1/2" max. and 1/2" flat |
| 1.277 | 1/12 | 20.0 | 1 D | Radial | 1,063 | 13.5% | 0.59 | Wane - 1/2" flat face |
| 1.251 | 1/12 | 18.4 | 1 D | Radial | 1,236 | 13.6% | 0.55 | |
| 1.275 | 1/12 | 18.4 | 1 D | Radial | 1,284 | 15.1% | 0.70 | Wane - 1/2" flat face |
| 1.258 | 1/12 | 11.2 | 1 D | Radial | 1,413 | 14.4% | 0.64 | Wane - 1/2" max. |
| 1.277 | 1/12 | 28.0 | 1 D | Tangential | 909 | 15.0% | 0.53 | Wane - 1/2" max. |
| 1.264 | 1/12 | 11.2 | 1 D | Tangential | 1,159 | 15.0% | 0.68 | Wane - 1/2" flat face |
| 1.255 | 1/12 | 15.2 | 1 D | Tangential | 1,171 | 14.0% | 0.68 | Wane - 1/2" flat face |
| 1.273 | 1/12 | 4.8 | 1 D | Tangential | 1,193 | 15.7% | 0.74 | Sm. 1/8" knot through upper third |
| 1.254 | 1/12 | 7.2 | 1 D | Tangential | 1,346 | 13.1% | 0.68 | Wane - 1/2" flat face |
| | | | | Mean | 1,180 | | | |
| | | | | Std. Dev. | 151 | K Factor 2.104 | | |
| | | | | 5% Exclusion | 862 [1] | | | |

[1] From ASTM D 2915

## Summary of 3/4" White Oak Shear Tests

Sorted By Yield Stress

| Avg. Dia. (in.) | Slope of Grain | No. Rings Per Inch | Span Lengths (in.) | Load Orientation | Yield Stress (psi) | Moisture Content | Dry Specific Gravity | Defects |
|---|---|---|---|---|---|---|---|---|
| 0.750 | 0/12 | 17.0 | 1/4D | Radial | 2,005 | 12.0% | 0.63 | |
| 0.746 | 1/12 | 8.0 | 1/4D | Radial | 2,132 | 11.6% | 0.61 | 2 pin dia. bore holes through section |
| 0.745 | 1/12 | 20.0 | 1/4D | Radial | 2,173 | 12.0% | 0.68 | |
| 0.740 | 1/12 | 6.7 | 1/4D | Radial | 2,592 | 12.1% | 0.73 | |
| 0.747 | 1/12 | 16.0 | 1/4D | Radial | 2,594 | 12.0% | 0.71 | |
| 0.737 | 1/12 | 12.0 | 1/4D | Tangential | 1,925 | 11.8% | 0.71 | |
| 0.750 | 1/12 | 13.3 | 1/4D | Tangential | 2,267 | 12.2% | 0.71 | |
| 0.736 | 0/12 | 9.3 | 1/4D | Tangential | 2,283 | 12.7% | 0.74 | |
| 0.749 | 1/12 | 8.0 | 1/4D | Tangential | 2,323 | 12.4% | 0.75 | |
| 0.746 | 1/12 | 9.3 | 1/4D | Tangential | 2,366 | 12.3% | 0.71 | |
| | | | | Mean | 2,266 | | | |
| | | | | Std. Dev. | 221 | K Factor 2.104 | | |
| | | | | 5% Exclusion | 1,802 [1] | | | |
| 0.743 | 1/12 | 10.7 | 1/2D | Radial | 2,003 | 11.8% | 0.72 | |
| 0.736 | 1/12 | 8.0 | 1/2D | Radial | 1,860 | 12.1% | 0.69 | |
| 0.749 | 0/12 | 12.0 | 1/2D | Radial | 1,951 | 11.9% | 0.58 | |
| 0.746 | 1/12 | 8.0 | 1/2D | Radial | 2,120 | 9.7% | 0.73 | |
| 0.737 | 1/12 | | 1/2D | Radial | 2,293 | 12.2% | 0.76 | |
| 0.729 | 0/12 | 12.0 | 1/2D | Tangential | 1,622 | 12.5% | 0.64 | |
| 0.746 | 1/12 | 12.0 | 1/2D | Tangential | 1,863 | 12.5% | 0.66 | |
| 0.717 | 1/12 | 20.0 | 1/2D | Tangential | 1,913 | 12.1% | 0.63 | |
| 0.725 | 1/12 | 6.7 | 1/2D | Tangential | 1,985 | 11.6% | 0.70 | |
| 0.730 | 1/12 | 8.0 | 1/2D | Tangential | 2,146 | 12.5% | 0.71 | |
| | | | | Mean | 1,976 | | | |
| | | | | Std. Dev. | 185 | K Factor 2.104 | | |
| | | | | 5% Exclusion | 1,587 [1] | | | |
| 0.736 | 1/12 | 8.0 | 1D | Radial | 1,275 | 12.0% | 0.68 | |
| 0.750 | 1/12 | 24.0 | 1D | Radial | 1,572 | 11.8% | 0.61 | |
| 0.747 | 1/12 | 26.0 | 1D | Radial | 1,729 | 11.6% | 0.67 | |
| 0.747 | 1/12 | 12.0 | 1D | Radial | 1,966 | 10.0% | 0.76 | |
| 0.742 | 1/12 | 8.0 | 1D | Radial | 1,999 | 11.8% | 0.74 | |
| 0.746 | 1/12 | 9.0 | 1D | Tangential | 1,186 | 11.9% | 0.61 | |
| 0.749 | 1/12 | 13.3 | 1D | Tangential | 1,550 | 10.7% | 0.61 | |
| 0.746 | 1/12 | 12.0 | 1D | Tangential | 1,581 | 11.5% | 0.67 | |
| 0.747 | 1/12 | 13.0 | 1D | Tangential | 1,615 | 12.1% | 0.66 | |
| 0.745 | 0/12 | 9.0 | 1D | Tangential | 1,693 | 11.4% | 0.72 | |
| | | | | Mean | 1,617 | | | |
| | | | | Std. Dev. | 258 | K Factor 2.104 | | |
| | | | | 5% Exclusion | 1,075 [1] | | | |

[1] From ASTM D 2915

## Summary of 1" White Oak Shear Tests

Sorted by Yield Stress

| Avg. Dia. (in.) | Slope of Grain | No. Rings Per Inch | Span Lengths (in.) | Load Orientation | Yield Stress (psi) | Moisture Content | Dry Specific Gravity | Defects |
|---|---|---|---|---|---|---|---|---|
| 0.991 | 1/12 | 10.0 | 0.25 | Radial | 1,932 | 10.2% | 0.59 | |
| 0.988 | 0/12 | 10.7 | 0.25 | Radial | 2,278 | 10.3% | 0.62 | |
| 0.993 | 1/12 | | 0.25 | Radial | 2,443 | 10.4% | 0.68 | |
| 0.975 | 0/12 | | 0.25 | Radial | 2,746 | 10.7% | 0.77 | |
| 0.990 | 1/12 | | 0.25 | Radial | 2,765 | 10.5% | 0.74 | |
| 0.988 | 0/12 | 11.0 | 0.25 | Tangential | 1,915 | 9.6% | 0.62 | |
| 0.991 | 1/12 | 9.0 | 0.25 | Tangential | 2,326 | 10.1% | 0.73 | |
| 0.990 | 0/12 | 10.0 | 0.25 | Tangential | 2,365 | 10.1% | 0.72 | |
| 0.984 | 0/12 | 10.7 | 0.25 | Tangential | 2,376 | 10.1% | 0.72 | |
| 0.992 | 1/12 | 15.0 | 0.25 | Tangential | 2,459 | 9.6% | 0.63 | |
| 0.979 | 1/12 | 6.7 | 0.25 | Tangential | 2,578 | 10.5% | 0.78 | |
| | | | | Mean | 2,380 | | | |
| | | | | Std. Dev. | 276 | K Factor 2.074 | | |
| | | | | 5% Exclusion | 1,808 [1] | | | |
| 0.993 | 1/12 | 9.0 | 0.50 | Radial | 1,950 | 10.3% | 0.68 | |
| 0.991 | 1/12 | 20.0 | 0.50 | Radial | 1,994 | 10.4% | 0.59 | |
| 0.988 | 1/12 | 16.0 | 0.50 | Radial | 1,995 | 9.6% | 0.62 | |
| 0.990 | 1/12 | 16.0 | 0.50 | Radial | 2,066 | 9.5% | 0.64 | |
| 0.990 | 1/12 | 12.0 | 0.50 | Radial | 2,161 | 9.7% | 0.62 | |
| 0.988 | 0/12 | 10.7 | 0.50 | Tangential | 1,805 | 10.0% | 0.65 | |
| 0.991 | 0/12 | 9.3 | 0.50 | Tangential | 1,829 | 9.9% | 0.64 | |
| 0.992 | 2/12 | 12.0 | 0.50 | Tangential | 2,014 | 9.4% | 0.66 | Chips missing out of sides |
| 0.980 | 1/12 | 6.7 | 0.50 | Tangential | 2,179 | 10.0% | 0.77 | |
| 0.990 | 1/12 | 9.3 | 0.50 | Tangential | 2,315 | 9.6% | 0.64 | |
| | | | | Mean | 2,031 | | | |
| | | | | Std. Dev. | 157 | K Factor 2.104 | | |
| | | | | 5% Exclusion | 1,700 [1] | | | |
| 1.000 | 1/12 | 19.0 | 1.00 | Radial | 1,310 | 10.0% | 0.52 | |
| 0.984 | 1/12 | 9.3 | 1.00 | Radial | 1,635 | 10.7% | 0.63 | |
| 0.990 | 1/12 | 8.0 | 1.00 | Radial | 1,863 | 10.7% | 0.68 | |
| 0.992 | 0/12 | 12.0 | 1.00 | Radial | 1,934 | 10.8% | 0.70 | |
| 0.992 | 1/12 | 10.7 | 1.00 | Radial | 1,974 | 10.8% | 0.74 | |
| 0.987 | 0/12 | 11.0 | 1.00 | Tangential | 1,408 | 10.4% | 0.59 | |
| 0.979 | 1/12 | 10.0 | 1.00 | Tangential | 1,429 | 10.7% | 0.66 | |
| 0.987 | 1/12 | 11.0 | 1.00 | Tangential | 1,629 | 10.5% | 0.67 | |
| 0.986 | 1/12 | 10.0 | 1.00 | Tangential | 1,630 | 10.3% | 0.69 | |
| 0.993 | 0/12 | | 1.00 | Tangential | 1,869 | 10.1% | 0.72 | |
| | | | | Mean | 1,668 | | | |
| | | | | Std. Dev. | 236 | K Factor 2.104 | | |
| | | | | 5% Exclusion | 1,173 [1] | | | |

[1] From ASTM D 2915

## Summary of 1 1/4" White Oak Shear Tests

Sorted By Yield Stress

| Avg. Dia. (in.) | Slope of Grain | No. Rings Per Inch | Span Lengths (in.) | Load Orientation | Yield Stress (psi) | Moisture Content | Dry Specific Gravity | Defects |
|---|---|---|---|---|---|---|---|---|
| 1.245 | 1/12 | 8.0 | 1/4D | Radial | 2,017 | 13.7% | 0.68 | Wane - 1/2" flat face |
| 1.242 | 0/12 | 11.2 | 1/4D | Radial | 2,088 | 13.4% | 0.65 | Wane - 1/2" flat face |
| 1.242 | 0/12 | 21.6 | 1/4D | Radial | 2,159 | 13.2% | 0.67 | Wane - 1/2" max. |
| 1.242 | 0/12 | 20.8 | 1/4D | Radial | 2,192 | 13.3% | 0.74 | Wane - 1/2" max. 1/8" knot through shear plane |
| 1.243 | 1/12 | 8.8 | 1/4D | Radial | 2,275 | 13.5% | 0.75 | Wane - 1/2" flat face |
| 1.250 | 0/12 | 16.8 | 1/4D | Tangential | 1,877 | 13.9% | 0.64 | Wane - 1/2" max. |
| 1.242 | 0/12 | 13.6 | 1/4D | Tangential | 1,900 | 13.9% | 0.68 | Wane - 1/2" flat face |
| 1.246 | 0/12 | 28.0 | 1/4D | Tangential | 2,007 | 13.4% | 0.66 | Wane - 1/2" flat face |
| 1.243 | 1/12 | 5.6 | 1/4D | Tangential | 2,088 | 13.5% | 0.73 | Wane - 1/2" max. |
| 1.242 | 0/12 | 19.2 | 1/4D | Tangential | 2,291 | 14.0% | 0.79 | Wane - 1/2" max. |
| | | | | Mean | 2,090 | | | |
| | | | | Std. Dev. | 143 | K Factor 2.104 | | |
| | | | | 5% Exclusion | 1,789 [1] | | | |
| 1.241 | 1/12 | 6.4 | 1/2D | Radial | 1,863 | 14.0% | 0.71 | Wane - 1/2" flat face |
| 1.238 | 1/12 | 10.4 | 1/2D | Radial | 1,883 | 14.2% | 0.72 | Wane - 1/2" flat face |
| 1.242 | 1/12 | | 1/2D | Radial | 1,973 | 13.7% | 0.68 | Wane - 1/2" flat face |
| 1.233 | 1/12 | 13.6 | 1/2D | Radial | 2,124 | 13.8% | 0.74 | Wane - 1/2" flat face |
| 1.237 | 1/12 | 11.2 | 1/2D | Radial | 2,228 | 13.7% | 0.81 | Wane - 1/2" flat face |
| 1.241 | 1/12 | 18.4 | 1/2D | Tangential | 1,514 | 14.2% | 0.60 | Wane - 1/2" flat face |
| 1.233 | 0/12 | 20.0 | 1/2D | Tangential | 1,620 | 13.7% | 0.63 | Wane - 3/8" flat face |
| 1.243 | 1/12 | 22.4 | 1/2D | Tangential | 1,819 | 13.5% | 0.66 | Wane - 1/2" flat face |
| 1.240 | 1/12 | 25.6 | 1/2D | Tangential | 1,893 | 13.6% | 0.69 | Wane - 1/2" flat face |
| 1.241 | 1/12 | 20.0 | 1/2D | Tangential | 1,965 | 13.7% | 0.75 | Wane - 1/2" flat face |
| | | | | Mean | 1,888 | | | |
| | | | | Std. Dev. | 211 | K Factor 2.104 | | |
| | | | | 5% Exclusion | 1,443 [1] | | | |
| 1.243 | 1/12 | 23.2 | 1D | Radial | 1,635 | 13.1% | 0.67 | Wane - 1/2" flat (2 sides) |
| 1.243 | 1/12 | 12.0 | 1D | Radial | 1,667 | 13.3% | 0.71 | |
| 1.243 | 0/12 | 16.8 | 1D | Radial | 1,686 | 13.2% | 0.67 | Wane - 1/2" max. |
| 1.243 | 1/12 | 7.2 | 1D | Radial | 1,695 | 11.9% | 0.66 | Wane - 1/2" max. (2 sides) |
| 1.247 | 1/12 | 12.8 | 1D | Radial | 1,756 | 13.8% | 0.73 | Wane - 1/2" flat face |
| 1.237 | 1/12 | 24.0 | 1D | Tangential | 1,487 | 13.2% | 0.67 | Wane - 1/2" flat face |
| 1.238 | 1/12 | | 1D | Tangential | 1,213 | 13.1% | 0.55 | |
| 1.242 | 2/12 | 7.2 | 1D | Tangential | 1,402 | 12.9% | 0.70 | Wane - 1/2" max. Burl wood at big end |
| 1.240 | 1/12 | 7.2 | 1D | Tangential | 1,525 | 13.6% | 0.67 | Wane - 1/2" flat face |
| 1.240 | 0/12 | 25.6 | 1D | Tangential | 1,528 | 13.9% | 0.75 | Wane - 1/2" flat face |
| | | | | Mean | 1,559 | | | |
| | | | | Std. Dev. | 164 | K Factor 2.104 | | |
| | | | | 5% Exclusion | 1,214 [1] | | | |

[1] From ASTM D 2915

# Appendix I Dowel Bearing Data

## Summary of Dowel Bearing Tests
## RO Pegs, RDF-LT Base

Sorted By Yield Stress

| Peg Orient. | Avg. Peg Dia. (in.) | Grain Slope | Peg Rings / Inch | Base Rings / Inch | Yield Stress (psi) | Peg Moisture Content | Peg Dry SG | Base Moisture Content | Base Dry SG | Stiffness (lb/in) | Peg / Base Defects |
|---|---|---|---|---|---|---|---|---|---|---|---|
| R | 1.010 | 1/12 | 17.0 | 25.0 | 1,714 | 11.9% | 0.54 | 12.9% | 0.47 | 62,386 | |
| R | 1.014 | 1/12 | 12.0 | 23.0 | 1,856 | 11.3% | 0.61 | 12.5% | 0.51 | 50,599 | |
| R | 1.025 | 0/12 | 18.0 | 16.0 | 1,927 | 11.3% | 0.55 | 12.9% | 0.47 | 57,576 | |
| R | 1.009 | 1/12 | 10.0 | 11.0 | 2,001 | 11.3% | 0.62 | 13.2% | 0.48 | 63,738 | |
| R | 1.007 | 0/12 | 9.0 | 13.0 | 2,607 | 11.7% | 0.68 | 13.2% | 0.47 | 107,832 | |
| T | 1.010 | 0/12 | 13.0 | 17.0 | 1,874 | 11.7% | 0.56 | 13.3% | 0.47 | 60,118 | |
| T | 1.010 | 0/12 | 12.0 | 16.0 | 1,930 | 11.4% | 0.55 | 13.0% | 0.47 | 49,439 | |
| T | 1.012 | 1/12 | 11.0 | 13.0 | 2,189 | 11.7% | 0.64 | 12.4% | 0.47 | 73,504 | |
| T | 1.017 | 0/12 | 12.0 | 22.0 | 2,251 | 11.6% | 0.67 | 12.5% | 0.47 | 54,083 | |
| T | 1.017 | 0/12 | 11.0 | 13.0 | 2,347 | 10.7% | 0.59 | 12.5% | 0.48 | 60,545 | |
| | | | | Mean | 2,070 | | | | | | |
| | | | | Std. Dev. | 272 | K Factor | 2.104 | | | | |
| | | | | 5% Exclusion | 1,497 | [1] | | | | | |

[1] From ASTM D 2915

## Summary of Embedment Tests
## RO Pegs, RDF-RT Base

Sorted By Yield Stress

| Peg Orient. | Avg. Peg Dia. (in.) | Grain Slope | Peg Rings / Inch | Base Rings / Inch | Yield Stress (psi) | Peg Moisture Content | Peg Dry SG | Base Moisture Content | Base Dry SG | Stiffness | Peg / Base Defects |
|---|---|---|---|---|---|---|---|---|---|---|---|
| R | 1.010 | 0/12 | 8.0 | 11.0 | 1,604 | 12.2% | 0.65 | 11.9% | 0.50 | 32,855 | |
| R | 1.012 | 0/12 | 19.0 | 10.0 | 1,899 | 11.6% | 0.53 | 11.6% | 0.47 | 44,055 | |
| R | 1.014 | 2/12 | 9.0 | 9.0 | 1,937 | 11.6% | 0.63 | 11.4% | 0.47 | 46,152 | |
| R | 1.009 | 1/12 | 22.4 | 21.0 | 1,617 | 11.1% | 0.56 | 11.1% | 0.47 | 22,833 | |
| R | 1.013 | 1/12 | 8.0 | 22.0 | 1,585 | 11.3% | 0.67 | 11.0% | 0.48 | 29,617 | |
| | | | | Mean | 1,728 | | | | | | |
| | | | | Std. Dev. | 174 | K Factor | 2.464 | | | | |
| | | | | 5% Exclusion | 1,300 | [1] | | | | | |

[1] From ASTM D 2915

## Summary of Embedment Tests
## RO Pegs, EWP-LT Base

Sorted By Yield Stress

| Peg Orient. | Avg. Peg Dia. (in.) | Grain Slope | Peg Rings / Inch | Base Rings / Inch | Yield Stress (psi) | Peg Moisture Content | Peg Dry SG | Base Moisture Content | Base Dry SG | Stiffness (lb/in) | Peg / Base Defects |
|---|---|---|---|---|---|---|---|---|---|---|---|
| R | 1.022 | 0/12 | 11.0 | 6.0 | 2,152 | 11.1% | 0.61 | 11.9% | 0.40 | 65,809 | |
| R | 1.004 | 0/12 | 12.0 | 9.0 | 2,228 | 11.7% | 0.58 | 12.3% | 0.35 | 62,972 | |
| R | 1.004 | 0/12 | 7.0 | 9.0 | 2,235 | 11.5% | 0.67 | 11.8% | 0.35 | 48,147 | |
| R | 1.007 | 0/12 | 14.0 | 6.0 | 2,398 | 11.7% | 0.54 | 12.2% | 0.34 | 71,865 | |
| R | 1.014 | 0/12 | 7.0 | 5.0 | 2,414 | 12.0% | 0.62 | 12.6% | 0.40 | 67,209 | |
| T | 1.013 | 1/12 | 16.0 | 6.0 | 1,944 | 11.7% | 0.57 | 11.6% | 0.34 | 62,873 | |
| T | 1.014 | 0/12 | 11.0 | 7.0 | 2,262 | 15.4% | 0.68 | 13.0% | 0.39 | 49,307 | |
| T | 1.013 | 1/12 | 13.0 | 8.0 | 2,309 | 11.8% | 0.59 | 12.0% | 0.37 | 73,168 | |
| T | 1.005 | 0/12 | 11.0 | 6.0 | 2,342 | 11.8% | 0.60 | 12.3% | 0.37 | 54,844 | |
| T | 1.009 | 0/12 | 9.0 | 6.0 | 2,483 | 12.0% | 0.67 | 12.5% | 0.36 | 65,005 | |
| | | | | Mean | 2,277 | | | | | | |
| | | | | Std. Dev. | 153 | K Factor | 2.104 | | | | |
| | | | | 5% Exclusion | 1,954 | [1] | | | | | |

[1] From ASTM D 2915

## Summary of Embedment Tests
## RO Pegs, EWP-RT Base

Sorted By Yield Stress

| Peg Orient. | Avg. Peg Dia. (in.) | Grain Slope | Peg Rings / Inch | Base Rings / Inch | Yield Stress (psi) | Peg Moisture Content | Peg Dry SG | Base Moisture Content | Base Dry SG | Stiffness (lb/in) | Peg / Base Defects |
|---|---|---|---|---|---|---|---|---|---|---|---|
| R | 1.021 | 1/12 | 15.0 | 10.0 | 1,289 | 11.7% | 0.55 | 12.7% | 0.38 | 20,530 | |
| R | 1.000 | 0/12 | 8.0 | 10.0 | 1,309 | 12.0% | 0.68 | 12.4% | 0.32 | 24,077 | |
| R | 1.008 | 0/12 | 16.0 | 5.0 | 1,434 | 12.0% | 0.61 | 12.8% | 0.35 | 23,757 | |
| R | 1.007 | 0/12 | 11.0 | 7.0 | 1,453 | 11.7% | 0.61 | 13.2% | 0.35 | 19,708 | |
| R | 1.016 | 0/12 | 11.0 | 7.0 | 1,705 | 12.3% | 0.59 | 13.5% | 0.32 | 35,807 | |
| T | 1.014 | 1/12 | 8.0 | 7.0 | 1,447 | 11.5% | 0.62 | 11.5% | 0.40 | 18,830 | |
| T | 1.008 | 1/12 | 13.0 | 7.0 | 1,453 | 11.4% | 0.65 | 12.2% | 0.35 | 28,350 | |
| T | 1.005 | 0/12 | 10.0 | 6.0 | 1,485 | 10.7% | 0.56 | 10.7% | 0.33 | 24,393 | Tree center below bearing area |
| T | 1.021 | 1/12 | 17.0 | 6.0 | 1,542 | 11.9% | 0.59 | 11.9% | 0.37 | 25,598 | |
| T | 1.009 | 1/12 | 8.0 | 7.0 | 1,578 | 11.3% | 0.62 | 11.2% | 0.39 | 28,724 | |
| | | | | Mean | 1,469 | | | | | | |
| | | | | Std. Dev. | 122 | K Factor | 2.104 | | | | |
| | | | | 5% Exclusion | 1,213 | [1] | | | | | |

[1] From ASTM D 2915

## Bibliography


Abe M., and Kawaguchi, M., (1995). "Structural Development of the Japanese Timber Pagoda," *Structural Engineering International* 5(4), 241-243.

American Forest & Paper Association (1991). "National Design Specification for Wood Construction," American Forest & Paper Association (AFPA), Washington, DC.

ASTM, (1995a). *1995 Annual Book of ASTM Standards, 04.10 Wood,* Philadelphia, PA.

ASTM, (1995b). "Standard Method for Evaluating Dowel Bearing Strength of Wood and Wood-Base Products," Draft 10, January 1995.

Aune P., and Patton-Mallory, M., (1986). "Lateral Load-Bearing Capacity of Nailed Joints Based on the Yield Theory." No. FPL-469, Forest Products Laboratory, U.S. Dept. of Agriculture, Washington, DC.

Benson, T. and Gruber, J., (1980). "Building the Timber Frame House, The Revival of a Forgotten Craft," Charles Schribner's Sons, New York.

Benson, T. (1997). "The Timber-Frame Home - Design, Construction, Finishing," Second Edition, Taunton Press, Inc., 4-22.

Bulleit, W. M., Sandberg, L. B., O'Bryant, T. L., Weaver, D. A., and Pattison, W. E., (1996). "Analysis of Frames with Traditional Timber Connections," *Proceedings*, International Wood Engineering Conference, New Orleans, LA. 4, 232-239.

Brungraber, R. L. (1992a). "Engineered Tension Joinery," *Timber Framing.* 23, 10-12.

Brungraber, R. L. (1992b). "Assessing Capacities of Traditional Timber Connections," *Wood Design Focus.* 3(4), 17-21.

Brungraber, R. L. (1985). "Traditional Timber Joinery: A Modern Analysis," Ph.D. Dissertation, Stanford University, Palo Alto, California.

Brungraber, R. L., and Morse-Fortier, L., (1996). "Wooden Peg Tests - Their Behavior and Capacities as Used in Town Lattice Trusses," Contract Report to Vermont Department of Transportation, Contract No. TH 9290 - Long Term Covered Bridge Study, March.

Charles, F. W. B. (1984). "Conservation of Timber Buildings," Hutchinson & Co. (Publishers) Ltd., 10-12.

Church, J. R. (1995). "Characterization of Factors Influencing the Bearing Strength of Wood Pegged Connections," M.S. Thesis, University of Idaho.

Church, J. R. and Tew, B. W. (1997). "Characterization of Bearing Strength Factors in Pegged Timber Connections," *Journal of Structural Engineering*, March 1997, 326-332.

Duff, S. F., Black, R. G., Mahin, S. A., and Blondet, M. (1996). "Parameter Study of an Internal Timber Tension Connections," *Journal of Structural Engineering*, 122(4), 446-452.

Eckelman, C. A. (1970). "How to Design Dowel Joints," *Research Progress Report*, Purdue University, Agricultural Experiment Station, 7 p.

Eckelman, C. A. (1979). "Out-of-Plane Strength and Stiffness of Dowel Joints," *Forest Products Journal*, 29(8), 32-38.

Elliot, S. and Wallas, E., (1977). "The Timber Framing Book," Housesmiths Press, 1-4.

Hewett, Cecil A., (1980). "English Historic Carpentry," Phillimore and Co., Glossary.

Hill, M. D. and Eckelman, C. A., (1973). "Flexibility and Bending Strength of Mortise and Tenon Joints," *Furniture Design and Manufacturing*, January, 54-60.

Hoadley, R. B. (1980). "Understanding Wood - A Craftsman's Guide to Wood Technology," The Taunton Press, 1-17.

Johansen, K. W. (1949). "Theory of Timber Connections," International Association for Bridge and Structural Engineering, 9, 249-262.

Kessel, M. H. (1988). "The Reconstruction of an Eight-Floor Timber Frame House at Hildesheim (FRG)," *Proceedings,* 1988 International Conference on Timber Engineering, Seattle, WA, 415-421.

Kessel, (1996). - Personal communication with Dr. Richard Schmidt

King, W. S., Yen, J. Y. R., and Yen, Y. N. A., (1996). "Joint Characteristics of Traditional Chinese Wooden Frames," *Engineering Structures*, 18(8), 635-644.

Larsen, H. J. (1973). "The Yield Load of Bolted and Nailed Joints," *Proceedings of the International Union of Forestry Research Organization*—Division V Conference, 645-654.

Macmillan, Inc. (1996). "Webster's New World Dictionary and Thesaurus," Macmillan, Inc. 135.

McLain, T. E., and Thangjitham, S., (1983). "Bolted Wood-Joint Yield Model," *Journal of Structural Engineering*. 109(8), 1820-1835.

Peavy, M. D., and Schmidt, R. J. (1995). "Load Behavior of Connections With Oak Pegs", *Timber Framing.* 38, 6-9. *Translation of:* Kessel, M. H., and Augustin, R., 1990, "Untersuchungen über das Tragverhalten von Verbindungen mit Eichenholznägeln," *Bauen mit Holz*, 246-250, April.

Peavy, M. D., and Schmidt, R. J. (1996). "Load Bearing Capacity of Timber Connections with Wood Pegs", *Timber Framing.* 39, 8-11. *Translation of:* Kessel, M. H., and Augustin, R., 1994. "Untersuchungen der Tragfähigkeit von Holzverbindungen mit Holznägeln für Sanierung und Rekonstruktion alter Bausubstanz," *Bauen mit Holz*, 484-487, June.

Sandberg, L. B., Bulleit, W. M., O'Bryant, T. L., Postlewaite, J. J., and Schaffer, J. J.(1996). "Experimental Evaluation of Traditional Timber Connections," *Proceedings*, International Wood Engineering Conference, New Orleans, LA., 4, 225-231.

Schmidt, R. J., MacKay, R. B., and Leu, B. L. (1996). "Design of Joints in Traditional Timber Frame Buildings," *Proceedings*, International Wood Engineering Conference, New Orleans, LA. 4, 240-247.

Seike, K. (1977). "The Art of Japanese Joinery," New York: J. Weatherhill.

Sobon, J., and Schroeder, R. (1984). "Timber Frame Construction," Garden Way Publishing, 3-15.

Sobon, J. (1994). "Build a Classic Timber-Framed House," Garden Way Publishing.

Soltis, L. A., Hubbard, F. K. and Wilkinson, T. L. (1986). "Bearing Strength of Bolted Timber Joints," *Journal of Structural Engineering*, 112(9), 2141-2154.

Soltis, L. A.; Karnasudirdja, S.; Little, J. K. (1987). "Angle to Grain Strength of Dowel–type Fasteners." Wood and Fiber Science. 19(1), 68-80.

Soltis, L. A., and Wilkinson, T. L. (1987). "Bolted-Connection Design." No. FPL-GTR-54, Forest Products Laboratory, U.S. Dept. of Agriculture, Washington, DC.

Soltis, L. A. (1994). "Bolted Connection Research: Present and Future." *Wood Design Focus*, Summer 1994, 5(2), 3-5.

Thangjitham, S. (1981). "A Method of Evaluating The Probabilistic Resistance of Bolted Wood Joints", Master's Thesis, Virginia Polytechnic Institute and State University, Blacksburg, Virginia.